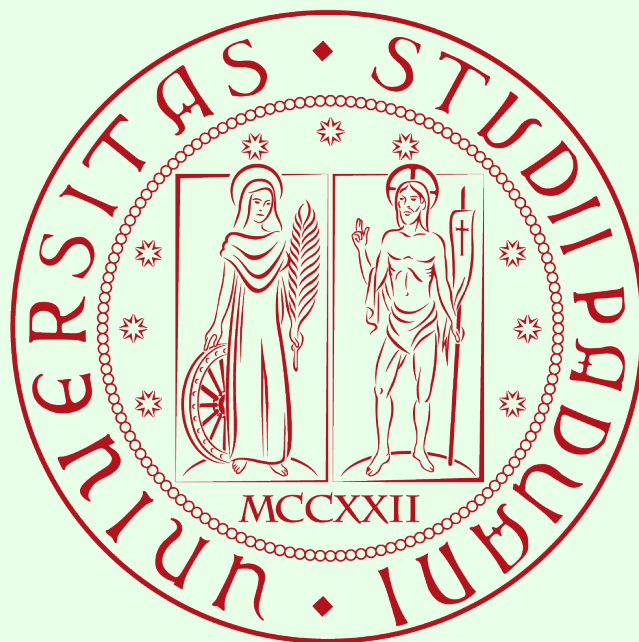

LECTURE NOTES
OF
DIGITAL SIGNAL PROCESSING

COLLECTION OF THE LECTURES NOTES OF PROFESSOR FEDERICA BATTISTI.

EDITED BY
ARDINO ROCCO
ACADEMIC YEAR 2020-2021



Abstract

In this document I have tried to reorder the notes of the Digital Signal Processing course held by Professor Federica Battisti at DEI of the University of Padua during the first semester of the 2020-21 academic year of the master's degree in Physics of Data.

The notes are fully integrated with the material provided by the professor in the Moodle platform. In addition, I will integrate them, as best as possible, with the books recommended by the professor.

There may be formatting errors, wrong marks, missing exponents and even missing parts, since I'm still working on them. If you find errors or if you have any suggestions, let me know (you can send an e-mail at rocco.ardino@studenti.unipd.it, labeled with **DSP::TYPO/SUGGESTION**) and I will correct/integrate them, so that this document can be a good study support. However, these notes are not to be intended as a substitute of the lectures held by the professor or of lecture notes made by other people.

Padova, Tuesday 22nd December, 2020
Rocco Ardino

Contents

1	Introduction	1
1.1	What is a signal?	1
1.2	Is sampling of a continuous signal always possible?	3
1.3	Discrete time and amplitude	3
1.4	Advantages and disadvantages of digital signals	5
2	Discrete-Time signals	7
2.1	Time-Domain representation	7
2.2	Operations on sequences	7
2.3	Classification of sequences	7
3	Discrete-Time systems	9
3.1	Linear systems	9
3.2	Shift-Invariant systems	9
3.3	Causal systems	9
3.4	Stable systems	9
3.5	Passive and lossless systems	9
3.6	Impulse and step response	9
3.7	Shift-Invariant systems	9
3.8	Time domain characterizatio of LTI discrete-time system	9
3.9	Convolution sum	9
3.10	Stablility and causality conditions	9
3.11	Correlation and autocorrelation	9
4	Fourier Analysis	11
4.1	Continuous-time Fourier transform	11
4.1.1	Energy density spectrum	12
4.1.2	Band-limited continuous-time signals	12
4.1.3	Discrete-time fourier transform	13
4.1.4	DTFT properties	18
4.1.5	Energy density spectrum	20
4.1.6	Band-limited discrete-time signals	21
4.2	Linear convolution using DTFT	22
4.3	The frequency response	24
4.4	The concept of filtering	28
4.5	Discrete Fourier Transform	30
4.5.1	Matrix relations	33
4.5.2	DTFT from DFT by interpolation	34
4.5.3	Sampling the DTFT	35
4.5.4	DFT properties	36
4.5.5	Circular shift of a sequence	36
4.5.6	Circular convolution	37

4.5.7	DFT of real sequences	38
4.6	Linear convolution using the DFT	40
5	The Z transform	45
5.1	The definition	45
5.2	Rational z-transforms	47
5.3	Inverse z-transform	51
5.4	Z-transform properties	53
5.5	Stability condition	55
6	Filter design	59
6.1	Phase and group delay	59
6.1.1	Phase delay	59
6.1.2	Group delay	59
6.2	Type of transfer functions	60
6.2.1	Ideal filters	60
6.2.2	Bounded Real transfer functions	61
6.2.3	Allpass transfer function	63
6.2.4	Phase characteristics	66
6.2.5	Frequency response from transfer function	68
6.2.6	Geometric interpretation of frequency response	69
6.3	Simple digital filters	70
6.3.1	Lowpass FIR digital filters	70
6.3.2	Highpass FIR digital filters	72
6.3.3	Lowpass IIR digital filters	73
6.3.4	Highpass IIR digital filters	74
6.3.5	Bandpass IIR digital filters	75
6.3.6	Bandstop IIR digital filters	76
6.3.7	Higher-Order IIR digital filters	77
	Bibliography	79

Chapter 1

Introduction

In this course we will enter into the world of Digital Signal Processing, trying to understand the theoretical fundations of this field with several examples. In particular, we will follow this outline of arguments:

- What is Digital Signal Processing?
- Discrete-time signals.
- Signals and Hilbert spaces.
- Fourier analysis.
- Discrete-time filters.
- The z-transform.
- Filter design, in particular A/D and D/A conversions and the design of a digital communication system.

Concerning the study material, along with the teaching professor's notes and slides, several textbooks are suggested to integrate the study material:

- [1] *Signal Processing for Communication*, P. Prandoni and M. Vetterli.
- [2] *Digital Signal Processing*, A. V. Oppenheim and R. W. Schafer.
- [3] *Digital Signal Processing: A Computer-Based Approach*, S. K. Mitra.

1.1 What is a signal?

Let us start with a definition of what we are going to deal with for most of our time. A signal is the description of the evolution of a physical phenomenon. For example, we can have:

- **continuous-time signals**, such as voltage, current, temperature and speed, whose spectrum is sketched in Figure 1.1;
- **discrete-time signals**, such as minimum/maximum temperature, lap intervals in races, sampled continuous signals, with an example spectrum showed in Figure 1.2.

Signals may have to be transformed in order to:

Lecture 1.
Tuesday 29th
September, 2020.

Signal definition
and types of signals

Operations on
signals

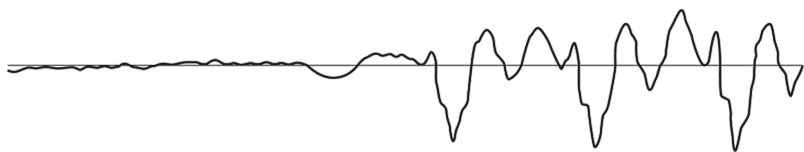


Figure 1.1: Example of continuous-time signal spectrum.

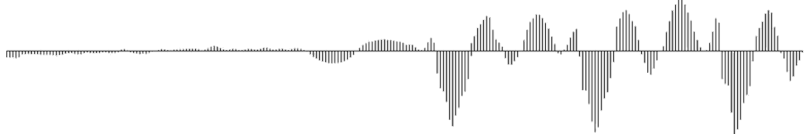


Figure 1.2: Example of discrete-time signal spectrum, obtained from sampling of the signal in Figure 1.1.

- be analyzed: this is necessary to **understand** the informations carried by the signal itself. For example, we can amplify or filter out embedded information, detect patterns, prepare the signal to survive a transmission channel and much more;
- be synthesized: this is necessary to **create** a signal to contain a specific information. Some common examples in this case are the cellphones, tv, radio and synthetic music.

Therefore, to do these operations we need specific methods to measure, characterize, model and simulate transmission channels, but also mathematical tools that split common channels and transformations into easily manipulated building blocks.

From analog to digital signals

Now, we enter more into the detail of digital signals. When we are dealing with analog signals, we can record them but we can hardly find a function that can describe them. In order to have an idea of the difficulty of this task, let us look at the signal in Figure 1.3: how can we describe this function? This is where the digital part comes into practice.

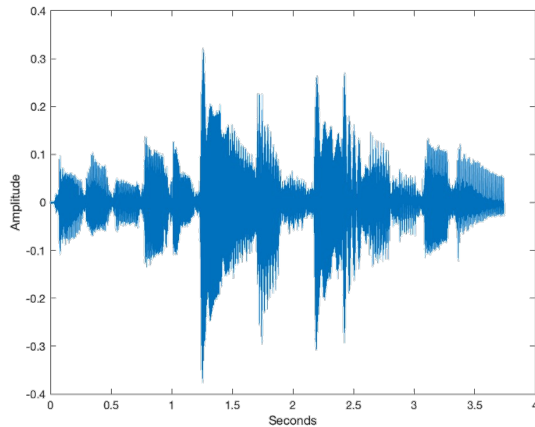


Figure 1.3: Example of analog signal.

Mathematical definition of digital signals

A continuous-time (analog) signal is defined along a continuum of time and is thus represented by a continuous independent variable. Discrete-time signals are defined at discrete times, and thus, the independent variable has discrete values. Therefore, the ladders are represented as sequences of numbers x , in which the n^{th} number in the sequence is denoted $x[n]$, and it is formally written as:

$$x = \{x[n]\}, \quad -\infty < n < \infty \quad (1.1)$$

where n is an integer. An example is showed in Figure 1.4.

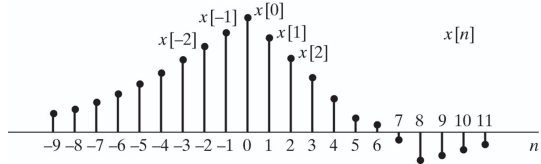


Figure 1.4: Example of graphic representation of a discrete-time signal.

Such sequences can arise from periodic sampling of an analog signal $x_a(t)$. In this case the numeric value of the n^{th} number in the sequence is equal to the value of the analog signal, namely $x_a(t)$, at time nT :

$$x[n] = x_a(nT), \quad -\infty < n < \infty \quad (1.2)$$

where T is the sampling period.

Digital signal
sampled from
periodic signals

1.2 Is sampling of a continuous signal always possible?

At this point we ask ourselves a question: when we represent an analog signal as a digital one, are we loosing information? The question has been answered by C. Shannon and H. Nyquist: under specific conditions, the analog and the digital representations of a signal are equivalent. Here we come to the sampling theorem. An analog signal can be represented as a linear combination of cardinal sine (denoted by sinc and plotted in Figure 1.5) functions shifted ad scaled by the values of the discrete time sequence. Mathematically, this translates into:

$$x(t) = \sum_{n=-\infty}^{\infty} x[n] \operatorname{sinc}\left(\frac{t - nT_S}{T_S}\right) \quad (1.3)$$

Sampling theorem

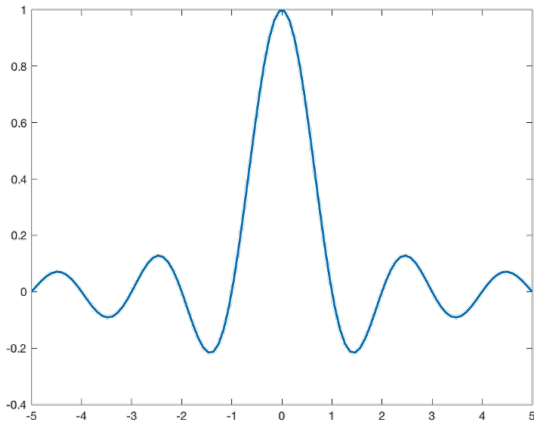


Figure 1.5: Cardinal sine sinc function.

It is important to determine the value of T_S so that the sampling theorem holds. The Fourier transform helps us understanding how fast the signal moves and consequently guides us to the selection of T_S .

Utility of Fourier
transform

1.3 Discrete time and amplitude

Till now we discussed the discretization of time. What if we discretize also the amplitude of the signal? In this case each sample can take predetermined values

in a countable set. Moreover, as consequence, we can always map the level of the sample onto an integer. An example of a sampled sin function is showed in Figure 1.6.

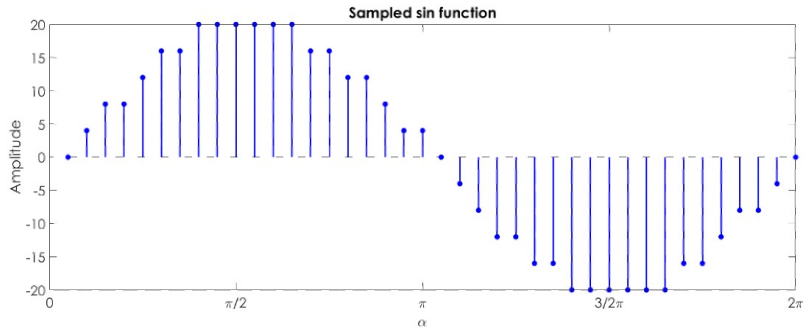


Figure 1.6: Sampled sin function.

It is of paramount importance to discretize both time and amplitude. By this way, we can ease tasks like storage, processing and transmission. In particular, let us describe the ladder.

Signal transmission

Transmission is one of the fields that most benefits from discrete signal representation. We give an idea of this fact through an example. Let us consider the channel scheme in Figure 1.7 and a sinusoidal analog signal, which is attenuated and acquires a noise component, as represented in Figure 1.9

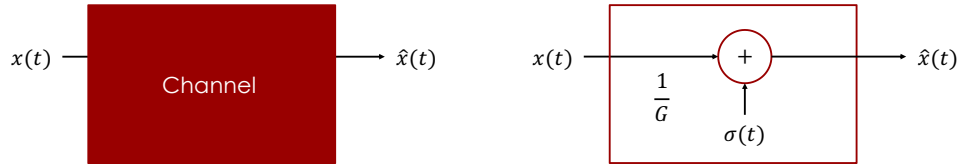


Figure 1.7: Scheme of an example of transmission channel.

We can counteract this problem by trying to undo the errors introduced by the signal (only the gain):

$$\hat{x}_1(t) = G \left[\frac{x(t)}{G} + \sigma(t) \right] = x(t) + G\sigma(t) \quad (1.4)$$

By this way, we also amplify the noise. Sometimes this is unavoidable, but what we can do is to amplify the signal as near to the place where it is acquired as possible, so that the noise is amplified before it increases in the transmission to the place where it is analyzed. In particular, noise amplification becomes more relevant if we put in cascade several transmission blocks, as represented in Figure 1.8. In this case, the output of the transmission chain reads:

$$\hat{x}_N(t) = x(t) + NG\sigma(t) \quad (1.5)$$

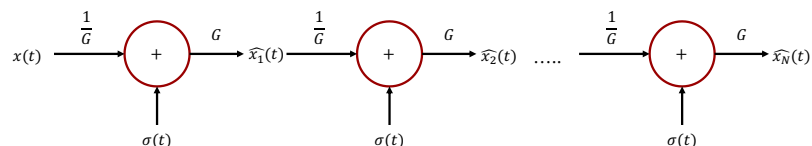


Figure 1.8: Scheme of an example of a cascade of transmission blocks.

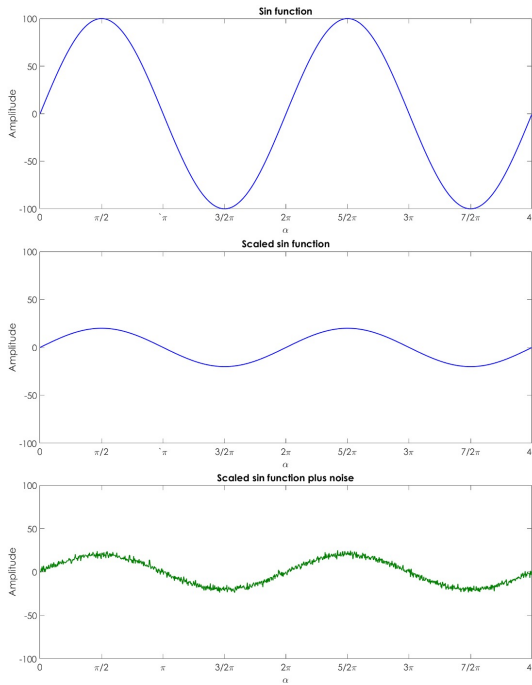


Figure 1.9: Sinusoidal analog signal (top), sinusoidal attenuated signal (center), sinusoidal attenuated noisy signal (bottom).

This discussion was mainly related to analog signals. Now, if we take into account the transmission of a digital signal, we have to perform other operations, such as introducing a thresholding operator to discretize the signal. With respect to the previous example, the new transmission block is showed in Figure 1.10 and the output reads:

$$\hat{x}_1(t) = \text{sign} [x(t) + G\sigma(t)] \quad (1.6)$$

which is in practice a square wave.

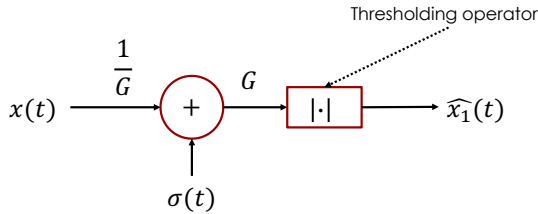


Figure 1.10: Scheme of an example of transmission channel for digital signals.

1.4 Advantages and disadvantages of digital signals

To conclude this introduction, we have still to present the main advantage of digital signals, but also their drawbacks:

Pro and cons

- ✓ noise is easy to control after initial quantization;
- ✓ highly linear (within limited dynamic range);
- ✓ complex algorithms fit into a single chip;
- ✓ flexibility, parameters can easily be varied in software;

- ✓ digital processing is insensitive to component tolerances, aging, environmental conditions, electromagnetic interference;
- ✗ discrete-time processing artifacts (aliasing);
- ✗ a significantly large amount of power can be required (battery, cooling);
- ✗ digital clock and switching cause interference.

Chapter 2

Discrete-Time signals

- 2.1 Time-Domain representation
- 2.2 Operations on sequences
- 2.3 Classification of sequences

Lecture 2.
*Thursday 1st
October, 2020.*

Chapter 3

Discrete-Time systems

3.1 Linear systems

Lecture 3.
Tuesday 6th
October, 2020.

3.2 Shift-Invariant systems

3.3 Causal systems

3.4 Stable systems

3.5 Passive and lossless systems

3.6 Impulse and step response

Lecture 5.
Tuesday 13th
October, 2020.

3.7 Shift-Invariant systems

3.8 Time domain characterizatio of LTI discrete-time system

3.9 Convolution sum

3.10 Stablility and causality conditions

Lecture 6.
Thursday 15th
October, 2020.

3.11 Correlation and autocorrelation

Chapter 4

Fourier Analysis

4.1 Continuous-time Fourier transform

Let us start with the definition of this very important tool

Lecture 8.
Thursday 22nd
October, 2020.

Definition 1: Fourier transform of a continuous-time signal

The CTFT of a continuous-time signal $x_a(t)$ is given by:

$$X_a(j\Omega) = \int_{-\infty}^{\infty} x_a(t)e^{-j\Omega t} dt \quad (4.1)$$

often referred to as the Fourier spectrum or simply the spectrum of the continuous-time signal.

Definition 2: Inverse Fourier transform of a continuous-time signal

The inverse CTFT of a Fourier transform $X_a(j\Omega)$ is given by:

$$x_a(t) = \frac{1}{2\pi} \int_{-\infty}^{\infty} X_a(j\Omega)e^{+j\Omega t} d\Omega \quad (4.2)$$

often referred to as the Fourier integral.

A CTFT pair will be denoted as:

$$x_a(t) \longleftrightarrow X_a(j\Omega) \quad (4.3)$$

Note that Ω is real and denotes the continuous-time angular frequency variable in radians. In general, the CTFT is a complex function of Ω in the range $-\infty < \Omega < \infty$. It can be expressed in the polar form as:

$$X_a(j\Omega) = |X_a(j\Omega)|e^{j\theta_a(\Omega)} \quad (4.4)$$

where $\theta_a(\Omega) = \arg X_a(j\Omega)$. The quantity $|X_a(j\Omega)|$ is called the magnitude spectrum and the quantity $\theta_a(\Omega)$ is called the phase spectrum. Both spectra are real function of Ω and in general the CTFT $X_a(j\Omega)$ exists if $x_a(t)$ satisfies the Dirichlet conditions:

- the signal $x_a(t)$ has a finite number of discontinuities and a finite number of maxima and minima in any finite interval;
- the signal is absolutely integrable, i.e.:

$$\int_{-\infty}^{\infty} |x_a(t)| dt < \infty \quad (4.5)$$

If the Dirichlet conditions are satisfied, then:

$$\frac{1}{2\pi} \int_{-\infty}^{\infty} X_a(j\Omega) e^{+j\Omega t} d\Omega \quad (4.6)$$

converges to $x_a(t)$ except at values of t where $x_a(t)$ has discontinuities. Moreover, it can be showed that if $x_a(t)$ is absolutely integrable, then proving the existence of the CTFT reduces to proving:

$$|X_a(t\Omega)| < \infty \quad (4.7)$$

4.1.1 Energy density spectrum

The total energy E_x of a finite energy continuous-time complex signal $x_a(t)$ is given by:

$$\begin{aligned} E_x &= \int_{-\infty}^{\infty} |x_a(t)|^2 dt \\ &= \int_{-\infty}^{\infty} x_a(t) x_a^*(t) dt \\ &= \int_{-\infty}^{\infty} x_a(t) \left[\frac{1}{2\pi} \int_{-\infty}^{\infty} X_a^*(j\Omega) e^{-j\Omega t} d\Omega \right] dt \end{aligned} \quad (4.8)$$

Interchanging the order of the integration we get:

$$\begin{aligned} E_x &= \frac{1}{2\pi} \int_{-\infty}^{\infty} X_a^*(j\Omega) \left[\int_{-\infty}^{\infty} x_a(t) e^{-j\Omega t} dt \right] d\Omega \\ &= \frac{1}{2\pi} \int_{-\infty}^{\infty} X_a^*(j\Omega) X_a(j\Omega) d\Omega \\ &= \frac{1}{2\pi} \int_{-\infty}^{\infty} |X_a(j\Omega)|^2 d\Omega \end{aligned} \quad (4.9)$$

Hence:

$$\int_{-\infty}^{\infty} |x(t)|^2 dt = \frac{1}{2\pi} \int_{-\infty}^{\infty} |X_a(j\Omega)|^2 d\Omega \quad (4.10)$$

The above relation is more commonly known as the Parseval's relation for finite-energy continuous-time signals. The quantity $|X_a(j\Omega)|^2$ is called the energy density spectrum of $x_a(t)$ and it is usually denoted as:

$$S_{xx}(\Omega) = |X_a(j\Omega)|^2 \quad (4.11)$$

The energy over a specified range of frequencies $\Omega_a \leq \Omega \leq \Omega_b$ can be computed using:

$$E_{x,r} = \frac{1}{2\pi} \int_{\Omega_a}^{\Omega_b} S_{xx}(\Omega) d\Omega \quad (4.12)$$

4.1.2 Band-limited continuous-time signals

A full-band, finite-energy, continuous-time signal has a spectrum occupying the whole frequency range $-\infty \leq \Omega \leq \infty$. A band-limited continuous-time signal has a spectrum that is limited to a portion of the frequency range $-\infty \leq \Omega \leq \infty$. An ideal band-limited signal has a spectrum that is zero outside a finite frequency range $\Omega_a \leq |\Omega| \leq \Omega_b$ can be computed using:

$$X_a(j\Omega) = \begin{cases} 0 & 0 \leq |\Omega| < \Omega_a \\ 0 & \Omega_b < |\Omega| < \infty \end{cases} \quad (4.13)$$

However, an ideal band-limited signal cannot be generated in practice.

Band-limited signals are classified according to the frequency range where most of the signal's is concentrated:

- a lowpass, continuous-time signal has a spectrum occupying the frequency range $0 < |\Omega| \leq \Omega_p < \infty$, where Ω_p is called the bandwidth of the signal;
- a highpass, continuous-time signal has a spectrum occupying the frequency range $0 < \Omega_p \leq |\Omega| < \infty$, where the bandwidth of the signal is from Ω_p to ∞ ;
- a bandpass, continuous-time signal has a spectrum occupying the frequency range $0 < \Omega_L \leq |\Omega| \leq \Omega_H < \infty$, where $\Omega_H - \Omega_L$ is the bandwidth.

4.1.3 Discrete-time fourier transform

Let us introduce the definition of this concept.

Definition 3: Discrete-time Fourier transform

The discrete-time Fourier transform (DTFT) $X(e^{j\omega})$ of a sequence $x[n]$ is given by:

$$X(e^{j\omega}) = \sum_{n=-\infty}^{\infty} x[n]e^{-j\omega n} \quad (4.14)$$

where in general $X(e^{j\omega})$ is a complex function of the real variable ω and can be written as:

$$X(e^{j\omega}) = X_{\text{re}}(e^{j\omega}) + jX_{\text{im}}(e^{j\omega}) \quad (4.15)$$

$X_{\text{re}}(e^{j\omega})$ and $X_{\text{im}}(e^{j\omega})$ are respectively, the real and imaginary parts of $X(e^{j\omega})$, and are real functions of ω . $X(e^{j\omega})$ can alternately be expressed as:

$$X(e^{j\omega}) = |X(e^{j\omega})|e^{j\theta(\omega)} \quad (4.16)$$

where $\theta(\omega) = \arg X(e^{j\omega})$. $|X(e^{j\omega})|$ and $\arg X(e^{j\omega})$ are called respectively magnitude function and phase function. Both quantities are again real functions of ω . In many applications, the DTFT is called the Fourier spectrum. Likewise, $|X(e^{j\omega})|$ and $\theta(\omega)$ are called respectively the magnitude and phase spectra.

For a real sequence $x[n]$, $|X(e^{j\omega})|$ and $X_{\text{re}}(e^{j\omega})$ are even functions of ω , whereas, $\theta(\omega)$ and $X_{\text{im}}(e^{j\omega})$ are odd functions of ω . Note also that $X(e^{j\omega}) = |X(e^{j\omega})|e^{j\theta(\omega+2\pi k)} = |X(e^{j\omega})|e^{j\theta(\omega)}$ for any integer k . The phase function $\theta(\omega)$ cannot be uniquely specified for any DTFT. Unless otherwise stated, we shall assume that the phase function $\theta(\omega)$ is restricted to the range of values $-\pi \leq \theta(\omega) < \pi$, called the principal value.

Example 1: DTFT of the unit sample sequence

The DTFT of the unit sample sequence $\delta[n]$ is given by:

$$\Delta(e^{j\omega}) = \sum_{n=-\infty}^{\infty} \delta[n]e^{-j\omega n} = \delta[0] = 1 \quad (4.17)$$

Example 2: DTFT of a causal sequence

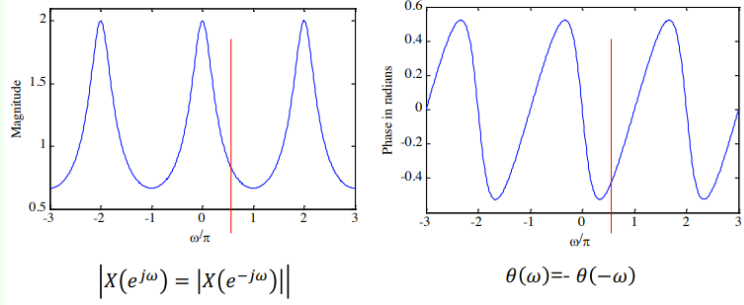
Consider the causal sequence:

$$x[n] = \alpha^n \mu[n], \quad |\alpha| < 1 \quad (4.18)$$

Its DTFT is given by:

$$\begin{aligned}
 X(e^{j\omega}) &= \sum_{n=-\infty}^{\infty} \alpha^n \mu[n] e^{-j\omega n} \\
 &= \sum_{n=0}^{\infty} \alpha^n e^{-j\omega n} \\
 &= \sum_{n=0}^{\infty} (\alpha e^{-j\omega})^n \\
 &= \frac{1}{1 - \alpha e^{-j\omega}}
 \end{aligned} \tag{4.19}$$

as $|\alpha e^{-j\omega}| = |\alpha| < 1$. If we take for example $\alpha = 0.5$, we get the plot below for the magnitude and phase of the DTFT.



The DTFT $X(e^{j\omega})$ of a sequence $x[n]$ is a continuous function of ω . It is also a periodic function of ω with a period 2π :

$$X\left(e^{j(\omega+2\pi k)}\right) = \sum_{n=-\infty}^{\infty} x[n] e^{-j\omega n} e^{-j2\pi kn} = \sum_{n=-\infty}^{\infty} x[n] e^{-j\omega n} = X(e^{j\omega}) \tag{4.20}$$

Therefore:

$$X(e^{j\omega}) = \sum_{n=-\infty}^{\infty} x[n] e^{-j\omega n} \tag{4.21}$$

represents the Fourier series representation of the periodic function. As a result, the Fourier coefficients $x[n]$ can be computed from $X(e^{j\omega})$ using the Fourier integral:

$$x[n] = \frac{1}{2\pi} \int_{-\pi}^{\pi} X(e^{j\omega}) e^{j\omega n} d\omega \tag{4.22}$$

Proof. Consider:

$$x[n] = \frac{1}{2\pi} \int_{-\pi}^{\pi} \left(\sum_{\ell=-\infty}^{\infty} x[\ell] e^{-j\omega \ell} \right) e^{j\omega n} d\omega \tag{4.23}$$

The order of integration and summation can be interchanged if the summation inside

the brackets converges uniformly, i.e. $X(e^{j\omega})$ exists. Then:

$$\begin{aligned} \frac{1}{2\pi} \int_{-\pi}^{\pi} \left(\sum_{\ell=-\infty}^{\infty} x[\ell] e^{-j\omega\ell} \right) e^{j\omega n} d\omega &= \sum_{\ell=-\infty}^{\infty} x[\ell] \left(\frac{1}{2\pi} \int_{-\pi}^{\pi} e^{j\omega(n-\ell)} d\omega \right) \\ &= \sum_{\ell=-\infty}^{\infty} x[\ell] \frac{\sin(\pi(n-\ell))}{\pi(n-\ell)} \\ &= \sum_{\ell=-\infty}^{\infty} x[\ell] \delta[n-\ell] \\ &= x[n] \end{aligned} \quad (4.24)$$

For the convergence condition, an infinite series of the form:

$$X(e^{j\omega}) = \sum_{n=-\infty}^{\infty} x[n] e^{-j\omega n} \quad (4.25)$$

may or may not converge. Therefore, let us consider:

$$X_k(e^{j\omega}) = \sum_{n=-k}^k x[n] e^{-j\omega n} \quad (4.26)$$

Then for uniform convergence of $X_k(e^{j\omega})$:

$$\lim_{k \rightarrow \infty} X_k(e^{j\omega}) = X(e^{j\omega}) \quad (4.27)$$

Now, if $x[n]$ is an absolutely summable sequence, i.e., if $\sum_{n=-\infty}^{\infty} |x[n]| < \infty$, then:

$$|X(e^{j\omega})| = \left| \sum_{n=-k}^k x[n] e^{-j\omega n} \right| \leq \sum_{n=-k}^k |x[n]| < \infty \quad (4.28)$$

for all values of ω . Thus, the absolute summability of $x[n]$ is a sufficient condition for the existence of the DTFT $X(e^{j\omega})$. ■

Example 3: Absolute summability condition

The sequence $x[n] = \alpha^n \mu[n]$ for $|\alpha| < 1$ is absolutely summable as:

$$\sum_{n=-k}^k |\alpha^n| \mu[n] = \sum_{n=0}^{\infty} |\alpha^n| = \frac{1}{1 - |\alpha|} < \infty \quad (4.29)$$

and its DTFT $X(e^{j\omega})$ therefore converges to $\frac{1}{1 - \alpha e^{j\omega}}$ uniformly.

Note that since:

$$\sum_{n=-\infty}^{\infty} |x[n]|^2 \leq \left(\sum_{n=-\infty}^{\infty} |x[n]| \right)^2 \quad (4.30)$$

an absolutely summable sequence has always a finite energy. However, a finite-energy sequence is not necessarily absolutely summable.

Example 4: Absolute summability

The sequence:

$$x[n] = \begin{cases} \frac{1}{n} & n \geq 1 \\ 0 & n \leq 0 \end{cases} \quad (4.31)$$

has finite energy equal to:

$$E_x = \sum_{n=1}^{\infty} \left(\frac{1}{n} \right)^2 = \frac{\pi^2}{6} \quad (4.32)$$

but $x[n]$ is not absolutely summable.

In order to represent a finite energy sequence $x[n]$ that is not absolutely summable by a DTFT $X(e^{j\omega})$, it is necessary to consider a mean-square convergence of $X(e^{j\omega})$:

$$\lim_{k \rightarrow \infty} \int_{-\pi}^{\pi} |X(e^{j\omega}) - X_k(e^{j\omega})|^2 d\omega = 0 \quad (4.33)$$

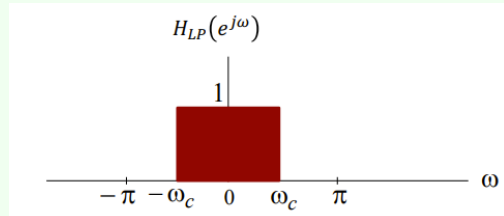
The total energy of the error $X(e^{j\omega}) - X_k(e^{j\omega})$ must approach zero at each value of ω as k goes to ∞ . In such a case, the absolute value of the error $|X(e^{j\omega}) - X_k(e^{j\omega})|$ may not go to zero as k goes to ∞ and the DTFT is no longer bounded.

Example 5: Mean-square convergence

Consider the DTFT:

$$H_{LP}(e^{j\omega}) = \begin{cases} 1 & 0 \leq |\omega| \leq \omega_c \\ 0 & \omega < |\omega| \leq \pi \end{cases} \quad (4.34)$$

showed in the plot below.



The inverse DTFT of $H_{LP}(e^{j\omega})$ is given by:

$$h_{LP}[n] = \frac{1}{2\pi} \int_{-\omega_c}^{\omega_c} e^{j\omega n} d\omega = \frac{1}{2\pi} \left(\frac{e^{j\omega_c n}}{jn} - \frac{e^{-j\omega_c n}}{jn} \right) = \frac{\sin(\omega_c n)}{\pi n} \quad (4.35)$$

for $-\infty < n < \infty$. The energy of $h_{LP}[n]$ is given by $\frac{\omega_c}{\pi}$. $h_{LP}[n]$ is a finite-energy sequence, but it is not absolutely summable. In fact, the result:

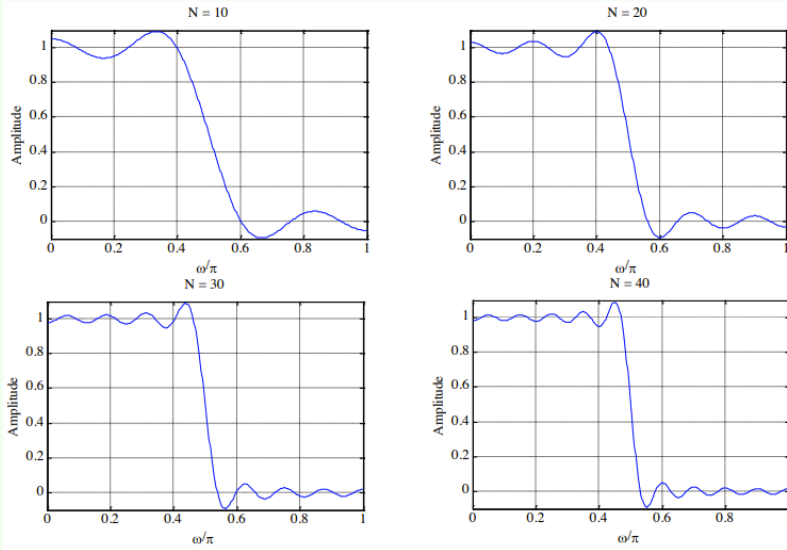
$$\sum_{n=-k}^{n=k} h_{LP}[n] e^{-j\omega n} = \sum_{n=-k}^{n=k} \frac{\sin(\omega_c n)}{\pi n} e^{-j\omega n} \quad (4.36)$$

does not uniformly converge to $H_{LP}(e^{j\omega})$ for all values of ω , but converges to $H_{LP}(e^{j\omega})$ in the mean-square sense.

The mean-square convergence property of the sequence $h_{LP}[n]$ can be further illustrated by examining the plot of the function:

$$H_{LP,k}(e^{j\omega}) = \sum_{n=-k}^k \frac{\sin(\omega_c n)}{\pi n} e^{-j\omega n} \quad (4.37)$$

for various values of k , as showed below.



As can be seen from these plots, independently of the value of k there are ripples in the plot of $H_{LP,k}(e^{j\omega})$ around both sides of the point $\omega = \omega_c$. The number of ripples increases as k increases with the height of the largest ripple remaining the same for all values of k . As k goes to ∞ , the condition:

$$\lim_{k \rightarrow \infty} \int_{-\pi}^{\pi} |H_{LP}(e^{j\omega}) - H_{LP,k}(e^{j\omega})|^2 d\omega = 0 \quad (4.38)$$

holds indicating the convergence of $H_{LP,k}(e^{j\omega})$ to $H_{LP}(e^{j\omega})$.

The oscillatory behaviour of $H_{LP,k}(e^{j\omega})$ approximating $H_{LP}(e^{j\omega})$ in the mean-square sense at a point of discontinuity is known as the Gibbs phenomenon

The DTFT can also be defined for a certain class of sequences which are neither absolutely summable nor square summable. Examples of such sequences are the unit step sequence $\mu[n]$, the sinusoidal sequence $\cos(\omega_0 n + \varphi)$ and the exponential sequence $A\alpha^n$. For this type of sequences, a DTFT representation is possible using the Dirac delta function $\delta(\omega)$.

A Dirac delta function $\delta(\omega)$ is a function of ω with infinite height, zero width, and unit area. It is the limiting form of a unit area pulse function p_Δ as Δ goes to zero satisfying:

$$\lim_{\Delta \rightarrow 0} \int_{-\infty}^{\infty} p_\Delta(\omega) d\omega = \int_{-\infty}^{\infty} \delta(\omega) d\omega \quad (4.39)$$

Example 6: Dirac δ application

Consider the complex exponential sequence:

$$x[n] = e^{j\omega_0 n} \quad (4.40)$$

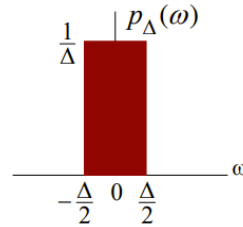


Figure 4.1: Plot and area of $p_{\Delta}(\omega)$ function.

Its DTFT is given by:

$$X(e^{j\omega}) = \sum_{k=-\infty}^{\infty} 2\pi\delta(\omega - \omega_0 + 2k\pi) \quad (4.41)$$

where $\delta(\omega)$ is an impulse function of ω and $-\pi \leq \omega_0 \leq \pi$. The function in Eq. 4.41 is periodic in ω with a period 2π and it is called periodic impulse train. In order to verify that $X(e^{j\omega})$ given above is indeed the DTFT of $x[n] = e^{j\omega_0 n}$ we compute the inverse DTFT of $X(e^{j\omega})$:

$$\begin{aligned} x[n] &= \frac{1}{2\pi} \int_{-\pi}^{\pi} \sum_{k=-\infty}^{\infty} 2\pi\delta(\omega - \omega_0 + 2\pi k) e^{j\omega n} d\omega \\ &= \int_{-\pi}^{\pi} \delta(\omega - \omega_0) e^{j\omega n} d\omega \\ &= e^{j\omega_0 n} \end{aligned} \quad (4.42)$$

where we have used the sampling property of the impulse function $\delta(\omega)$.

Last but not least, we list in Table 4.1 a set of commonly used DTFT pairs.

Sequence	DTFT
$\delta[n]$	1
1	$\sum_{k=-\infty}^{\infty} 2\pi\delta(\omega + 2\pi k)$
$e^{j\omega_0 n}$	$\sum_{k=-\infty}^{\infty} 2\pi\delta(\omega - \omega_0 + 2\pi k)$
$\mu[n]$	$\frac{1}{1 - e^{-j\omega}} + \sum_{k=-\infty}^{\infty} \pi\delta(\omega + 2\pi k)$
$\alpha^n \mu[n] \quad (\alpha < 1)$	$\frac{1}{1 - \alpha e^{-j\omega}}$

Table 4.1: Commonly used DTFT pairs.

4.1.4 DTFT properties

There are a number of important properties of the DTFT that are useful in signal processing applications. These are listed here in Figures 4.2, 4.3, 4.4 without proof, since it is quite straightforward to derive them. We illustrate the applications of some of the DTFT properties.

Sequence	Discrete-Time Fourier Transform
$x[n]$	$X(e^{j\omega})$
$x[-n]$	$X(e^{-j\omega})$
$x^*[-n]$	$X^*(e^{j\omega})$
$\operatorname{Re}\{x[n]\}$	$X_{\text{cs}}(e^{j\omega}) = \frac{1}{2}\{X(e^{j\omega}) + X^*(e^{-j\omega})\}$
$j\operatorname{Im}\{x[n]\}$	$X_{\text{ca}}(e^{j\omega}) = \frac{1}{2}\{X(e^{j\omega}) - X^*(e^{-j\omega})\}$
$x_{\text{cs}}[n]$	$X_{\text{re}}(e^{j\omega})$
$x_{\text{ca}}[n]$	$jX_{\text{im}}(e^{j\omega})$

Figure 4.2: DTFT symmetry relations for a complex sequence $x[n]$.

Sequence	Discrete-Time Fourier Transform
$x[n]$	$X(e^{j\omega}) = X_{\text{re}}(e^{j\omega}) + jX_{\text{im}}(e^{j\omega})$
$x_{\text{ev}}[n]$	$X_{\text{re}}(e^{j\omega})$
$x_{\text{od}}[n]$	$jX_{\text{im}}(e^{j\omega})$
Symmetry relations	
$X(e^{j\omega}) = X^*(e^{-j\omega})$	
$X_{\text{re}}(e^{j\omega}) = X_{\text{re}}(e^{-j\omega})$	
$X_{\text{im}}(e^{j\omega}) = -X_{\text{im}}(e^{-j\omega})$	
$ X(e^{j\omega}) = X(e^{-j\omega}) $	
$\arg\{X(e^{j\omega})\} = -\arg\{X(e^{-j\omega})\}$	

Figure 4.3: DTFT symmetry realtions for a real sequence $x[n]$.**Example 7: DTFT properties**

We determine the DTFT $Y(e^{j\omega})$ of:

$$y[n] = (n+1)\alpha^n \mu[n], \quad |\alpha| < 1 \quad (4.43)$$

Let $x[n] = \alpha^n \mu[n]$, with $\alpha < 1$. We can therefore write:

$$y[n] = nx[n] + x[n] \quad (4.44)$$

The DTFT of $x[n]$ is given by:

$$X(e^{j\omega}) = \frac{1}{1 - \alpha e^{-j\omega}} \quad (4.45)$$

Using the differentiation property of the DTFT, we observe that the DTFT of $nx[n]$ is given by:

$$j \frac{dX(e^{j\omega})}{d\omega} = j \frac{d}{d\omega} \left(\frac{1}{1 - \alpha e^{-j\omega}} \right) = \frac{\alpha e^{-j\omega}}{(1 - \alpha e^{-j\omega})^2} \quad (4.46)$$

Type of Property	Sequence	Discrete-Time Fourier Transform
	$g[n]$ $h[n]$	$G(e^{j\omega})$ $H(e^{j\omega})$
Linearity	$\alpha g[n] + \beta h[n]$	$\alpha G(e^{j\omega}) + \beta H(e^{j\omega})$
Time-shifting	$g[n - n_0]$	$e^{-j\omega n_0} G(e^{j\omega})$
Frequency-shifting	$e^{j\omega_0 n} g[n]$	$G(e^{j(\omega - \omega_0)})$
Differentiation in frequency	$ng[n]$	$j \frac{dG(e^{j\omega})}{d\omega}$
Convolution	$g[n] \circledast h[n]$	$G(e^{j\omega}) H(e^{j\omega})$
Modulation	$g[n]h[n]$	$\frac{1}{2\pi} \int_{-\pi}^{\pi} G(e^{j\theta}) H(e^{j(\omega - \theta)}) d\theta$
Parseval's relation	$\sum_{n=-\infty}^{\infty} g[n]h^*[n]$	$\frac{1}{2\pi} \int_{-\pi}^{\pi} G(e^{j\omega}) H^*(e^{j\omega}) d\omega$

Figure 4.4: DTFT general properties.

Next, using the linearity property of the DTFT, we arrive at:

$$Y(e^{j\omega}) = \frac{\alpha e^{-j\omega}}{(1 - \alpha e^{-j\omega})^2} + \frac{1}{1 - \alpha e^{-j\omega}} = \frac{1}{(1 - \alpha e^{-j\omega})^2} \quad (4.47)$$

Example 8: DTFT properties

We determine the DTFT $V(e^{j\omega})$ of the sequence $v[n]$, defined by:

$$d_0 v[n] + d_1 v[n - 1] = p_0 \delta[n] + p_1 \delta[n - 1] \quad (4.48)$$

The DTFT of $\delta[n]$ is 1. Using the time-shifting property of the DTFT, we observe that the DTFT of $\delta[n-1]$ is $e^{-j\omega}$ and the DTFT of $v[n-1]$ is $e^{-j\omega} V(e^{j\omega})$. Using the linearity property we then obtain the frequency-domain representation of $d_0 v[n] + d_1 v[n - 1]$ as:

$$d_0 V(e^{j\omega}) + d_1 e^{-j\omega} V(e^{j\omega}) = p_0 + p_1 e^{-j\omega} \quad (4.49)$$

Solving the above equation we get:

$$V(e^{j\omega}) = \frac{p_0 + p_1 e^{-j\omega}}{d_0 + d_1 e^{-j\omega}} \quad (4.50)$$

4.1.5 Energy density spectrum

The total energy of a finite-energy sequence $g[n]$ is given by:

$$E_g = \sum_{n=-\infty}^{\infty} |g[n]|^2 \quad (4.51)$$

From Parseval's relation we observe that:

$$E_g = \sum_{n=-\infty}^{\infty} |g[n]|^2 = \frac{1}{2\pi} \int_{-\pi}^{\pi} |G(e^{j\omega})|^2 d\omega \quad (4.52)$$

The quantity:

$$S_{gg}(\omega) = |G(e^{j\omega})|^2 \quad (4.53)$$

is called the energy density spectrum. The area under this curve in the range $-\pi \leq \omega \leq \pi$ divided by 2π is the energy of the sequence.

4.1.6 Band-limited discrete-time signals

Since the spectrum of a discrete-time signal is a periodic function of ω with a period 2π , a full-band signal has a spectrum occupying the frequency range $-\pi \leq \omega \leq \pi$. A band-limited discrete-time signal has a spectrum that is limited to a portion of the frequency range $-\pi \leq \omega \leq \pi$.

An ideal band-limited signal has a spectrum that is zero outside a frequency range $0 < \omega_a \leq |\omega| \leq \omega_b < \pi$, that is:

$$X(e^{j\omega}) = \begin{cases} 0 & 0 \leq |\omega| < \omega_a \\ 0 & \omega_b < |\omega| < \pi \end{cases} \quad (4.54)$$

However, an ideal band-limited discrete-time signal cannot be generated in practice. A classification of a band-limited discrete-time signal is based on the frequency range where most of the signal energy is concentrated. A lowpass discrete-time real signal has a spectrum occupying the frequency range $0 < |\omega| \leq \omega_p < \pi$ and has a bandwidth of ω_p .

A highpass discrete-time real signal has a spectrum occupying the frequency range $0 < \omega_p \leq |\omega| < \pi$ and has a bandwidth of $\pi - \omega_p$.

A bandpass discrete-time real signal has a spectrum occupying the frequency range $0 < \omega_L \leq |\omega| \leq \omega_H < \pi$ and has a bandwidth of $\omega_H - \omega_L$.

Example 9: Band-limited discrete-time signals

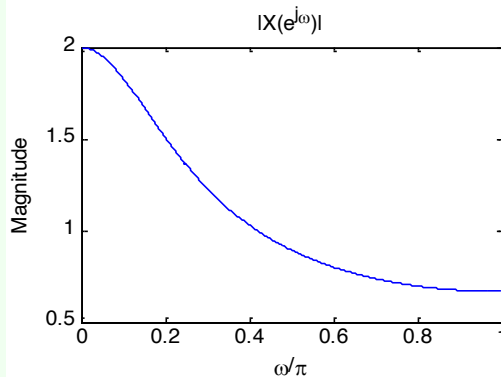
Consider the sequence:

$$x[n] = (0.5)^n \mu[n] \quad (4.55)$$

The DTFT is:

$$X(e^{j\omega}) = \frac{1}{1 - 0.5e^{-j\omega}} \quad (4.56)$$

and the magnitude spectrum is showed below.



It can be showed that 80% of the energy of this lowpass signal is contained in the frequency range $0 \leq |\omega| \leq 0.5081\pi$. Hence, we can define the 80% bandwidth to be 0.5081π radians.

Returning to the energy density spectrum, we consider some other examples introducing also the concept of band-limited signals.

Example 10: Energy density spectrum

We compute the energy of the sequence:

$$h_{LP}[n] = \frac{\sin(\omega_c n)}{\pi n}, \quad -\infty < n < \infty \quad (4.57)$$

Here:

$$\sum_{n=-\infty}^{\infty} |h_{LP}[n]|^2 = \frac{1}{2\pi} \int_{-\pi}^{\pi} |H_{LP}(e^{j\omega})|^2 d\omega \quad (4.58)$$

where:

$$H_{LP}(e^{j\omega}) = \begin{cases} 1 & 0 \leq |\omega| \leq \omega_c \\ 0 & \omega_c < |\omega| \leq \pi \end{cases} \quad (4.59)$$

Therefore:

$$\sum_{n=-\infty}^{\infty} |h_{LP}[n]|^2 = \frac{1}{2\pi} \int_{-\omega_c}^{\omega_c} d\omega = \frac{\omega_c}{\pi} < \infty \quad (4.60)$$

Hence, $h_{LP}[n]$ is a finite-energy lowpass sequence.

4.2 Linear convolution using DTFT

An important property of the DTFT is given by the convolution theorem. It states that if $y[n] = x[n] * h[n]$, then the DTFT $Y(e^{j\omega})$ of $y[n]$ is given by:

$$Y(e^{j\omega}) = X(e^{j\omega})H(e^{j\omega}) \quad (4.61)$$

An implication of this result is that the linear convolution $y[n]$ of the sequences $x[n]$ and $h[n]$ can be performed as follows:

- compute the DTFTs $X(e^{j\omega})$ and $H(e^{j\omega})$ of the sequences $x[n]$ and $h[n]$, respectively;
- form the DTFT $Y(e^{j\omega}) = X(e^{j\omega})H(e^{j\omega})$;
- compute the IDFT $y[n]$ of $Y(e^{j\omega})$.

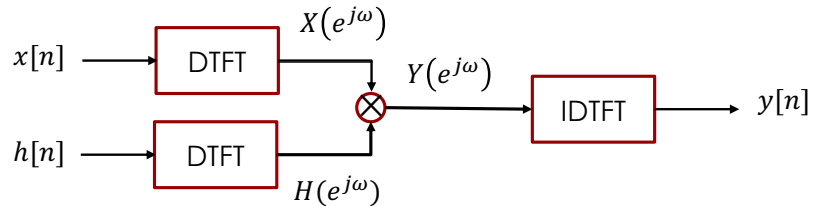


Figure 4.5: Scheme of the computation of linear convolution $y[n]$ of the sequences $x[n]$ and $h[n]$.

Note that in numerical computation, when the computed phase function is outside the range $[-\pi, \pi]$, the phase is computed modulo 2π , to bring the computed value to this range. Thus, the phase functions of some sequences exhibit discontinuities of 2π radians in the plot. For example, there is a discontinuity of 2π at $\omega = 0.72$ in the

phase response below:

$$X(e^{j\omega}) = \frac{0.008 - 0.033e^{-j\omega} + 0.05e^{-2j\omega} - 0.033e^{-3j\omega} + 0.008e^{-4j\omega}}{1 + 2.37e^{-j\omega} + 2.7e^{-2j\omega} + 1.6e^{-3j\omega} + 0.41e^{-4j\omega}} \quad (4.62)$$

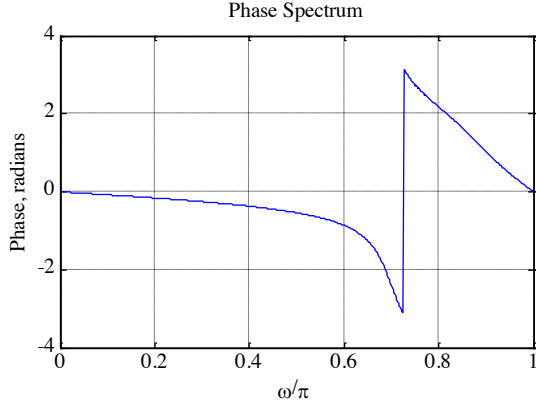


Figure 4.6: Discontinuity in the phase response of Eq. 4.62.

In such cases, often an alternate type of phase function that is continuous function of ω is derived from the original phase function by removing the discontinuities of 2π . Process of discontinuity removal is called unwrapping the phase and the unwrapped phase function will be denoted as $\theta_c(\omega)$.

For example, the unwrapped phase function of the DTFT in Eq. 4.62 is showed in Figure 4.7.

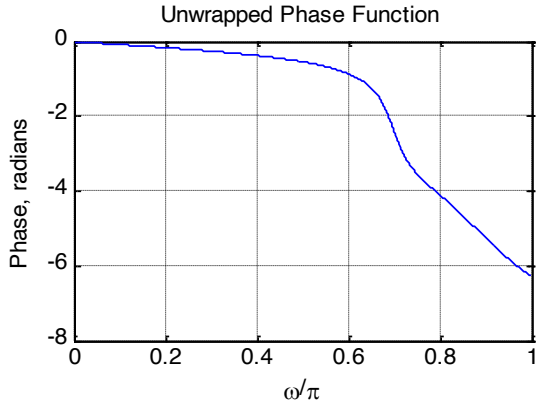


Figure 4.7: Unwrapped phase function of Eq. 4.62.

The conditions under which the phase function will be a continuous function of ω is next derived. Now consider:

$$\ln X(e^{j\omega}) = \ln |X(e^{j\omega})| + j\theta(\omega) \quad (4.63)$$

where:

$$\theta(\omega) = \arg \{X(e^{j\omega})\} \quad (4.64)$$

From $\ln X(e^{j\omega})$ we can also compute $\frac{d \ln X(e^{j\omega})}{d\omega}$:

$$\frac{d \ln X(e^{j\omega})}{d\omega} = \frac{d \ln |X(e^{j\omega})|}{d\omega} + j \frac{d\theta(\omega)}{d\omega} \quad (4.65)$$

Thus, $\frac{d\theta(\omega)}{d\omega}$ is given by the imaginary part of:

$$\frac{1}{X(e^{j\omega})} \left[\frac{dX_{\text{re}}(e^{j\omega})}{d\omega} + j \frac{dX_{\text{im}}(e^{j\omega})}{d\omega} \right] \quad (4.66)$$

Hence:

$$\frac{d\theta(\omega)}{d\omega} = \frac{1}{|X(e^{j\omega})|^2} \left[X_{\text{re}}(e^{j\omega}) \frac{dX_{\text{im}}(e^{j\omega})}{d\omega} - X_{\text{im}}(e^{j\omega}) \frac{dX_{\text{re}}(e^{j\omega})}{d\omega} \right] \quad (4.67)$$

The phase function can thus be defined unequivocally by its derivative:

$$\theta(\omega) = \int_0^\omega \left[\frac{d\theta(\eta)}{d\eta} \right] d\eta \quad (4.68)$$

with the constraint $\theta(0) = 0$.

The phase function defined by Eq. 4.68 is called the unwrapped phase function of $X(e^{j\omega})$ and it is a continuous function of ω . Therefore, $\ln X(e^{j\omega})$ exists. Moreover, the phase function will be an odd function of ω if:

$$\frac{1}{\pi} \int_0^{2\pi} \left[\frac{d\theta(\eta)}{d\eta} \right] d\eta = 0 \quad (4.69)$$

If the above constraint is not satisfied, then the computed phase function will exhibit absolute jumps greater than π .

4.3 The frequency response

Most discrete-time signals encountered in practice can be represented as a linear combination of a very large, maybe infinite, number of sinusoidal discrete-time signals of different angular frequencies. Thus, knowing the response of the LTI system to a single sinusoidal signal, we can determine its response to more complicated signals by making use of the superposition property.

An important property of an LTI system is that for certain types of input signals, called eigen functions, the output signal is the input signal multiplied by a complex constant. We consider here one such eigen function as the input.

Consider the LTI discrete-time system with an impulse response $\{h[n]\}$. Its input-output relationship in the time-domain is given by the convolution sum:

$$y[n] = \sum_{k=-\infty}^{\infty} h[k]x[n-k] \quad (4.70)$$

If the input is of the form:

$$x[n] = e^{j\omega n}, \quad -\infty < n < \infty \quad (4.71)$$

then it follows that the output is given by:

$$y[n] = \sum_{k=-\infty}^{\infty} h[k]x[n-k] = \left(\sum_{k=-\infty}^{\infty} h[k]e^{-j\omega k} \right) e^{j\omega n} \quad (4.72)$$

Now, let:

$$H(e^{j\omega}) = \sum_{k=-\infty}^{\infty} h[k]e^{-j\omega k} \quad (4.73)$$

Then we can write:

$$y[n] = H(e^{j\omega})e^{j\omega n} \quad (4.74)$$

Thus for a complex exponential input signal $e^{j\omega n}$, the output of an LTI discrete-time system is also a complex exponential signal of the same frequency multiplied by a complex constant $H(e^{j\omega})$. Thus $e^{j\omega n}$ is an eigen function of the system.

The quantity $H(e^{j\omega})$ is called the frequency response of the LTI discrete-time system. $H(e^{j\omega})$ provides a frequency-domain description of the system and is precisely the DTFT of the impulse response $\{h[n]\}$ of the system. $H(e^{j\omega})$, in general, is a complex function of ω with a period 2π . It can be expressed in terms of its real and imaginary parts:

$$H(e^{j\omega}) = H_{\text{re}}(e^{j\omega}) + jH_{\text{im}}(e^{j\omega}) \quad (4.75)$$

or, in terms of its magnitude and phase:

$$H(e^{j\omega}) = |H(e^{j\omega})|e^{j\theta(\omega)} \quad (4.76)$$

where:

$$\theta(\omega) = \arg\{H(e^{j\omega})\} \quad (4.77)$$

The function $|H(e^{j\omega})|$ is called the magnitude response and the function $\theta(\omega)$ is called the phase response of the LTI discrete-time system. Design specifications for the LTI discrete-time system, in many applications, are given in terms of the magnitude response or the phase response or both.

In some cases, the magnitude function is specified in decibels as:

$$g(\omega) = 20 \log_{10} |H(e^{j\omega})| \text{dB} \quad (4.78)$$

where $G(\omega)$ is called the gain function. The negative of the gain function $A(\omega) = -G(\omega)$ is called the attenuation or loss function.

Note that magnitude and phase functions are real functions of ω , whereas the frequency response is a complex function of ω . If the impulse response $h[n]$ is real then it follows that the magnitude function is an even function of ω :

$$|H(e^{j\omega})| = |H(e^{-j\omega})| \quad (4.79)$$

and the phase function is an odd function of ω :

$$\theta(\omega) = -\theta(-\omega) \quad (4.80)$$

Likewise, for a real impulse response $h[n]$, $H_{\text{re}}(e^{j\omega})$ is even and $H_{\text{im}}(e^{j\omega})$ is odd.

Example 11: M-point moving average filter

Consider the M -point moving average filter with an impulse response given by:

$$h[n] = \begin{cases} \frac{1}{M} & 0 \leq n \leq M-1 \\ 0 & \text{otherwise} \end{cases} \quad (4.81)$$

Its frequency response is then given by:

$$H(e^{j\omega}) = \frac{1}{M} \sum_{n=0}^{M-1} e^{-j\omega n} \quad (4.82)$$

Performing all the calculations:

$$\begin{aligned}
 H(e^{j\omega}) &= \frac{1}{M} \left(\sum_{n=0}^{\infty} e^{-j\omega n} - \sum_{n=M}^{\infty} e^{-j\omega n} \right) \\
 &= \frac{1}{M} \left(\sum_{n=0}^{\infty} e^{-j\omega n} \right) (1 - e^{-jM\omega}) \\
 &= \frac{1}{M} \frac{1 - e^{-jM\omega}}{1 - e^{-j\omega}} \\
 &= \frac{1}{M} \frac{\sin(\frac{M\omega}{2})}{\sin(\frac{\omega}{2})} e^{-j\frac{(M-1)\omega}{2}}
 \end{aligned} \tag{4.83}$$

Thus, the magnitude response of the M -point moving average filter is given by:

$$|H(e^{j\omega})| = \left| \frac{1}{M} \frac{\sin(\frac{M\omega}{2})}{\sin(\frac{\omega}{2})} \right| \tag{4.84}$$

and the phase response is given by

$$\theta(\omega) = -\frac{(M-1)\omega}{2} + \pi \sum_{k=1}^{\lfloor \frac{M}{2} \rfloor} \mu \left[\omega - \frac{2\pi k}{M} \right] \tag{4.85}$$

Note that the frequency response also determines the steady-state response of an LTI discrete-time system to a sinusoidal input.

Example 12: Steady-state response

We determine the steady-state output $y[n]$ of a real coefficient LTI discrete-time system with a frequency response $H(e^{j\omega})$ for an input:

$$x[n] = A \cos(\omega_0 n + \varphi), \quad -\infty < n < \infty \tag{4.86}$$

We can express the input $x[n]$ as:

$$x[n] = g[n] + g^*[n] \tag{4.87}$$

where:

$$g[n] = \frac{1}{2} A e^{j\varphi} e^{j\omega_0 n} \tag{4.88}$$

Now the output of the system for an input $e^{j\omega_0 n}$ is simply $H(e^{j\omega_0})e^{j\omega_0 n}$. Because of linearity, the response $v[n]$ to an input $g[n]$ is given by:

$$v[n] = \frac{1}{2} A e^{j\varphi} H(e^{j\omega_0}) e^{j\omega_0 n} \tag{4.89}$$

Likewise, the output $v^*[n]$ to the input $g^*[n]$ is:

$$v^*[n] = \frac{1}{2} A e^{-j\varphi} H(e^{-j\omega_0}) e^{-j\omega_0 n} \tag{4.90}$$

Combining the last two equations we get:

$$\begin{aligned}
 y[n] &= v[n] + v^*[n] \\
 &= \frac{1}{2}Ae^{j\varphi}H(e^{j\omega_0})e^{j\omega_0 n} + \frac{1}{2}Ae^{-j\varphi}H(e^{-j\omega_0})e^{-j\omega_0 n} \\
 &= \frac{1}{2}A|H(e^{j\omega_0})|\left\{e^{j\theta(\omega_0)}e^{j\varphi}e^{j\omega_0 n} + e^{-j\theta(\omega_0)}e^{-j\varphi}e^{-j\omega_0 n}\right\} \\
 &= A|H(e^{j\omega_0})|\cos(\omega_0 n + \theta(\omega_0) + \varphi)
 \end{aligned} \tag{4.91}$$

Thus, the output $y[n]$ has the same sinusoidal waveform as the input with two differences:

- the amplitude is multiplied by $|H(e^{j\omega_0})|$, the value of the magnitude function at $\omega = \omega_0$;
- the output has a phase lag relative to the input by an amount $\theta(\omega_0)$, the value of the phase function at $\omega = \omega_0$.

The expression for the steady-state response developed earlier assumes that the system is initially relaxed before the application of the input $x[n]$. In practice, excitation $x[n]$ to a discrete-time system is usually a right-sided sequence applied at some sample index $n = n_0$. Now, we develop the expression for the output for such an input.

Without any loss of generality, assume $x[n] = 0$ for $n < 0$. From the input-output relation in Eq. 4.70, we observe that for an input:

$$x[n] = e^{j\omega n} \mu[n] \tag{4.92}$$

the output is given by:

$$y[n] = \left(\sum_{k=-\infty}^{\infty} h[k]e^{j\omega(n-k)} \right) \mu[n] = \left(\sum_{k=-\infty}^{\infty} h[k]e^{-j\omega k} \right) e^{j\omega n} \mu[n] \tag{4.93}$$

The output for $n < 0$ is $y[n] = 0$, while for $n \geq 0$ it is given by:

$$\begin{aligned}
 y[n] &= \left(\sum_{k=0}^{\infty} h[k]e^{-j\omega k} \right) e^{j\omega n} - \left(\sum_{k=n+1}^{\infty} h[k]e^{-j\omega k} \right) e^{j\omega n} \\
 &= H(e^{j\omega})e^{j\omega n} - \left(\sum_{k=n+1}^{\infty} h[k]e^{-j\omega k} \right) e^{j\omega n}
 \end{aligned} \tag{4.94}$$

The first term on the RHS is the same as that obtained when the input is applied at $n = 0$ to an initially relaxed system and it is the steady-state response:

$$y_{\text{sr}}[n] = H(e^{j\omega})e^{j\omega n} \tag{4.95}$$

The second term on the RHS is called the transient response:

$$y_{\text{tr}}[n] = - \left(\sum_{k=n+1}^{\infty} h[k]e^{-j\omega k} \right) e^{j\omega n} \tag{4.96}$$

To determine the effect of the above term on the total output response, we observe:

$$|y_{\text{tr}}[n]| = \left| \sum_{k=n+1}^{\infty} h[k]e^{-j\omega(k-n)} \right| \leq \sum_{k=n+1}^{\infty} |h[k]| \leq \sum_{k=0}^{\infty} |h[k]| \tag{4.97}$$

For a causal, stable LTI IIR discrete-time system, $h[n]$ is absolutely summable. As a result, the transient response $y_{\text{tr}}[n]$ is a bounded sequence. Moreover, as $n \rightarrow \infty$:

$$\sum_{k=n+1}^{\infty} |h[k]| \rightarrow 0 \quad (4.98)$$

and hence, the transient response decays to zero as n gets very large.

For a causal FIR LTI discrete-time system with an impulse response $h[n]$ of length $N + 1$, $h[n] = 0$ for $n > N$. Hence, $y_{\text{tr}}[n] = 0$ for $n > N - 1$. Here the output reaches the steady-state value $y_{\text{sr}}[n] = H(e^{j\omega})e^{j\omega n}$ at $n = N$.

4.4 The concept of filtering

One application of an LTI discrete-time system is to pass certain frequency components in an input sequence without any distortion (if possible) and to block other frequency components. Such systems are called digital filters and one of the main subjects of discussion in this course.

The key to the filtering process is the Fourier transform

$$x[n] = \frac{1}{2\pi} \int_{-\pi}^{\pi} H(e^{j\omega}) e^{j\omega n} d\omega \quad (4.99)$$

It expresses an arbitrary input as a linear weighted sum of an infinite number of exponential sequences, or equivalently, as a linear weighted sum of sinusoidal sequences. Thus, by appropriately choosing the values of the magnitude function $|H(e^{j\omega})|$ of the LTI digital filter at frequencies corresponding to the frequencies of the sinusoidal components of the input, some of these components can be selectively heavily attenuated or filtered with respect to the others.

To understand the mechanism behind the design of frequency-selective filters, consider a real-coefficient LTI discrete-time system characterized by a magnitude function:

$$|H(e^{j\omega})| \approx \begin{cases} 1 & |\omega| \leq \omega_c \\ 0 & \omega_c < |\omega| \leq \pi \end{cases} \quad (4.100)$$

We apply to the system an input:

$$x[n] = A \cos(\omega_1 n) + B \cos(\omega_2 n), \quad 0 < \omega_1 < \omega_c < \omega_2 < \pi \quad (4.101)$$

Because of linearity, the output of this system is of the form:

$$y[n] = A |H(e^{j\omega_1})| \cos(\omega_1 n + \theta(\omega_1)) + B |H(e^{j\omega_2})| \cos(\omega_2 n + \theta(\omega_2)) \quad (4.102)$$

As $|H(e^{j\omega_1})| \approx 1$ and $|H(e^{j\omega_2})| \approx 0$, the output reduces to:

$$y[n] \approx A |H(e^{j\omega_1})| \cos(\omega_1 n + \theta(\omega_1)) \quad (4.103)$$

Thus, the system acts like a lowpass filter.

Now we consider an example of design of a very simple digital filter.

Example 13: Design of a simple digital filter

The input consists of a sum of two sinusoidal sequences of angular frequencies 0.1 rad/sample and 0.4 rad/sample. We need to design a highpass filter that will pass the high-frequency component of the input but block the low-frequency component.

For simplicity, assume the filter to be an FIR filter of length 3 with an impulse response:

$$h[0] = h[2] = \alpha \quad (4.104)$$

$$h[1] = \beta \quad (4.105)$$

The convolution sum description of this filter is then given by:

$$\begin{aligned} y[n] &= h[0]x[n]h[1]x[n-1] + h[2]x[n-2] \\ &= \alpha x[n] + \beta x[n-1] + \alpha x[n-2] \end{aligned} \quad (4.106)$$

$y[n]$ and $x[n]$ are, respectively, the output and the input sequences.

The design objective is to choose suitable values of α and β so that the output is a sinusoidal sequence with a frequency of 0.4 rad/sample.

Now, the frequency response of the FIR filter is given by:

$$\begin{aligned} H(e^{j\omega}) &= h[0] + h[1]e^{-j\omega} + h[2]e^{-j2\omega} \\ &= \alpha(1 + e^{-j2\omega}) + \beta e^{-j\omega} \\ &= 2\alpha \left(\frac{e^{j\omega} + e^{-j\omega}}{2} \right) e^{-j\omega} + \beta e^{-j\omega} \\ &= (2\alpha \cos \omega + \beta) e^{-j\omega} \end{aligned} \quad (4.107)$$

The magnitude and phase functions are:

$$|H(e^{j\omega})| = 2\alpha \cos \omega + \beta \quad (4.108)$$

$$\theta(\omega) = -\omega \quad (4.109)$$

In order to block the low-frequency component, the magnitude function at $\omega = 0.1$ should be equal to zero. Likewise, to pass the high-frequency component, the magnitude function at $\omega = 0.4$ should be equal to one. Thus, the two conditions that must be satisfied are:

$$|H(e^{j0.1})| = 2\alpha \cos(0.1) + \beta = 0 \quad (4.110)$$

$$|H(e^{j0.4})| = 2\alpha \cos(0.4) + \beta = 1 \quad (4.111)$$

Solving the above two equations we get:

$$\alpha = -6.76195 \quad (4.112)$$

$$\beta = 13.456335 \quad (4.113)$$

$$(4.114)$$

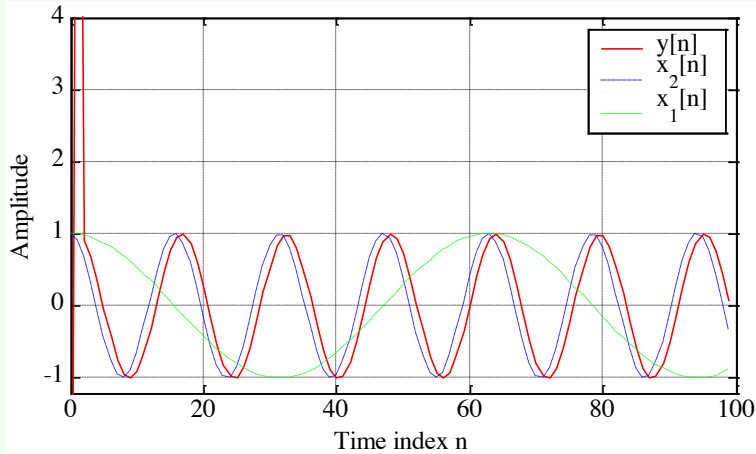
Thus the output-input relation of the FIR filter is given by:

$$y[n] = -6.76195(x[n] + x[n-2]) + 13.456335x[n-1] \quad (4.115)$$

where the input is:

$$x[n] = \{\cos(0.1n) + \cos(0.4n)\}\mu[n] \quad (4.116)$$

A plot of the signals of interests is showed below.



The first seven samples of the output are showed below as well.

n	$\cos(0.1n)$	$\cos(0.4n)$	$x[n]$	$y[n]$
0	1.0	1.0	2.0	-13.52390
1	0.9950041	0.9210609	1.9160652	13.956333
2	0.9800665	0.6967067	1.6767733	0.9210616
3	0.9553364	0.3623577	1.3176942	0.6967064
4	0.9210609	-0.0291995	0.8918614	0.3623572
5	0.8775825	-0.4161468	0.4614357	-0.0292002
6	0.8253356	-0.7373937	0.0879419	-0.4161467

From this table, it can be seen that, neglecting the least significant digit:

$$y[n] = \cos(0.4(n-1)), \quad n \geq 2 \quad (4.117)$$

Computation of the present value of the output requires the knowledge of the present and two previous input samples. Hence, the first two output samples, $y[0]$ and $y[1]$, are the result of assumed zero input sample values at $n = -1$ and $n = -2$. Therefore, first two output samples constitute the transient part of the output. Since the impulse response is of length 3, the steady-state is reached at $n = N = 2$. Note also that the output is delayed version of the high-frequency component $\cos(0.4n)$ of the input, and the delay is one sample period.

Lecture 12.
Thursday 5th
November, 2020.

4.5 Discrete Fourier Transform

We have discussed the DTFT for a discrete-time function given by:

$$X(e^{j\omega}) = \sum_{n=-\infty}^{\infty} x[n]e^{-j\omega n} \quad (4.118)$$

and the IDTFT:

$$x[n] = \frac{1}{2\pi} \int_{-\pi}^{\pi} X(e^{j\omega})e^{j\omega n} d\omega \quad (4.119)$$

The pair and their properties and applications have some limitations. The input signal is usually aperiodic and may be finite in length.

Moreover, we often do not have an infinite amount of data which is required by DTFT. For example in a computer we cannot calculate uncountable infinite (continuum) of

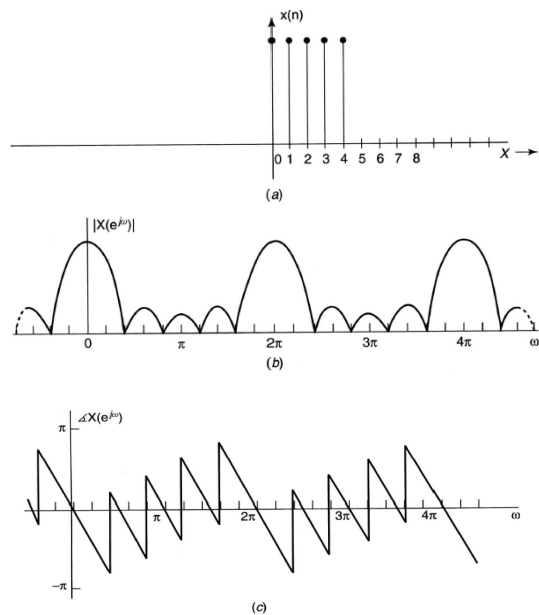


Figure 4.8: In order from top to bottom, a finite-length signal, its magnitude spectrum, its phase spectrum.

frequencies as required by DTFT. Thus, we use DTF to look at finite segment of data. We only observe the data through a window:

$$x_0[n] = x[n]w_R[n] \quad (4.120)$$

$$w_R[n] = \begin{cases} 1 & n = 0, 1, \dots, N-1 \\ 0 & \text{otherwise} \end{cases} \quad (4.121)$$

In this case, the $x_0[n]$ is just a sampled data between $n = 0, n = N-1$ (so, N points). The solution to our problems is given by the Discrete Fourier Transform (DFT).

Definition 4: Discrete Fourier Transform (DFT)

The simplest relation between a length- N sequence $x[n]$, defined for $0 \leq n \leq N-1$, and its DTFT $X(e^{j\omega})$ is obtained by uniformly sampling on the ω -axis between $0 \leq \omega \leq 2\pi$ at $\omega_k = \frac{2\pi k}{N}$, for $0 \leq k \leq N-1$. From the definition of the DTFT we thus have:

$$X[k] = [X(e^{j\omega})]_{\omega=\frac{2\pi k}{N}} = \sum_{n=0}^{N-1} x[n]e^{-j2\pi k \frac{n}{N}} \quad (4.122)$$

Note that $X[k]$ is also a length- N sequence in the frequency domain and it is called the Discrete Fourier Transform (DFT) of the sequence $x[n]$. Using the notation $W_N = e^{-j\frac{2\pi}{N}}$, the DFT is usually expressed as:

$$X[k] = \sum_{n=0}^{N-1} x[n]W_N^{kn}, \quad 0 \leq k \leq N-1 \quad (4.123)$$

Definition 5: Inverse Discrete Fourier Transform (IDFT)

The Inverse Discrete Fourier Transform (IDFT) is given by:

$$x[n] = \frac{1}{N} \sum_{k=0}^{N-1} X[k] W_N^{-kn}, \quad 0 \leq n \leq N-1 \quad (4.124)$$

To verify the above expression we multiply both sides of the above equation by $W_N^{\ell n}$ and sum the result from $n = 0$ to $n = N - 1$, resulting in:

$$\begin{aligned} \sum_{n=0}^{N-1} x[n] W_N^{\ell n} &= \sum_{n=0}^{N-1} \left(\frac{1}{N} \sum_{k=0}^{N-1} X[k] W_N^{-kn} \right) W_N^{\ell n} \\ &= \frac{1}{N} \sum_{n=0}^{N-1} \sum_{k=0}^{N-1} X[k] W_N^{-(k-\ell)n} \\ &= \frac{1}{N} \sum_{k=0}^{N-1} \sum_{n=0}^{N-1} X[k] W_N^{-(k-\ell)n} \end{aligned} \quad (4.125)$$

Making use of the identity:

$$\sum_{n=0}^{N-1} W_N^{-(k-\ell)n} = \begin{cases} N & k - \ell = rN, \quad n \in \mathbb{Z} \\ 0 & \text{otherwise} \end{cases} \quad (4.126)$$

we observe that the right-hand-side of the last equation is equal to $X[\ell]$. Hence:

$$\sum_{n=0}^{N-1} x[n] W_N^{\ell n} = X[\ell] \quad (4.127)$$

Example 14: Discrete Fourier Transform

Consider the length- N sequence:

$$x[n] = \begin{cases} 1 & n = 0 \\ 0 & 1 \leq n \leq N-1 \end{cases} \quad (4.128)$$

Its N -point DFT is given by:

$$X[k] = \sum_{n=0}^{N-1} x[n] W_N^{kn} = x[0] W_N^0 = 1 \quad (4.129)$$

with $0 \leq k \leq N-1$.

Example 15: Discrete Fourier Transform

Consider the length- N sequence:

$$y[n] = \begin{cases} 1 & n = m \\ 0 & 0 \leq n \leq m-1, \quad m+1 \leq n \leq N-1 \end{cases} \quad (4.130)$$

Its N -point DFT is given by:

$$Y[k] = \sum_{n=0}^{N-1} y[n] W_N^{kn} = y[m] W_N^{km} = W_N^{km} \quad (4.131)$$

with $0 \leq k \leq N - 1$.

Example 16: Discrete Fourier Transform

Consider the length- N sequence defined for $0 \leq n \leq N - 1$:

$$g[n] = \cos\left(\frac{2\pi rn}{N}\right), \quad 0 \leq r \leq N - 1 \quad (4.132)$$

Using trigonometric identities, we can rewrite:

$$g[n] = \frac{1}{2} \left(e^{j2\pi r \frac{n}{N}} + e^{-j2\pi r \frac{n}{N}} \right) = \frac{1}{2} (W_N^{-rn} + W_N^{rn}) \quad (4.133)$$

The N -point DFT of $g[n]$ is thus given by:

$$G[k] = \sum_{n=0}^{N-1} g[n] W_N^{kn} = \frac{1}{2} \left(\sum_{n=0}^{N-1} W_N^{-(r-k)n} + \sum_{n=0}^{N-1} W_N^{(r+k)n} \right) \quad (4.134)$$

with $0 \leq k \leq N - 1$. Making use of the identity:

$$\sum_{n=0}^{N-1} W_N^{-(k-\ell)n} = \begin{cases} N & k - \ell = rN, \quad r \in \mathbb{Z} \\ 0 & \text{otherwise} \end{cases} \quad (4.135)$$

we get:

$$\begin{cases} \frac{N}{2} & k = r \\ \frac{N}{2} & k = N - r \\ 0 & \text{otherwise} \end{cases} \quad (4.136)$$

with $0 \leq k \leq N - 1$.

4.5.1 Matrix relations

The DFT samples defined by:

$$X[k] = \sum_{n=0}^{N-1} x[n] W_N^{kn}, \quad 0 \leq k \leq N - 1 \quad (4.137)$$

can be expressed in matrix form as:

$$\mathbf{X} = \mathbf{D}_N \mathbf{x} \quad (4.138)$$

where:

$$\mathbf{X} = [X[0] \ X[1] \ \dots \ X[N - 1]]^T \quad (4.139)$$

$$\mathbf{x} = [x[0] \ x[1] \ \dots \ x[N - 1]]^T \quad (4.140)$$

and \mathbf{D}_N is the $N \times N$ DFT matrix given by:

$$\mathbf{D}_N = \begin{bmatrix} 1 & 1 & 1 & \dots & 1 \\ 1 & W_N^1 & W_N^2 & \dots & W_N^{(N-1)} \\ 1 & W_N^2 & W_N^4 & \dots & W_N^{2(N-1)} \\ \vdots & \vdots & \vdots & \ddots & \vdots \\ 1 & W_N^{(N-1)} & W_N^{2(N-1)} & \dots & W_N^{(N-1)^2} \end{bmatrix} \quad (4.141)$$

Likewise, the IDFT relation given by:

$$x[n] = \frac{1}{N} \sum_{k=0}^{N-1} X[k] W_N^{-kn}, \quad 0 \leq n \leq N-1 \quad (4.142)$$

can be expressed in matrix form as:

$$\mathbf{x} = \mathbf{D}_N^{-1} \mathbf{X} \quad (4.143)$$

where \mathbf{D}_N^{-1} is the $N \times N$ IDFT matrix, given by:

$$\mathbf{D}_N^{-1} = \begin{bmatrix} 1 & 1 & 1 & \cdots & 1 \\ 1 & W_N^{-1} & W_N^{-2} & \cdots & W_N^{-(N-1)} \\ 1 & W_N^{-2} & W_N^{-4} & \cdots & W_N^{-2(N-1)} \\ \vdots & \vdots & \vdots & \ddots & \vdots \\ 1 & W_N^{-(N-1)} & W_N^{-2(N-1)} & \cdots & W_N^{-(N-1)^2} \end{bmatrix} = \frac{1}{N} \mathbf{D}_N^* \quad (4.144)$$

4.5.2 DTFT from DFT by interpolation

The N -point DFT $X[k]$ of a length- N sequence $x[n]$ is simply the frequency samples of its DTFT $X(e^{j\omega})$ evaluated at N uniformly spaced frequency points:

$$\omega = \omega_k = \frac{2\pi k}{N}, \quad 0 \leq k \leq N-1 \quad (4.145)$$

Given the N -point DFT $X[k]$ of a length- N sequence $x[n]$, its DTFT $X(e^{j\omega})$ can be uniquely determined from $X[k]$. Thus:

$$\begin{aligned} X(e^{j\omega}) &= \sum_{n=0}^{N-1} x[n] e^{-j\omega n} \\ &= \sum_{n=0}^{N-1} \left[\frac{1}{N} \sum_{k=0}^{N-1} X[k] W_N^{-kn} \right] e^{-j\omega n} \\ &= \frac{1}{N} \sum_{k=0}^{N-1} X[k] \underbrace{\sum_{n=0}^{N-1} e^{-j(\omega - \frac{2\pi k}{N})n}}_S \end{aligned} \quad (4.146)$$

To develop a compact expression for the sum S , let $r = e^{-j(\omega - \frac{2\pi k}{N})}$. Then:

$$S = \sum_{n=0}^{N-1} r^n \quad (4.147)$$

From the above:

$$\begin{aligned} rS &= \sum_{n=1}^N r^n = 1 + \sum_{n=1}^{N-1} r^n r^N - 1 \\ &= \sum_{n=0}^{N-1} r^n + r^N - 1 = S + r^N - 1 \end{aligned} \quad (4.148)$$

or, equivalently:

$$S - rS = (1 - r)S = 1 - r^N \quad (4.149)$$

Hence:

$$\begin{aligned} S &= \frac{1 - r^N}{1 - r} \\ &= \frac{1 - e^{-j(\omega n - 2\pi k)}}{1 - e^{-j(\omega - \frac{2\pi k}{N})}} \\ &= \frac{\sin\left(\frac{\omega N 2\pi k}{2}\right)}{\sin\left(\frac{\omega N - 2\pi k}{2N}\right)} e^{-j\left(\frac{\omega - 2\pi k}{N}\right)\left(\frac{N-1}{2}\right)} \end{aligned} \quad (4.150)$$

Therefore:

$$X(e^{j\omega}) = \frac{1}{N} \sum_{k=0}^{N-1} X[k] \frac{\sin\left(\frac{\omega N 2\pi k}{2}\right)}{\sin\left(\frac{\omega N - 2\pi k}{2N}\right)} e^{-j\left(\frac{\omega - 2\pi k}{N}\right)\left(\frac{N-1}{2}\right)} \quad (4.151)$$

4.5.3 Sampling the DTFT

Consider a sequence $x[n]$ with a DTFT $X(e^{j\omega})$. We sample $X(e^{j\omega})$ at N equally spaced points $\omega_k = \frac{2\pi k}{N}$, $0 \leq k \leq N-1$, developing the N frequency samples $\{X(e^{j\omega_k})\}$. These N frequency samples can be considered as an N -point DFT $Y[k]$ whose N -point IDFT is a length- N sequence $y[n]$. Now:

$$X(e^{j\omega}) = \sum_{\ell=-\infty}^{\infty} x[\ell] e^{-j\omega\ell} \quad (4.152)$$

Thus:

$$Y[k] = X(e^{j\omega_k}) = X(e^{j\frac{2\pi k}{N}}) = \sum_{\ell=-\infty}^{\infty} x[\ell] e^{-j2\pi k \frac{\ell}{N}} = \sum_{\ell=-\infty}^{\infty} x[\ell] W_N^{k\ell} \quad (4.153)$$

An IDFT of $Y[k]$ yields:

$$\begin{aligned} y[n] &= \frac{1}{N} \sum_{k=0}^{N-1} Y[k] W_N^{-kn} \\ &= \frac{1}{N} \sum_{k=0}^{N-1} \sum_{\ell=-\infty}^{\infty} x[\ell] W_N^{k\ell} W_N^{-kn} \\ &= \sum_{\ell=-\infty}^{\infty} x[\ell] \left[\sum_{k=0}^{N-1} W_N^{-k(n-\ell)} \right] \\ &= \sum_{m=-\infty}^{\infty} x[n+mN] \end{aligned} \quad (4.154)$$

with $0 \leq n \leq N-1$, where in the last passage the identity in Eq. 4.135 is employed. Thus, $y[n]$ is obtained from $x[n]$ by adding an infinite number of shifted replicas of $x[n]$, with each replica shifted by an integer multiple of N sampling instants, and observing the sum only for the interval $0 \leq n \leq N-1$.

To apply the last result to finite-length sequences, we assume that the samples outside the specified range are zeros. Thus, if $x[n]$ is a length- M sequence with $M \leq N$, then $y[n] = x[n]$ for $0 \leq n \leq N-1$. If $M > N$, there is a time-domain aliasing of samples of $x[n]$ in generating $y[n]$, and $x[n]$ cannot be recovered from $y[n]$.

Example 17: Aliasing

Let $x[n] = \{0, 1, 2, 3, 4, 5\}$. By sampling its DTFT $X(e^{j\omega})$ at $\omega_k = \frac{2\pi k}{4}$, with $0 \leq k \leq 3$, and then applying a 4-point IDFT to these samples, we arrive at the sequence $y[n]$ given by:

$$y[n] = x[n] + x[n+4] + x[n-4], \quad 0 \leq n \leq 3 \quad (4.155)$$

We get $y[n] = \{4, 6, 2, 3\}$. $x[n]$ cannot be recovered from $y[n]$.

4.5.4 DFT properties

Like the DTFT, the DFT also satisfies a number of properties that are useful in signal processing applications. Some of these properties are essentially identical to those of the DTFT, while some others are somewhat different. A summary of the DFT properties are given in Figures 4.9, 4.10 and 4.11.

Length- N Sequence	N -point DFT
$x[n]$	$X[k]$
$x^*[n]$	$X^*[(-k)_N]$
$x^*[(-n)_N]$	$X^*[k]$
$\text{Re}\{x[n]\}$	$X_{\text{pcs}}[k] = \frac{1}{2}\{X[(k)_N] + X^*[(-k)_N]\}$
$j \text{Im}\{x[n]\}$	$X_{\text{pca}}[k] = \frac{1}{2}\{X[(k)_N] - X^*[(-k)_N]\}$
$x_{\text{pcs}}[n]$	$\text{Re}\{X[k]\}$
$x_{\text{pca}}[n]$	$j \text{Im}\{X[k]\}$

Note: $x_{\text{pcs}}[n]$ and $x_{\text{pca}}[n]$ are the periodic conjugate-symmetric and periodic conjugate-antisymmetric parts of $x[n]$, respectively. Likewise, $X_{\text{pcs}}[k]$ and $X_{\text{pca}}[k]$ are the periodic conjugate-symmetric and periodic conjugate-antisymmetric parts of $X[k]$, respectively.

Figure 4.9: Symmetry relations of DFT for a complex sequence $x[n]$.

Length- N Sequence	N -point DFT
$x[n]$	$X[k] = \text{Re}\{X[k]\} + j \text{Im}\{X[k]\}$
$x_{\text{pe}}[n]$	$\text{Re}\{X[k]\}$
$x_{\text{po}}[n]$	$j \text{Im}\{X[k]\}$
Symmetry relations	$\begin{aligned} X[k] &= X^*[(-k)_N] \\ \text{Re } X[k] &= \text{Re } X[(-k)_N] \\ \text{Im } X[k] &= -\text{Im } X[(-k)_N] \\ X[k] &= X[(-k)_N] \\ \arg X[k] &= -\arg X[(-k)_N] \end{aligned}$

Note: $x_{\text{pe}}[n]$ and $x_{\text{po}}[n]$ are the periodic even and periodic odd parts of $x[n]$, respectively.

Figure 4.10: Symmetry relations of DFT for a real sequence $x[n]$.

4.5.5 Circular shift of a sequence

This property is analogous to the time-shifting property of the DTFT but with a difference. Consider length- N sequences defined for $0 \leq n \leq N-1$. Sample values

Type of Property	Length- N Sequence	N -point DFT
	$\frac{g[n]}{h[n]}$	$\frac{G[k]}{H[k]}$
Linearity	$\alpha g[n] + \beta h[n]$	$\alpha G[k] + \beta H[k]$
Circular time-shifting	$g[(n - n_0)_N]$	$W_N^{kn_0} G[k]$
Circular frequency-shifting	$W_N^{-k_0 n} g[n]$	$G[\langle k - k_0 \rangle_N]$
Duality	$G[n]$	$N g[\langle -k \rangle_N]$
N -point circular convolution	$\sum_{m=0}^{N-1} g[m]h[\langle n - m \rangle_N]$	$G[k]H[k]$
Modulation	$g[n]h[n]$	$\frac{1}{N} \sum_{m=0}^{N-1} G[m]H[\langle k - m \rangle_N]$

Parseval's relation	$\sum_{n=0}^{N-1} x[n] ^2 = \frac{1}{N} \sum_{k=0}^{N-1} X[k] ^2$
---------------------	---------------------------------------------------------------------

Figure 4.11: General properties of DFT.

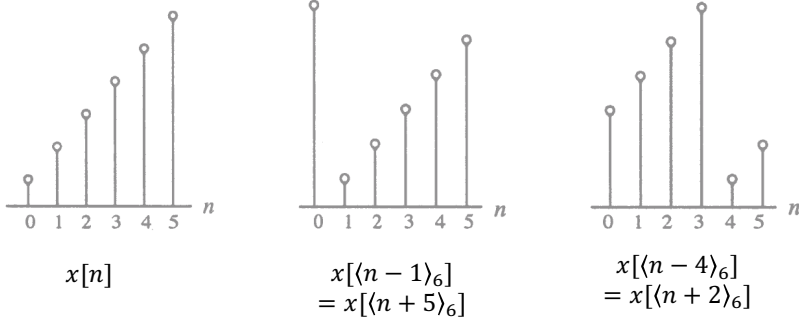
of such sequences are equal to zero for values of $n < 0$ and $n \geq N$. If $x[n]$ is such a sequence, then for any arbitrary integer n_0 , the shifted sequence $x_1[n] = x[n - n_0]$ is no longer defined for the range $0 \leq n \leq N - 1$. We thus need to define another type of shift that will always keep the shifted sequence in the range $0 \leq n \leq N - 1$. The desired shift, called the circular shift, is defined using a modulo operation:

$$x_c[n] = x[\langle n - n_0 \rangle_N] \quad (4.156)$$

For $n_0 > 0$ (right circular shift), the above equation implies:

$$x_c[n] = \begin{cases} x[n - n_0] & n_0 \leq n \leq N - 1 \\ x[N - n_0 + n] & 0 \leq n \leq n_0 \end{cases} \quad (4.157)$$

An illustration of the concept of circular shift is showed in Figure 4.12. As it is possible to observe, a right circular shift by n_0 is equivalent to a left circular shift by $N - n_0$ sample periods. A circular shift by an integer number n_0 greater than N is equivalent to a circular shift by $\langle n_0 \rangle_N$.

**Figure 4.12:** Illustration of circular shift.

4.5.6 Circular convolution

This operation is analogous to linear convolution, but with a difference. Consider two length- N sequences, $g[n]$ and $h[n]$, respectively. Their linear convolution results in a length- $(2N - 1)$ sequence $y_L[n]$ given by:

$$y_L[n] = \sum_{m=0}^{N-1} g[m]h[n - m], \quad 0 \leq n \leq 2N - 2 \quad (4.158)$$

In computing $y_L[n]$ we have assumed that both length- N sequences have been zero-padded to extend their lengths to $2N - 1$. The longer form of $y_L[n]$ results from the time-reversal of the sequence $h[n]$ and its linear shift to the right. The first nonzero value of $y_L[n]$ is $y_L[0] = g[0]h[0]$ and the last nonzero value is $y_L[2N - 2] = g[N - 1]h[N - 1]$.

To develop a convolution-like operation resulting in a length- N sequence $y_C[n]$, we need to define a circular time-reversal, and then apply a circular time-shift. Resulting operation, called a circular convolution, is defined by:

$$y_C[n] = \sum_{m=0}^{N-1} g[m]h[\langle n-m \rangle_N], \quad 0 \leq n \leq N-1 \quad (4.159)$$

Since the operation defined involves two length- N sequences, it is often referred to as an N -point circular convolution, denoted as:

Lecture 13.
Tuesday 10th
November, 2020.

4.5.7 DFT of real sequences

In most practical applications, sequences of interest are real. In such cases, the symmetry properties of the DFT can be exploited to make the DFT computations more efficient.

Let $g[n]$ and $h[n]$ be two length- N real sequences with $G[k]$ and $H[k]$ denoting their respective N -point DFTs. These two N -point DFTs can be computed efficiently using a single N -point DFT. Now, define a complex length- N sequence:

$$x[n] = g[n] + jh[n] \quad (4.160)$$

Hence, $g[n] = \text{Re}\{x[n]\}$ and $h[n] = \text{Im}\{x[n]\}$. Let $X[k]$ denote the N -point DFT of $x[n]$. Then, we arrive at:

$$G[k] = \frac{1}{2}\{X[k] + X^*[\langle -k \rangle_N]\} \quad (4.161)$$

$$H[k] = \frac{1}{2j}\{X[k] - X^*[\langle -k \rangle_N]\} \quad (4.162)$$

Note that for $0 \leq k \leq N-1$:

$$X^*[\langle -k \rangle_N] = X^*[\langle N-k \rangle_N] \quad (4.163)$$

Example 18: DFT of real sequences

We compute the 4-point DFTs of the two real sequences $g[n]$ and $h[n]$:

$$g[n] = \{1, 2, 0, 1\} \quad (4.164)$$

$$h[n] = \{2, 2, 1, 1\} \quad (4.165)$$

Then $x[n] = g[n] + jh[n]$ is given by:

$$x[n] = \{1 + j2, 2 + j2, 1 + j\} \quad (4.166)$$

Its DFT $X[k]$ is:

$$\begin{bmatrix} X[0] \\ X[1] \\ X[2] \\ X[3] \end{bmatrix} = \begin{bmatrix} 1 & 1 & 1 & 1 \\ 1 & -j & -1 & j \\ 1 & -1 & 1 & -1 \\ 1 & j & -1 & -1 \end{bmatrix} \begin{bmatrix} 1+j2 \\ 2+j2 \\ j \\ 1+j \end{bmatrix} = \begin{bmatrix} 4+j6 \\ 2 \\ -2 \\ j2 \end{bmatrix} \quad (4.167)$$

From the above:

$$X^*[k] = [4 - j6, 2, -2, -j2] \quad (4.168)$$

Hence:

$$X^*[\langle 4 - k \rangle_4] = [4 - j6, -j2, -2, 2] \quad (4.169)$$

Therefore:

$$G[k] = [4, 1 - j, -2, 1 + j] \quad (4.170)$$

$$H[k] = [6, 1 - j, 0, 1 + j] \quad (4.171)$$

verifying the results derived in Lecture 12

Now, let $v[n]$ be a length- $2N$ real sequence with a $2N$ -point DFT $V[k]$. Define two length- N real sequences $g[n]$ and $h[n]$ as follows. Let $G[k]$ and $H[k]$ denote their respective N -point DFTs:

$$\begin{cases} g[n] = v[2n] \\ h[n] = v[2n + 1] \end{cases} \quad 0 \leq n \leq N \quad (4.172)$$

We define a length- N complex sequence $x[n] = g[n] + jh[n]$ with an N -point DFT $X[k]$. Then, as showed earlier:

$$G[k] = \frac{1}{2}\{X[k] + X^*[\langle -k \rangle_N]\} \quad (4.173)$$

$$H[k] = \frac{1}{2j}\{X[k] - X^*[\langle -k \rangle_N]\} \quad (4.174)$$

Now, for $0 \leq k \leq 2N - 1$:

$$\begin{aligned} V[k] &= \sum_{n=0}^{2N-1} v[n]W_{2N}^{nk} \\ &= \sum_{n=0}^{N-1} v[2n]W_{2N}^{2nk} + \sum_{n=0}^{N-1} v[2n+1]W_{2N}^{(2n+1)k} \\ &= \sum_{n=0}^{N-1} g[n]W_N^{nk} + \sum_{n=0}^{N-1} W_N^{nk}W_{2N}^k \\ &= \sum_{n=0}^{N-1} g[n]W_N^{nk} + W_{2N}^k \sum_{n=0}^{N-1} h[n]W_N^{nk} \\ &= G[\langle k \rangle_N] + W_{2N}^k H[\langle k \rangle_N] \end{aligned} \quad (4.175)$$

Example 19: DFT of real sequences

Let us determine the 8-point DFT $V[k]$ of the length-8 real sequence:

$$v[n] = \{1, 2, 2, 2, 0, 1, 1, 1\} \quad (4.176)$$

We form two length-4 real sequences as follows:

$$g[n] = v[2n] = \{1, 2, 0, 1\} \quad (4.177)$$

$$h[n] = v[2n+1] = \{2, 2, 1, 1\} \quad (4.178)$$

Now:

$$V[k] = G[\langle k \rangle_4] + W_8^k H[\langle k \rangle_4] \quad 0 \leq k \leq 7 \quad (4.179)$$

Substituting the values of the 4-point DFTs $G[k]$ and $H[k]$ computed earlier, we get:

$$V[0] = G[0] + H[0] = 4 + 6 = 10 \quad (4.180)$$

$$V[1] = G[1] + W_1^0 H[1] = (1 - j) + e^{-j\frac{\pi}{4}}(1 - j) = 1 - j2.4142 \quad (4.181)$$

$$V[2] = G[2] + W_2^0 H[2] = -2 + e^{-j\frac{3\pi}{4}} \cdot 0 = -2 \quad (4.182)$$

$$V[3] = G[3] + W_3^0 H[3] = (1 + j) + e^{-j\frac{3\pi}{4}}(1 + j) = 1 - j0.4142 \quad (4.183)$$

$$V[4] = G[0] + W_4^0 H[0] = 4 + e^{-j\pi} \cdot 6 = -2 \quad (4.184)$$

$$V[5] = G[1] + W_5^0 H[1] = (1 - j) + e^{-j\frac{5\pi}{4}}(1 - j) = 1 + j0.4142 \quad (4.185)$$

$$V[6] = G[2] + W_6^0 H[2] = -2 + e^{-j\frac{3\pi}{2}} \cdot 0 = -2 \quad (4.186)$$

$$V[7] = G[3] + W_7^0 H[3] = (1 + j) + e^{-j\frac{7\pi}{4}}(1 + j) = 1 + j2.4142 \quad (4.187)$$

4.6 Linear convolution using the DFT

Linear convolution is a key operation in many signal processing applications. Since a DFT can be efficiently implemented using FFT algorithms, it is of interest to develop methods for the implementation of linear convolution using the DFT.

Let $g[n]$ and $h[n]$ be two finite-length sequences of length N and M , respectively. Moreover, we denote with $L = N + M + 1$. Then, we define two length- L sequences:

$$g_e[n] = \begin{cases} g[n] & 0 \leq n \leq N - 1 \\ 0 & N \leq n \leq L - 1 \end{cases} \quad (4.188)$$

$$h_e[n] = \begin{cases} h[n] & 0 \leq n \leq M - 1 \\ 0 & M \leq n \leq L - 1 \end{cases} \quad (4.189)$$

Then:

$$y_L[n] = g[n] * h[n] = y_C[n] = g_e[n] \overset{L}{*} h_e[n] \quad (4.190)$$

The corresponding implementation scheme is illustrated in Figure 4.13.

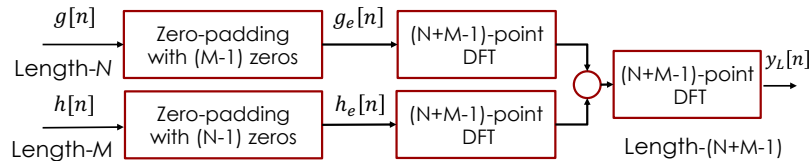


Figure 4.13: Scheme of linear convolution of two finite-length sequences.

We next consider the DFT-based implementation of:

$$y[n] = \sum_{\ell=0}^{M-1} h[\ell]x[n-\ell] = h[n] * x[n] \quad (4.191)$$

where $h[n]$ is a finite-length sequence of length M and $x[n]$ is an infinite length (or a finite length sequence of length much greater than M). We first segment $x[n]$, assumed to be a causal sequence here without any loss of generality, into a set of contiguous finite-length subsequences $x_m[n]$ of length N each:

$$x[n] = \sum_{m=0}^{\infty} x_m[n - mN] \quad (4.192)$$

where:

$$x_m[n] = \begin{cases} x[n + mN] & 0 \leq n \leq N - 1 \\ 0 & \text{otherwise} \end{cases} \quad (4.193)$$

Thus, we can write:

$$y[n] = h[n] * x[n] = \sum_{m=0}^{\infty} y_m[n - mN] \quad (4.194)$$

where:

$$y_m = h[n] * x_m[n] \quad (4.195)$$

Since $h[n]$ is of length M and $x_m[n]$ is of length N , the linear convolution $h[n] * x_m[n]$ is of length $N + M - 1$.

As a result, the desired linear convolution $y[n] = h[n] * x[n]$ has been broken up into a sum of infinite numbers of short-length linear convolutions of length $N + M - 1$ each:

$$y_m[n] = h[n] * x_m[n] \quad (4.196)$$

Each of these short convolutions can be implemented using the DFT-based method discussed earlier, where now the DFTs (and the IDFT) are computed on the basis of $N + M - 1$ points.

There is one more subtlety to take care of before we can implement:

$$y[n] = \sum_{m=0}^{\infty} y_m[n - mN] \quad (4.197)$$

using the DFT-based approach. Now the first convolution in Eq. 4.197, namely $y_0 = h[n] * x_0[n]$, is of length $N + M - 1$ and is defined for $0 \leq n \leq N + M - 2$. The second short convolution, namely $y_1[n] = h[n] * x_1[n]$, is also of length $N + M - 1$ but it is defined for $N \leq n \leq 2N + M - 2$. There is an overlap of $M - 1$ samples between these two short linear convolutions. Likewise the third short convolution, namely $y_2[n] = h[n] * x_2[n]$, is also of length $N + M - 1$ but is defined for $2N \leq n \leq 3N + M - 2$. Thus, there is an overlap of $M - 1$ samples between $h[n] * x_1[n]$ and $h[n] * x_2[n]$.

In general, there will be an overlap of $M - 1$ samples between the samples of the short convolutions $h[n] * x_{r-1}[n]$ and $h[n] * x_r[n]$ for $(r-1)N \leq n \leq rN + M - 1$. This process is illustrated in Figures 4.14 and 4.15 for $M = 5$ and $N = 7$.

Therefore, $y[n]$ obtained by a linear convolution of $x[n]$ and $h[n]$ is given by:

$$y[n] = y_0[n] \quad 0 \leq n \leq 6 \quad (4.198)$$

$$y[n] = y_0[n] + y_1[n - 7] \quad 7 \leq n \leq 10 \quad (4.199)$$

$$y[n] = y_1[n - 7] \quad 11 \leq n \leq 13 \quad (4.200)$$

$$y[n] = y_1[n - 7] + y_2[n - 14] \quad 14 \leq n \leq 17 \quad (4.201)$$

$$y[n] = y_2[n - 14] \quad 18 \leq n \leq 20 \quad (4.202)$$

$$\vdots \quad \vdots$$

The above procedure is called the overlap-add method since the results of the short linear convolutions overlap and the overlapped portions are added to get the correct final result.

In implementing the overlap-add method using the DFT, we need to compute two $(N + M - 1)$ -point DFTs and one $(N + M - 1)$ -point IDFT since the overall linear

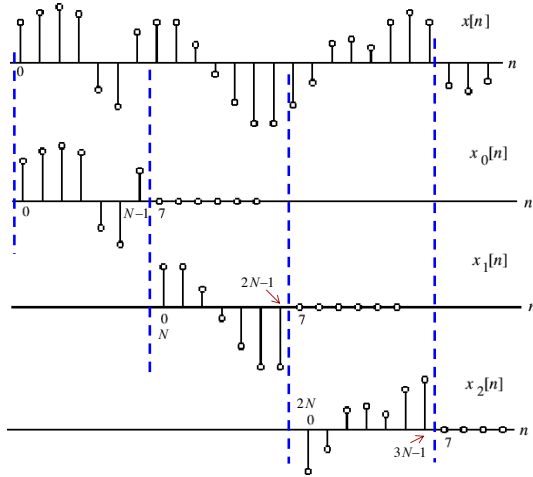


Figure 4.14: Overlap-add method for $M = 5$ and $N = 7$.

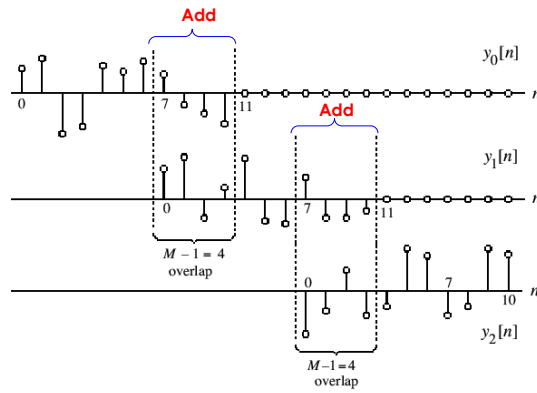


Figure 4.15: Overlap-add method for $M = 5$ and $N = 7$.

convolution was expressed as a sum of short-length linear convolutions of length $N + M - 1$ each. It is possible to implement the overall linear convolution by performing instead circular convolution of length shorter than $N + M - 1$. To this end, it is necessary to segment $x[n]$ into overlapping blocks $x_m[n]$, keep the terms of the circular convolution of $h[n]$ with $x_m[n]$ that corresponds to the terms obtained by a linear convolution of $h[n]$ and $x_m[n]$, and throw away the other parts of the circular convolution.

To understand the correspondence between the linear and circular convolutions, consider a length-4 sequence $x[n]$ and a length-3 sequence $h[n]$. Let $y_L[n]$ denote the result of a linear convolution of $x[n]$ with $h[n]$. The six samples of $y_L[n]$ are given by:

$$y_L[0] = h[0]x[0] \quad (4.203)$$

$$y_L[1] = h[0]x[1] + h[1]x[0] \quad (4.204)$$

$$y_L[2] = h[0]x[2] + h[1]x[1] + h[2]x[0] \quad (4.205)$$

$$y_L[3] = h[0]x[3] + h[1]x[2] + h[2]x[1] \quad (4.206)$$

$$y_L[4] = h[1]x[3] + h[2]x[2] \quad (4.207)$$

$$y_L[5] = h[2]x[3] \quad (4.208)$$

If we append $h[n]$ with a single zero-valued sample and convert it into a length-4

sequence $h_e[n]$, the 4-point circular convolution $y_C[n]$ of $h_e[n]$ and $x[n]$ is given by:

$$y_C[0] = h[0]x[0] + h[1]x[3] + h[2]x[2] \quad (4.209)$$

$$y_C[1] = h[0]x[1] + h[1]x[0] + h[2]x[3] \quad (4.210)$$

$$y_C[2] = h[0]x[2] + h[1]x[1] + h[2]x[0] \quad (4.211)$$

$$y_C[3] = h[0]x[3] + h[1]x[2] + h[2]x[1] \quad (4.212)$$

If we compare the expressions for the samples of $y_L[n]$ with the samples of $y_C[n]$, we observe that the first 2 terms of $y_C[n]$ do not correspond to the first 2 terms of $y_L[n]$, whereas the last 2 terms of $y_C[n]$ are precisely the same as the third and the forth terms of $y_L[n]$.

In general, if we consider the N -point circular convolution of a length- M sequence $h[n]$ with a length- N sequence $x[n]$ with $N > M$, the first $M - 1$ samples of the circular convolution are incorrect and are rejected. The remaining $N - M + 1$ samples correspond to the correct samples of the linear convolution of $h[n]$ with $x[n]$.

Now we consider an infinitely long or very long sequence $x[n]$. We break it up as a collection of smaller length (length-4) overlapping sequences $x_m[n]$ as $x_m[n] = x[n + 2m]$, with $0 \leq n \leq 3$, $0 \leq m \leq \infty$. Next, we form:

$$w_m[n] = h[n] \stackrel{4}{\ast} x_m[n] \quad (4.213)$$

or, equivalently

$$w_m[0] = h[0]x_m[0] + h[1]x_m[3] + h[2]x_m[2] \quad (4.214)$$

$$w_m[1] = h[0]x_m[1] + h[1]x_m[0] + h[2]x_m[3] \quad (4.215)$$

$$w_m[2] = h[0]x_m[2] + h[1]x_m[1] + h[2]x_m[0] \quad (4.216)$$

$$w_m[3] = h[0]x_m[3] + h[1]x_m[2] + h[2]x_m[1] \quad (4.217)$$

Computing the above for $m = 0, 1, 2, 3, \dots$, and substituting the values of $x_m[n]$, we arrive at:

$w_0[0] = h[0]x[0] + h[1]x[3] + h[2]x[2]$	← Reject
$w_0[1] = h[0]x[1] + h[1]x[0] + h[2]x[3]$	← Reject
$w_0[2] = h[0]x[2] + h[1]x[1] + h[2]x[0] = y[2]$	← Save
$w_0[3] = h[0]x[3] + h[1]x[2] + h[2]x[1] = y[3]$	← Save
$w_1[0] = h[0]x[2] + h[1]x[5] + h[2]x[4]$	← Reject
$w_1[1] = h[0]x[3] + h[1]x[2] + h[2]x[5]$	← Reject
$w_1[2] = h[0]x[4] + h[1]x[3] + h[2]x[2] = y[4]$	← Save
$w_1[3] = h[0]x[5] + h[1]x[4] + h[2]x[3] = y[5]$	← Save
$w_2[0] = h[0]x[4] + h[1]x[5] + h[2]x[6]$	← Reject
$w_2[1] = h[0]x[5] + h[1]x[4] + h[2]x[7]$	← Reject
$w_2[2] = h[0]x[6] + h[1]x[5] + h[2]x[4] = y[6]$	← Save
$w_2[3] = h[0]x[7] + h[1]x[6] + h[2]x[5] = y[7]$	← Save

It should be noted that to determine $y[0]$ and $y[1]$ we need to form $x_{-1}[n]$, setting $x_{-1}[0] = x_{-1}[1] = 0$, $x_{-1}[2] = x[0]$, $x_{-1}[3] = x[1]$, and compute:

$$w_{-1}[n] = h[n] \stackrel{4}{\ast} x_{-1}[n] \quad 0 \leq n \leq 3 \quad (4.218)$$

then reject $w_{-1}[0]$ and $w_{-1}[1]$, and save $w_{-1}[2] = y[0]$ and $w_{-1}[3] = y[1]$.

In general, let $h[n]$ be a length- N sequence. Let $x_m[n]$ denote the m^{th} section of an infinitely long sequence $x[n]$ of length N and defined by:

$$x_m[n] = x[n + m(N - m + 1)] \quad 0 \leq n \leq N - 1 \quad (4.219)$$

with $M < N$. Let $w_m[n] = h[n] * x_m[n]$. Then, we reject the first $M - 1$ samples of $w_m[n]$ and “about” the remaining $M - M + 1$ samples of $w_m[n]$ to form $y_L[n]$, namely the linear convolution of $h[n]$ and $x[n]$. If $y_m[n]$ denotes the saved portion of $w_m[n]$, i.e.:

$$y_m[n] = \begin{cases} 0 & 0 \leq n \leq M - 2 \\ w_m[n] & M - 1 \leq n \leq N - 2 \end{cases} \quad (4.220)$$

then:

$$y_L[n + m(N - M + 1)] = y_m[n] \quad M - 1 \leq n \leq N - 1 \quad (4.221)$$

The approach is called overlap-save method since the input is segmented into overlapping sections and parts of the results of the circular convolutions are saved and abutted to determine the linear convolution result. The process is illustrated in Figure 4.16.

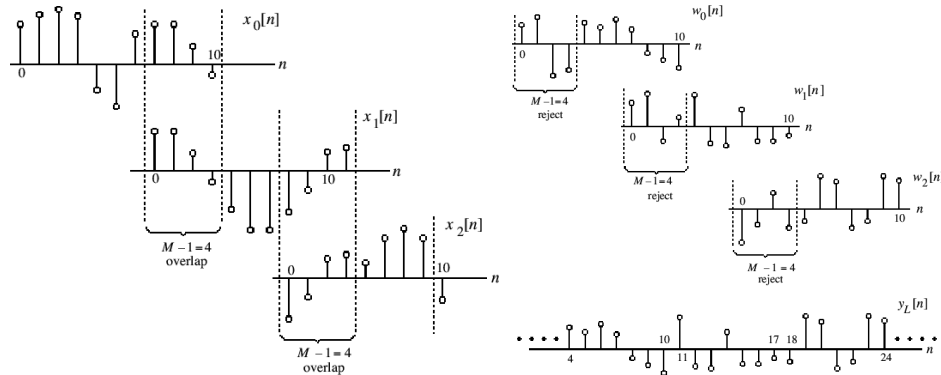


Figure 4.16: Illustration of the overlap-save method.

Chapter 5

The Z transform

We have seen that the DTFT provides a frequency-domain representation of discrete-time signals and LTI discrete-time systems. However, because of the convergence condition, in many cases, the DTFT of a sequence may not exist. As a result, it is not possible to make use of such frequency-domain characterization in these cases. A possible solution and alternative is a generalization of the DTFT, which leads to the z-transform. The ladder may exist for many sequences for which the DTFT does not exist. Moreover, use of z-transform techniques permits simple but powerful algebraic manipulations. Consequently, z-transform has become an important tool in the analysis and design of digital filters

Lecture 14.
Thursday 12th
November, 2020.

5.1 The definition

Definition 6: Z-transform

For a given sequence $g[n]$, its z-transform $G(z)$ is defined as:

$$G(z) = \sum_{n=-\infty}^{\infty} g[n]z^{-n} \quad (5.1)$$

where $z = \text{Re}[z] + j \text{Im}[z]$ is a complex variable.

If we let $z = re^{j\omega}$, then the z-transform reduces to:

$$G(re^{j\omega}) = \sum_{n=-\infty}^{\infty} g[n]r^{-n}e^{-j\omega n} \quad (5.2)$$

The above can be interpreted as the DTFT of the modified sequence $\{g[n]r^{-n}\}$. For $r = 1$ (i.e., $|z| = 1$), the z-transform reduces to its DTFT, provided the ladder exists. Like the DTFT, there are conditions on the convergence of the infinite series like:

$$\sum_{n=-\infty}^{\infty} g[n]z^{-n} \quad (5.3)$$

For a given sequence, the set R of values of z for which its z-transform converges is called the region of convergence (ROC).

From our earlier discussion on the uniform convergence of the DTFT, it follows that the series:

$$G(re^{j\omega}) = \sum_{n=-\infty}^{\infty} g[n]r^{-n}e^{-j\omega n} \quad (5.4)$$

converges if $\{g[n]r^{-n}\}$ is absolutely summable, i.e. if:

$$\sum_{n=-\infty}^{\infty} |g[n]r^{-n}| < \infty \quad (5.5)$$

In general, the ROC R of a z-transform of a sequence $g[n]$ is an annular region of the z-plane, namely:

$$R_{g^-} < |z| < R_{g^+} \quad (5.6)$$

where $0 \leq R_{g^-} < R_{g^+} < \infty$.

Example 20: Z-transform calculation

We determine the z-transform $X(z)$ of the causal sequence $x[n] = \alpha^n \mu[n]$ and its ROC. Now:

$$X(z) = \alpha^n \mu[n] z^{-n} = \sum_{n=0}^{\infty} \alpha^n z^{-n} \quad (5.7)$$

The above power series converges to:

$$X(z) = \frac{1}{1 - \alpha z^{-1}} \quad |\alpha z^{-1}| < 1 \quad (5.8)$$

ROC is the annular region $|z| > |\alpha|$.

Example 21: Z-transform calculation

The z-transform $\mu(z)$ of the unit step sequence $\mu[n]$ can be obtained from:

$$X(z) = \frac{1}{1 - \alpha z^{-1}} \quad |\alpha z^{-1}| < 1 \quad (5.9)$$

By setting $\alpha = 1$:

$$\mu(z) = \frac{1}{1 - z^{-1}} \quad |z^{-1}| < 1 \quad (5.10)$$

ROC is the annular region $1 < |z| < \infty$. Note that the unit step sequence $\mu[n]$ is not absolutely summable, and hence its DTFT does not converge uniformly.

Example 22: Z-transform calculation

Consider the anti-causal sequence:

$$y[n] = -\alpha^n \mu[-n - 1] \quad (5.11)$$

Its z-transform is given by:

$$\begin{aligned} Y(z) &= - \sum_{n=-\infty}^{-1} \alpha^n z^{-n} = - \sum_{m=1}^{\infty} \alpha^{-m} z^m \\ &= -\alpha^{-1} z \sum_{m=0}^{\infty} \alpha^{-m} z^m = -\frac{-\alpha^{-1} z}{1 - \alpha z^{-1}} \\ &= \frac{1}{1 - \alpha z^{-1}} \end{aligned} \quad (5.12)$$

for $|\alpha^{-1} z| < 1$. ROC is the annular region $|z| < |\alpha|$.

Note that the z-transforms of the two sequences $\alpha^n \mu[n]$ and $-\alpha^n \mu[-n-1]$ are identical even though the two parent sequences are different. The only way a unique sequence can be associated with a z-transform is by specifying its ROC.

Another important point is that the DTFT $G(e^{j\omega})$ of a sequence $g[n]$ converges uniformly if and only if the ROC of the z-transform $G(z)$ of $g[n]$ includes the unit circle. However, the existence of the DTFT does not always imply the existence of the z-transform.

Example 23: Z-transform

The finite energy sequence:

$$h_{LP}[n] = \frac{\sin(\omega_c n)}{\pi n} \quad -\infty < n < \infty \quad (5.13)$$

has a DTFT given by:

$$H_{LP}(e^{j\omega}) = \begin{cases} 1 & 0 \leq |\omega| \leq \omega_c \\ 0 & \omega_c < |\omega| \leq \pi \end{cases} \quad (5.14)$$

which converges in the mean-square sense. However, $h_{LP}[n]$ does not have a z-transform as it is not absolutely summable for any value of r .

Some commonly used z-transform pairs are listed in Figure 5.1.

Sequence	z -Transform	ROC
$\delta[n]$	1	All values of z
$\mu[n]$	$\frac{1}{1-z^{-1}}$	$ z > 1$
$\alpha^n \mu[n]$	$\frac{1}{1-\alpha z^{-1}}$	$ z > \alpha $
$(r^n \cos \omega_o n) \mu[n]$	$\frac{1-(r \cos \omega_o) z^{-1}}{1-(2r \cos \omega_o) z^{-1} + r^2 z^{-2}}$	$ z > r$
$(r^n \sin \omega_o n) \mu[n]$	$\frac{(r \sin \omega_o) z^{-1}}{1-(2r \cos \omega_o) z^{-1} + r^2 z^{-2}}$	$ z > r$

Figure 5.1: Common z-transform pairs.

5.2 Rational z-transforms

In the case of LTI discrete-time systems we are concerned with in this course, all pertinent z-transforms are rational functions of z^{-1} , that is, they are ratios of two polynomials in z^{-1} :

$$G(z) = \frac{P(z)}{D(z)} = \frac{p_0 + p_1 z^{-1} + \cdots + p_{M-1} z^{-(M-1)} + p_M z^{-M}}{d_0 + d_1 z^{-1} + \cdots + d_{N-1} z^{-(N-1)} + d_N z^{-N}} \quad (5.15)$$

The degree of the numerator polynomial $P(z)$ is M and the degree of the denominator polynomial $D(z)$ is N . An alternate representation of a rational z-transform is as a

ratio of two polynomials in z :

$$G(z) = z^{(N-M)} \frac{p_0 z^M + \cdots + p_{M-1} z + p_M}{d_0 z^N + \cdots + d_{N-1} z + d_N} \quad (5.16)$$

Again, a rational z-transform can be alternately written in factored form as:

$$G(z) = \frac{p_0 \prod_{\ell=1}^M (1 - \xi_\ell z^{-1})}{d_0 \prod_{\ell=1}^N (1 - \lambda_\ell z^{-1})} = z^{(N-M)} \frac{p_0 \prod_{\ell=1}^M (z - \xi_\ell)}{d_0 \prod_{\ell=1}^N (z - \lambda_\ell)} \quad (5.17)$$

We have as roots:

- $z = \xi_\ell$, roots of the numerator polynomial. These values of z are known as the zeros of $G(z)$;
- $z = \lambda_\ell$, roots of the denominator polynomial. These values of z are known as the poles of $G(z)$.

Example 24: Zeros and poles

The z-transform:

$$\mu(z) = \frac{1}{1 - z^{-1}} \quad |z| > 1 \quad (5.18)$$

has a zero at $z = 0$ and a pole at $z = 1$.

Example 25: ROC of a rational z-transform

The z-transform $H(z)$ of the sequence $h[n] = (-0.6)^n \mu[n]$ is given by:

$$H(z) = \frac{1}{1 + 0.6z^{-1}} \quad |z| > 0.6 \quad (5.19)$$

Here the ROC is just outside the circle going through the point $z = -0.6$.

A physical interpretation of the concepts of poles and zeros can be given by plotting the log-magnitude $20 \log_{10} |G(z)|$ as showed in Figure 5.2 for:

$$G(z) = \frac{1 - 2.4z^{-1} + 2.88z^{-2}}{1 - 0.8z^{-1} + 0.64z^{-2}} \quad (5.20)$$

Observe that the magnitude plot exhibits very large peaks around the points $z = 0.4 \pm j0.6928$, which are the poles of $G(z)$. It also exhibits very narrow and deep wells around the location of the zeros at $z = 1.2 \pm j1.2$.

ROC of a z-transform is an important concept. Without its knowledge, there is no unique relationship between a sequence and its z-transform. Hence, the z-transform must always be specified with its ROC. Moreover, there is a relationship between the ROC of the z-transform of the impulse response of a causal LTI discrete-time system and its BIBO stability.

Another important distinction is that a sequence can be one of the following types: finite-length, right-sided, left-sided and two-sided. In general, the ROC depends on the type of the sequence of interest.

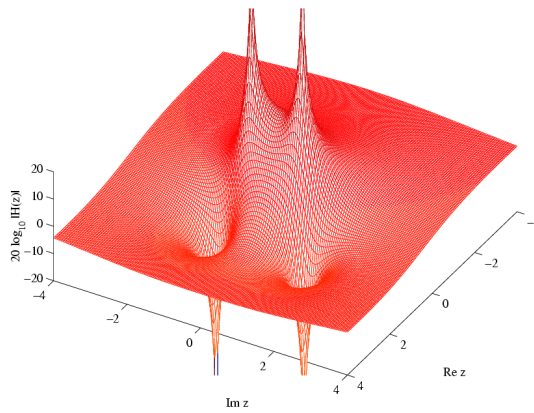


Figure 5.2: Log-magnitude plot for $G(z)$ in Eq. 5.20.

Example 26: Finite-length sequence z-transform

Consider a finite-length sequence $g[n]$ defined for $-M \leq n \leq N$, where M and N are non-negative integers and $|g[n]| < \infty$. Its z-transform is given by:

$$G(z) = \sum_{n=-M}^N g[n]z^{-n} = \frac{\sum_{n=0}^{N+M} g[n-M]z^{N+M-n}}{z^N} \quad (5.21)$$

Note that $G(z)$ has M zeros and N poles. As can be seen from the expression for $G(z)$, the z-transform of a finite-length bounded sequence converges everywhere in the z-plane except possibly at $z = 0$ and/or at $z = \infty$.

Example 27: Right-sided sequence z-transform

A right-sided sequence with nonzero sample values for $n \geq 0$ is sometimes called a causal sequence. So, consider a causal sequence $u_1[n]$. Its z-transform is given by:

$$U_1(z) = \sum_{n=0}^{\infty} u_1[n]z^{-n} \quad (5.22)$$

It can be showed that $U_1(z)$ converges exterior to a circle with $|z| = R_1$, including the point $z = \infty$.

On the other hand, a right-sided sequence $u_2[n]$ with nonzero sample values only for $n \geq -M$ with M non-negative has a z-transform $U_2(z)$ with M poles at $z = \infty$. The ROC of $U_2(z)$ is exterior to a circle $|z| = R_2$, excluding the point $z = \infty$.

Example 28: Left-sided sequence z-transform

A left-sided sequence with nonzero sample values for $n \leq 0$ is sometimes called anticausal sequence. So, consider an anticausal sequence $v_1[n]$. Its z-transform is given by:

$$V_1(z) = \sum_{n=-\infty}^0 v_1[n]z^{-n} \quad (5.23)$$

It can be showed that $V_1(z)$ converges interior to a circle $|z| = R_3$, including the

point $z = 0$.

On the other hand, a left-sided sequence with nonzero sample values only for $n \leq N$ with N non-negative has a z-transform $V_2(z)$ with N poles at $z = 0$. The ROC of $V_2(z)$ is interior to a circle $|z| = R_4$, excluding the point $z = 0$.

Example 29: Two-sided sequence z-transform

The z-transform of a two-sided sequence $w[n]$ can be expressed as:

$$W(z) = \sum_{n=-\infty}^{\infty} w[n]z^{-n} = \sum_{n=0}^{\infty} w[n]z^{-n} + \sum_{n=-\infty}^{-1} w[n]z^{-n} \quad (5.24)$$

The first term on the RHS can be interpreted as the z-transform of a right-sided sequence and it thus converges exterior to the circle $|z| = R_5$. The second term of the RHS can be interpreted as the z-transform of a left-sided sequence and it thus converges interior to the circle $|z| = R_6$. If $R_5 < R_6$, there is an overlapping ROC given by $R_5 < |z| < R_6$. If $R_5 > R_6$, there is no overlap and the z-transform does not exist.

In particular, let us consider as example the two-sided sequence:

$$u[n] = \alpha^n \quad (5.25)$$

where α can be either real or complex. Its z-transform is given by:

$$U(z) = \sum_{n=-\infty}^{\infty} \alpha^n z^{-n} = \sum_{n=0}^{\infty} \alpha^n z^{-n} + \sum_{n=-\infty}^{-1} \alpha^n z^{-n} \quad (5.26)$$

The first term on the RHS converges for $|z| > |\alpha|$, whereas the second term converges for $|z| < |\alpha|$. There is no overlap between these two regions, hence the z-transform of $u[n] = \alpha^n$ does not exist.

The ROC of a rational z-transform cannot contain any pole (since it is infinite at a pole) and is bounded by the poles. To show that the z-transform is bounded by the poles, assume that the z-transform $X(z)$ has simple poles at $z = \alpha$ and $z = \beta$. Assume that the corresponding sequence $x[n]$ is a right-sided sequence. Then, $x[n]$ has the form:

$$x[n] = (r_1 \alpha^n + r_2 \beta^n) \mu[n - N_0] \quad |\alpha| < |\beta| \quad (5.27)$$

where N_0 is a positive or negative integer. Now, the z-transform of the right-sided sequence $\gamma^n \mu[n - N_0]$ exists if:

$$\sum_{n=N_0}^{\infty} |\gamma^n z^{-n}| < \infty \quad (5.28)$$

for some z . The condition in Eq. 5.28 holds for $|z| > |\gamma|$, but not for $|z| \leq |\gamma|$. Therefore, the z-transform of Eq. 5.27 has a ROC defined by $|\beta| < |z| \leq \infty$. Likewise, the z-transform of a left-sided sequence:

$$x[n] = (r_1 \alpha^n + r_2 \beta^n) \mu[-n - N_0] \quad |\alpha| < |\beta| \quad (5.29)$$

has a ROC define by $0 \leq |z| < |\alpha|$.

5.3 Inverse z-transform

Firstly, we recall that, for $z = re^{j\omega}$, the z-transform $G(z)$ given by:

$$G(z) = \sum_{n=-\infty}^{\infty} g[n]z^{-n} = \sum_{n=-\infty}^{\infty} g[n]r^{-n}e^{-j\omega n} \quad (5.30)$$

is the DTFT of the modified sequence $g[n]r^{-n}$. Accordingly, the inverse DTFT is thus given by:

$$g[n]r^{-n} = \frac{1}{2\pi} \int_{-\pi}^{\pi} G(re^{j\omega})e^{j\omega n} d\omega \quad (5.31)$$

By making a change of variable $z = re^{j\omega}$, the previous equation can be converted into a contour integral given by:

$$g[n] = \frac{1}{2\pi j} \oint_{C'} G(z)z^{n-1} dz \quad (5.32)$$

where C' is a counterclockwise contour of integration defined by $|z| = r$. But the integral remains unchanged when is replaced with any contour C encircling the point $z = 0$ in the ROC of $G(z)$. The contour integral can be evaluated using the Cauchy's residue theorem resulting in:

$$g[n] = \sum \text{Res}_C [G(z)z^{n-1}] \quad (5.33)$$

Eq. 5.33 needs to be evaluated at all values of n and is not pursued here.

A rational z-transform $G(z)$ with a causal inverse transform $g[n]$ has an ROC that is exterior to a circle. Here, it is more convenient to express $G(z)$ in a partial-fraction expansion form and then determine $g[n]$ by summing the inverse transform of the individual simpler terms in the expansion. A rational $G(z)$ can be expressed as:

$$G(z) = \frac{P(z)}{D(z)} = \frac{\sum_{i=0}^M p_i z^{-i}}{\sum_{i=0}^N d_i z^{-i}} \quad (5.34)$$

If $M \geq N$, then $G(z)$ can be re-expressed as:

$$G(z) = \sum_{\ell=0}^{M-N} \eta_\ell z^{-\ell} + \frac{P_1(z)}{D(z)} \quad (5.35)$$

where the degree of $P_1(z)$ is less than N . The rational function $\frac{P_1(z)}{D(z)}$ is called a proper fraction. To develop the proper fraction part $\frac{P_1(z)}{D(z)}$ from $G(z)$, a long division of $P(z)$ by $D(z)$ should be carried out in a reverse order until the remainder polynomial $P_1(z)$ is of lower degree than that of the denominator $D(z)$.

Example 30: Inverse transform by partial-fraction expansion

Consider:

$$G(z) = \frac{2 + 0.8z^{-1} + 0.5z^{-2} + 0.3z^{-3}}{1 + 0.8z^{-1} + 0.2z^{-2}} \quad (5.36)$$

By long division in reverse order we arrive at:

$$G(z) = -3.5 + 1.5z^{-1} + \underbrace{\frac{5.5 + 2.1z^{-1}}{1 + 0.8z^{-1} + 0.2z^{-2}}}_{\text{Proper fraction}} \quad (5.37)$$

In most practical cases, the rational z-transform of interest $G(z)$ is a proper fraction with simple poles. Let the poles of $G(z)$ be at $z = \lambda_k$, with $1 \leq k \leq N$. A partial-fraction expansion of $G(z)$ is then of the form:

$$G(z) = \sum_{\ell=1}^N \left(\frac{\rho_\ell}{1 - \lambda_\ell z^{-1}} \right) \quad (5.38)$$

The constants ρ_ℓ in the partial-fraction expansion are called the residues and are given by:

$$\rho_\ell = [(1 - \lambda_\ell z^{-1})G(z)]_{z=\lambda_\ell} \quad (5.39)$$

Each term of the sum in partial-fraction expansion has a ROC given by $|z| > |\lambda_\ell|$ and thus has an inverse transform of the form $\rho_\ell(\lambda_\ell)^n \mu[n]$. Therefore, the inverse transform $g[n]$ of $G(z)$ is given by:

$$g[n] = \sum_{\ell=1}^N \rho_\ell (\lambda_\ell)^n \mu[n] \quad (5.40)$$

Note that the approach in Eq. 5.40 with a slight modification can also be used to determine the inverse of a rational z-transform of a noncausal sequence.

Example 31: Inverse transfrom of a causal sequence

Let the z-transform $H(z)$ of a causal sequence $h[n]$ be given by:

$$H(z) = \frac{z(z+2)}{(z-0.2)(z+0.6)} = \frac{1+2z^{-1}}{(1-0.2z^{-1})(1+0.6z^{-1})} \quad (5.41)$$

A partial-fraction expansion of $H(z)$ is then of the form:

$$H(z) = \frac{\rho_1}{1-0.2z^{-1}} + \frac{\rho_2}{1+0.6z^{-1}} \quad (5.42)$$

Now:

$$\rho_1 = [(1-0.2z^{-1})H(z)]_{z=0.2} = \left[\frac{1+2z^{-1}}{1+0.6z^{-1}} \right]_{z=0.2} = 2.75 \quad (5.43)$$

$$\rho_2 = [(1+0.6z^{-1})H(z)]_{z=-0.6} = \left[\frac{1+2z^{-1}}{1-0.2z^{-1}} \right]_{z=-0.6} = -1.75 \quad (5.44)$$

Hence:

$$H(z) = \frac{2.75}{1-0.2z^{-1}} - \frac{1.75}{1+0.6z^{-1}} \quad (5.45)$$

The inverse transform of the above is therefore given by:

$$h[n] = 2.75(0.2)^n \mu[n] - 1.75(-0.6)^n \mu[n] \quad (5.46)$$

In case $G(z)$ has multiple poles, the partial-fraction expansion is of slightly different form. Let the pole at $z = v$ be of multiplicity L and the remaining $N - L$ poles be simple and at $z = \lambda_\ell$, for $1 \leq \ell \leq N - L$. Then, the partial-fraction expansion of $G(z)$ is of the form:

$$G(z) = \sum_{\ell=0}^{M-N} \eta_\ell z^{-\ell} + \sum_{\ell=1}^{N-L} \frac{\rho_\ell}{1 - \lambda_\ell z^{-1}} + \sum_{i=1}^L \frac{\gamma_i}{(1 - vz^{-1})^i} \quad (5.47)$$

where the constants γ_i are computed using:

$$\gamma_i = \frac{1}{(L-i)!(-v)^{L-i}} \frac{d^{L-i}}{dz^{L-i}} [(1-vz^{-1})G(z)]_{z=v} \quad 1 \leq i \leq L \quad (5.48)$$

The residues ρ_ℓ are calculated as before.

5.4 Z-transform properties

A list of properties of the z-transform is showed in Figure 5.3.

Property	Sequence	z -Transform	ROC
	$g[n]$ $h[n]$	$G(z)$ $H(z)$	\mathcal{R}_g \mathcal{R}_h
Conjugation	$g^*[n]$	$G^*(z^*)$	\mathcal{R}_g
Time-reversal	$g[-n]$	$G(1/z)$	$1/\mathcal{R}_g$
Linearity	$\alpha g[n] + \beta h[n]$	$\alpha G(z) + \beta H(z)$	Includes $\mathcal{R}_g \cap \mathcal{R}_h$
Time-shifting	$g[n - n_o]$	$z^{-n_o} G(z)$	\mathcal{R}_g , except possibly the point $z = 0$ or ∞
Multiplication by an exponential sequence	$\alpha^n g[n]$	$G(z/\alpha)$	$ \alpha \mathcal{R}_g$
Differentiation of $G(z)$	$ng[n]$	$-z \frac{dG(z)}{dz}$	\mathcal{R}_g , except possibly the point $z = 0$ or ∞
Convolution	$g[n] \otimes h[n]$	$G(z)H(z)$	Includes $\mathcal{R}_g \cap \mathcal{R}_h$
Modulation	$g[n]h[n]$	$\frac{1}{2\pi j} \oint_C G(v)H(z/v)v^{-1} dv$	Includes $\mathcal{R}_g \mathcal{R}_h$
Parseval's relation		$\sum_{n=-\infty}^{\infty} g[n]h^*[n] = \frac{1}{2\pi j} \oint_C G(v)H^*(1/v^*)v^{-1} dv$	

Note: If \mathcal{R}_g denotes the region $R_{g-} < |z| < R_{g+}$ and \mathcal{R}_h denotes the region $R_{h-} < |z| < R_{h+}$, then $1/\mathcal{R}_g$ denotes the region $1/R_{g+} < |z| < 1/R_{g-}$ and $\mathcal{R}_g \mathcal{R}_h$ denotes the region $R_{g-} R_{h-} < |z| < R_{g+} R_{h+}$.

Figure 5.3: Properties of the z-transform.

Example 32: Z-transform properties

Consider the two-sided sequence:

$$v[n] = \alpha^n \mu[n] - \beta^n \mu[-n-1] \quad (5.49)$$

Let $x[n] = \alpha^n \mu[n]$ and $y = -\beta^n \mu[-n-1]$ with $X(z)$ and $Y(z)$ denoting, respectively, their z-transforms. Now:

$$X(z) = \frac{1}{1 - \alpha z^{-1}} \quad |z| > |\alpha| \quad (5.50)$$

$$Y(z) = \frac{1}{1 - \beta z^{-1}} \quad |z| < |\beta| \quad (5.51)$$

Using the linearity property we arrive at:

$$V(z) = X(z) + Y(z) = \frac{1}{1 - \alpha z^{-1}} + \frac{1}{1 - \beta z^{-1}} \quad (5.52)$$

The ROC of $V(z)$ is given by the overlap regions of $|z| > |\alpha|$ and $|z| < |\beta|$. We have that:

- if $|\alpha| < |\beta|$, then there is an overlap and the ROC is an annular region $|\alpha| < |z| < |\beta|$;
- if $|\alpha| > |\beta|$, then there is no overlap and $V(z)$ does not exist.

Example 33: Z-transform properties

We determine the z-transform and its ROC of the causal sequence:

$$x[n] = r^n (\cos(\omega_0 n)) \mu[n] \quad (5.53)$$

We can express $x[n] = v[n] + v^*[n]$, where:

$$v[n] = \frac{1}{2} r^n e^{j\omega_0 n} \mu[n] = \frac{1}{2} \alpha^n \mu[n] \quad (5.54)$$

The z-transform of $v[n]$ is given by:

$$V(z) = \frac{1}{2} \frac{1}{1 - \alpha z^{-1}} = \frac{1}{2} \frac{1}{1 - re^{j\omega_0 z^{-1}}} \quad |z| > |\alpha| = r \quad (5.55)$$

Using the conjugation property, we obtain the z-transform of $v^*[n]$ as:

$$V^*(z^*) = \frac{1}{2} \frac{1}{1 - \alpha^* z^{-1}} = \frac{1}{2} \frac{1}{1 - re^{-j\omega_0 z^{-1}}} \quad |z| > |\alpha| \quad (5.56)$$

Finally, using the linearity property we get:

$$X(z) = V(z) + V^*(z^*) = \frac{1}{2} \left(\frac{1}{1 - re^{j\omega_0 z^{-1}}} + \frac{1}{1 - re^{-j\omega_0 z^{-1}}} \right) \quad (5.57)$$

or:

$$X(z) = \frac{1 - (r \cos \omega_0) z^{-1}}{1 - (2r \cos \omega_0) z^{-1} + r^2 z^{-2}} \quad |z| > r \quad (5.58)$$

Example 34: Z-transform properties

We determine the z-transform $Y(z)$ and the ROC of the sequence:

$$y[n] = (n + 1) \alpha^n \mu[n] \quad (5.59)$$

We can write $y[n] = nx[n] + x[n]$ where:

$$x[n] = \alpha^n \mu[n] \quad (5.60)$$

Now, the z-transform $X(z)$ of $x[n] = \alpha^n \mu[n]$ is given by:

$$X(z) = \frac{1}{1 - \alpha z^{-1}} \quad |z| > |\alpha| \quad (5.61)$$

Using the differentiation property, we arrive at the z-transform of $nx[n]$ as:

$$-z \frac{dX(z)}{dz} = \frac{\alpha z^{-1}}{1 - \alpha z^{-1}} \quad |z| > |\alpha| \quad (5.62)$$

Using the linearity property we finally obtain:

$$Y(z) = \frac{1}{1 - \alpha z^{-1}} + \frac{\alpha z^{-1}}{(1 - \alpha z^{-1})^2} = \frac{1}{(1 - \alpha z^{-1})^2} \quad |z| > |\alpha| \quad (5.63)$$

Lecture 17.
Tuesday 24th
November, 2020.

5.5 Stability condition

A causal LTI digital filter is BIBO stable if and only if its impulse response $h[n]$ is absolutely summable, i.e.:

$$S = \sum_{n=-\infty}^{\infty} |h[n]| < \infty \quad (5.64)$$

We now develop a stability condition in terms of the pole locations of the transfer function $H(z)$.

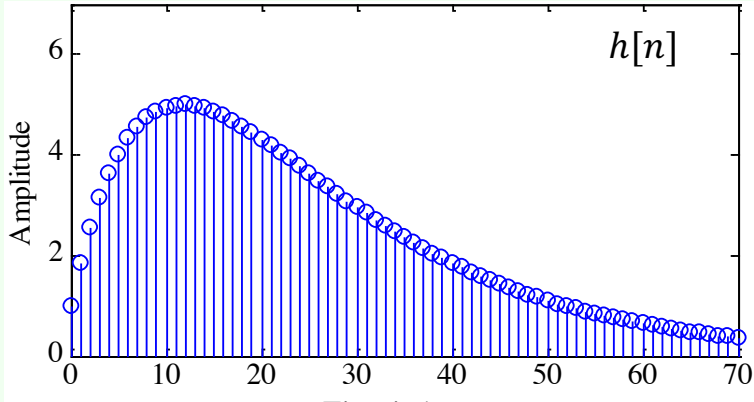
The ROC of the z-transform $H(z)$ of the impulse response sequence $h[n]$ is defined by values of $|z| = r$ for which $h[n]r^{-n}$ is absolutely summable. Thus, if the ROC includes the unit circle $|z| = 1$, then the digital filter is stable, and viceversa. In addition, for a stable and causal digital filter for which $h[n]$ is a right-sided sequence, the ROC will include the unit circle and entire z-plane including the point $z = \infty$. Note that a FIR digital filter with bounded impulse response is always stable. On the other hand, a IIR filter may be unstable if not designed properly. In addition, an originally stable IIR filter characterized by infinite precision coefficients may become unstable when coefficients get quantized due to implementation.

Example 35: Stability condition

Consider the causal IIR transfer function:

$$H(z) = \frac{1}{1 - 1.845z^{-1} + 0.850586z^{-2}} \quad (5.65)$$

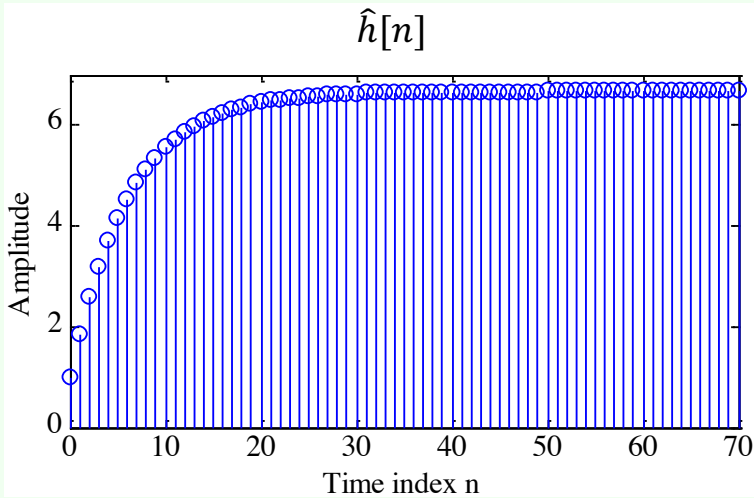
The plot of the impulse response coefficients is showed below. As can be seen from the plot, the impulse response coefficient $h[n]$ decays rapidly to zero value as n increases.



The absolute summability condition of $h[n]$ is satisfied. Hence, $H(z)$ is a stable transfer function. Now, consider the case when the transfer function coefficients are rounded to values with 2 digits after the decimal point:

$$\hat{H}(z) = \frac{1}{1 - 1.85z^{-1} + 0.85z^{-2}} \quad (5.66)$$

A plot of the impulse response of $\hat{h}[n]$ is showed below.



In this case, the impulse coefficient $\hat{h}[n]$ increases rapidly to a constant value as n increases. Hence, the absolute summability condition of $\hat{h}[n]$ is violated. Thus, $\hat{H}[z]$ is an unstable transfer function.

The stability testing of a IIR transfer function is therefore an important problem. In most cases it is difficult to compute the infinite sum in Eq. 5.64. For a causal IIR transfer function, the sum S can be computed approximately as:

$$S_k = \sum_{n=0}^{k-1} |h[n]| \quad (5.67)$$

The partial sum is computed for increasing values of k until the difference between a series of consecutive values of S_k is smaller than some arbitrarily chosen small number, which is typically 10^{-6} . For a transfer function of very high order this approach may not be satisfactory. An alternate, easy-to-test, stability condition is developed next. Let us consider the causal IIR digital filter with a rational transfer function $H(z)$

given by:

$$H(z) = \frac{\sum_{k=0}^M p_k z^{-k}}{\sum_{k=0}^N d_k z^{-k}} \quad (5.68)$$

Its impulse response $\{h[n]\}$ is a right-sided sequence. The ROC of $H(z)$ is exterior to a circle going through the pole furthest from $z = 0$. But stability requires that $\{h[n]\}$ is absolutely summable. This in turn implies that the DTFT $H(e^{j\omega})$ of $\{h[n]\}$ exists. Now, if the ROC of the x-transform $H(z)$ includes the unit circle, then:

$$H(e^{j\omega}) = [H(z)]_{z=e^{j\omega}} \quad (5.69)$$

In conclusion, all the poles of a causal stable transfer function $H(z)$ must be strictly inside the unit circle, as showed in Figure 5.4.

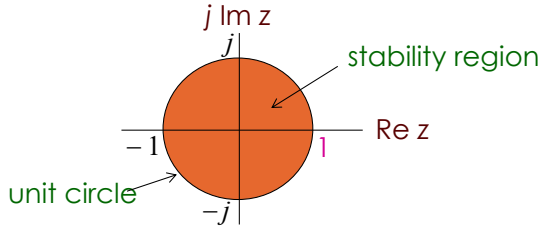


Figure 5.4: Stability condition (shaded area).

Example 36: Stability condition

The factored form of the previous example transfer function is:

$$H(z) = \frac{1}{1 - 1.845z^{-1} + 0.850586z^{-2}} = \frac{1}{(1 - 0.902z^{-1})(1 - 0.943z^{-1})} \quad (5.70)$$

which has a real pole at $z = 0.902$ and a real pole at $z = 0.943$. Since both poles are inside the unit circle, $H(z)$ is BIBO stable.

On the other hand, the factored form of $\hat{H}(z)$ is:

$$\hat{H}(z) = \frac{1}{1 - 1.85z^{-1} + 0.85z^{-2}} = \frac{1}{(1 - z^{-1})(1 - 0.85z^{-1})} \quad (5.71)$$

which has a real pole on the unit circle at $z = 1$ and the other pole inside the unit circle. Since not both the poles are inside the unit circle, $\hat{H}(z)$ is unstable.

Chapter 6

Filter design

Before starting with the discussion of filter design, we have to go some steps backward and introduce some concepts

6.1 Phase and group delay

6.1.1 Phase delay

If the input $x[n]$ to an LTI system $H(e^{j\omega})$ is a sinusoidal signal of frequency ω_0 , i.e.:

$$x[n] = A \cos(\omega_0 n + \varphi), \quad -\infty < n < \infty \quad (6.1)$$

then the output $y[n]$ is also a sinusoidal signal of the same frequency ω_0 , but lagging in phase by $\theta(\omega_0)$ radians:

$$y[n] = A |H(e^{j\omega_0})| \cos(\omega_0 n + \theta(\omega_0) + \varphi), \quad -\infty < n < \infty \quad (6.2)$$

We can rewrite the output expression as:

$$y[n] = A |H(e^{j\omega_0})| \cos(\omega_0(n - \tau_p(\omega_0) + \varphi)) \quad (6.3)$$

where:

$$\tau_p(\omega_0) = -\frac{\theta(\omega_0)}{\omega_0} \quad (6.4)$$

is called the phase delay. The minus sign in front indicates phase lag. Thus, the output $y[n]$ is a time-delayed version of the input $x[n]$. In general, $y[n]$ will not be a delayed replica of $x[n]$ unless the phase delay $\tau_p(\omega_0)$ is an integer.

6.1.2 Group delay

When the input is composed of many sinusoidal components with different frequencies that are not harmonically related, each component will go through different phase delays. In this case, the signal delay is determined using the group delay defined by:

$$\tau_g(\omega) = -\frac{d\theta(\omega)}{d\omega} \quad (6.5)$$

In defining the group delay, it is assumed that the phase function is unwrapped so that its derivatives exist.

Example 37: Phase and group delay

The phase function of the FIR filter:

$$y[n] = \alpha x[n] + \beta x[n - 1] + \gamma x[n - 2] \quad (6.6)$$

is:

$$\theta(\omega) = -\omega \quad (6.7)$$

Hence, its group delay is given by $\tau_g(\omega) = 1$.

6.2 Type of transfer functions

The time-domain classification of an LTI digital transfer function sequence is based on the length of its impulse response. We can have:

- Finite Impulse Response (FIR) transfer function;
- Infinite Impulse Response (IIR) transfer function.

In the case of digital transfer functions with frequency-selective frequency responses, there are two types of classifications:

- a classification based on the shape of the magnitude function $|H(e^{j\omega})|$;
- a classification based on the form of the phase function $\theta(\omega)$.

One common classification is based on an ideal magnitude response. A digital filter designed to pass signal components of certain frequencies without distortion should have a frequency response equal to one at these frequencies, and should have a frequency response equal to zero at all other frequencies.

6.2.1 Ideal filters

The range of frequencies where the frequency response takes the value of one is called the passband. The range of frequencies where the frequency response takes the value of zero is called the stopband.

Frequency responses of the four popular types of ideal digital filters with real impulse response coefficients are showed in Figure 6.1.

In particular, the passband and stopband of those filters are listed in Table 6.1. The frequencies ω_c , ω_{c_1} and ω_{c_2} are called the cutoff frequencies. An ideal filter has a magnitude response equal to one in the passband and zero in the stopband, and has a zero phase everywhere.

Type	Passband	Stopband
Lowpass	$0 \leq \omega \leq \omega_c$	$\omega_c < \omega \leq \pi$
Highpass	$\omega_c \leq \omega \leq \pi$	$0 \leq \omega < \omega_c$
Bandpass	$\omega_{c_1} \leq \omega \leq \omega_{c_2}$	$0 \leq \omega < \omega_{c_1}$ and $\omega_{c_2} < \omega \leq \pi$
Stopband	$0 \leq \omega \leq \omega_{c_1}$ and $\omega_{c_2} \leq \omega \leq \pi$	$\omega_{c_1} < \omega < \omega_{c_2}$

Table 6.1: Passband and stopband of the four popular types of ideal digital filters

Earlier in the course we derived the inverse DTFT of the frequency response $H_{LP}(e^{j\omega})$ of the ideal lowpass filter:

$$h_{LP}[n] = \frac{\sin(\omega_c n)}{\pi n}, \quad -\infty < n < \infty \quad (6.8)$$

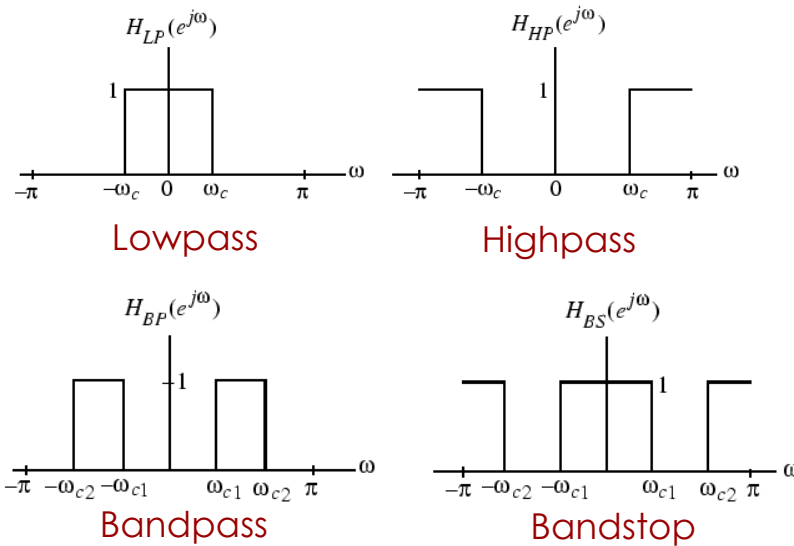


Figure 6.1: Frequency responses of the four popular types of ideal digital filters with real impulse response coefficients.

We have also shown that the above impulse response is not absolutely summable, and hence, the corresponding transfer function is not BIBO stable. Also, $h_{LP}[n]$ is not causal and is of doubly infinite length. The remaining three ideal filters are also characterized by doubly infinite, noncausal impulse responses and are not absolutely summable. Thus, the ideal filters with the ideal “brick wall” frequency responses cannot be realized with finite dimensional LTI filter.

To develop stable and realizable transfer functions, the ideal frequency response specifications are relaxed by including a transition band between the passband and the stopband. This permits the magnitude response to decay slowly from its maximum value in the passband to the zero value in the stopband. Moreover, the magnitude response is allowed to vary by a small amount both in the passband and the stopband. Typical magnitude response specifications of a lowpass filter are showed in Figure 6.2.

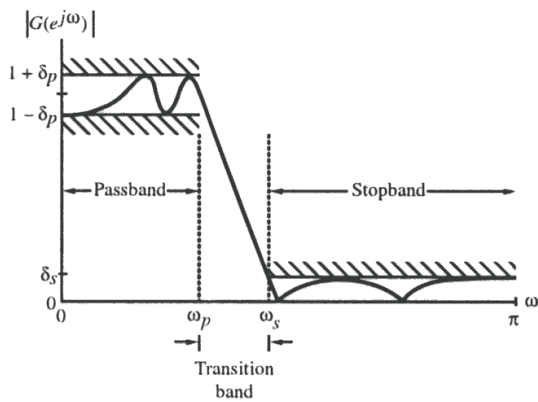


Figure 6.2: Typical magnitude response specifications of a lowpass filter.

6.2.2 Bounded Real transfer functions

A causal stable real-coefficient transfer function $H(z)$ is defined as a bounded real (BR) transfer function if:

$$|H(e^{j\omega})| \leq 1 \quad \forall \omega \quad (6.9)$$

Let $x[n]$ and $y[n]$ denote, respectively, the input and output of a digital filter characterized by a BR transfer function $H(z)$ with $X(e^{j\omega})$ and $Y(e^{j\omega})$ denoting their DTFTs. Then, the condition in Eq. 6.9 implies that:

$$|Y(e^{j\omega})|^2 \leq |X(e^{k\omega})|^2 \quad (6.10)$$

Integrating Eq. 6.10 from $-\pi$ to π and applying Parseval's relation, we get:

$$\sum_{n=-\infty}^{\infty} y[n]^2 \leq \sum_{n=-\infty}^{\infty} x[n]^2 \quad (6.11)$$

Thus, for all finite-energy inputs, the output energy is less than or equal to the input energy implying that a digital filter characterized by a BR transfer function can be viewed as a passive structure. If $|H(e^{j\omega})| = 1$, then the output energy is equal to the input energy, and such a digital filter is therefore a lossless system.

A causal stable real-coefficient transfer function $H(z)$ with $|H(e^{j\omega})| = 1$ is thus called a lossless bounded real (LBR) transfer function. The BR and LBR transfer functions are the keys to the realization of digital filters with low coefficient sensitivity.

Example 38: Bounded Real transfer functions

Consider the causal stable IIR transfer function:

$$H(z) = \frac{k}{1 - \alpha z^{-1}}, \quad 0 < |\alpha| < 1 \quad (6.12)$$

where k is a real constant. Its square-magnitude function is given by:

$$|H(e^{j\omega})|^2 = [H(z)H(z^{-1})]_{z=e^{j\omega}} = \frac{k^2}{(1 + \alpha^2) - 2\alpha \cos \omega} \quad (6.13)$$

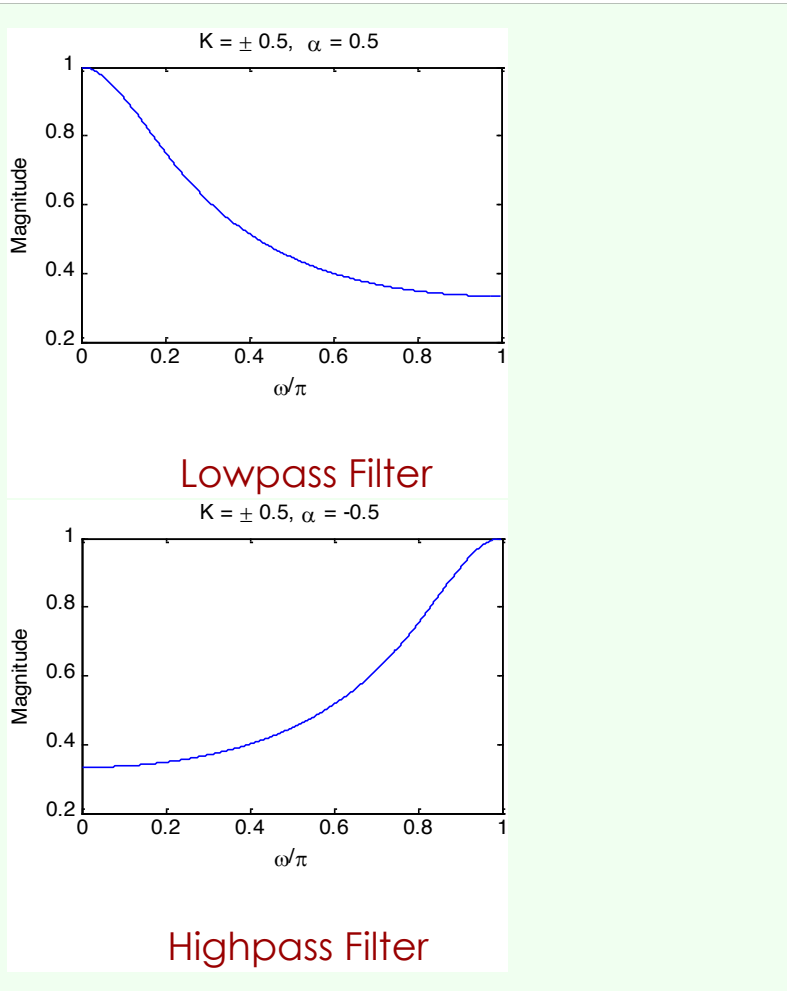
The maximum value of $|H(e^{j\omega})|^2$ is obtained when $2\alpha \cos \omega$ in the denominator is a maximum and the minimum value is obtained when $2\alpha \cos \omega$ is a minimum. For $\alpha > 0$, the maximum value of $2\alpha \cos \omega$ is equal to 2α at $\omega = 0$, and the minimum value is -2α at $\omega = \pi$.

Thus, for $\alpha > 0$, the maximum value of $|H(e^{j\omega})|^2$ is equal to $\frac{k^2}{(1-\alpha)^2}$ at $\omega = 0$ and the minimum value is equal to $\frac{k^2}{(1+\alpha)^2}$ at $\omega = \pi$.

On the other hand, for $\alpha < 0$, the maximum value of $2\alpha \cos \omega$ is equal to -2α at $\omega = \pi$ and the minimum value is equal to 2α at $\omega = 0$. Here, the maximum value of $|H(e^{j\omega})|^2$ is equal to $\frac{k^2}{(1-\alpha)^2}$ at $\omega = \pi$, and the minimum value is equal to $\frac{k^2}{(1+\alpha)^2}$ at $\omega = 0$. Hence, the maximum value can be made equal to 1 by choosing $k = \pm(1 - \alpha)$, in which case the minimum value becomes $\frac{(1-\alpha)^2}{(1+\alpha)^2}$. Hence:

$$H(z) = \frac{k}{1 - \alpha z^{-1}}, \quad 0 < |\alpha| < 1 \quad (6.14)$$

is a BR function for $k = \pm(1 - \alpha)$. Plots of the magnitude function for $\alpha = \pm 0.5$ with values of k chosen to make $H(z)$ a BR function are showed below.



6.2.3 Allpass transfer function

Definition 7: Allpass transfer function

An IIR transfer function $A(z)$ with unity magnitude response for all frequencies, i.e.:

$$|A(e^{j\omega})|^2 = 1 \quad \forall \omega \quad (6.15)$$

is called an allpass transfer function.

An M^{th} order causal real-coefficient allpass transfer function is of the form:

$$A_M(z) = \pm \frac{d_M + d_{M-1}z^{-1} + \dots + d_1z^{-M+1} + z^{-M}}{1 + d_1z^{-1} + \dots + d_{M-1}z^{-M+1} + d_Mz^{-M}} \quad (6.16)$$

If we denote the denominator polynomials of $A_M(z)$ as $D_M(z)$:

$$D_M(z) = 1 + d_1z^{-1} + \dots + d_{M-1}z^{-M+1} + d_Mz^{-M} \quad (6.17)$$

then it follows that $A_M(z)$ can be written as:

$$A_M(z) = \pm \frac{z^{-M} D_M(z^{-1})}{D_M(z)} \quad (6.18)$$

Note that if $z = re^{j\omega}$ is a pole of a real coefficient allpass transfer function, then it has a zero at $z = \frac{1}{r}e^{-j\varphi}$.

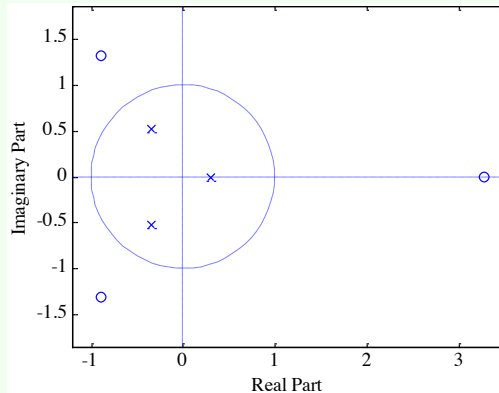
The numerator of a real-coefficient allpass transfer function is said to be the mirror-image polynomial of the denominator, and vice versa. We shall use the notation $\tilde{D}_M(z)$ to denote the mirror-image polynomial of a degree- M polynomial $D_M(z)$, i.e.:

$$\tilde{D}_M(z) = z^{-M} D_M(z^{-1}) \quad (6.19)$$

The expression in Eq. 6.18 implies that the poles and zeros of a real-coefficient allpass function exhibit mirror-image symmetry in the z -plane.

Example 39: Allpass transfer function

$$A_3(z) \frac{-0.2 + 0.81z^{-1} + 0.4z^{-2} + z^{-3}}{1 + 0.4z^{-1} + 0.18z^{-2} - 0.2z^{-3}} \quad (6.20)$$



To show that $|A_M(e^{j\omega})|^2 = 1$, we observe that:

$$A_M(z^{-1}) = \pm \frac{z^M D_M(z)}{D_M(z^{-1})} \quad (6.21)$$

Therefore:

$$A_M(z) A_M(z^{-1}) = \frac{z^{-M} D_M(z^{-1})}{D_M(z)} \frac{z^M D_M(z)}{D_M(z^{-1})} \quad (6.22)$$

Hence:

$$|A_M(e^{j\omega})|^2 = [A_M(z) A_M(z^{-1})]_{z=e^{j\omega}} = 1 \quad (6.23)$$

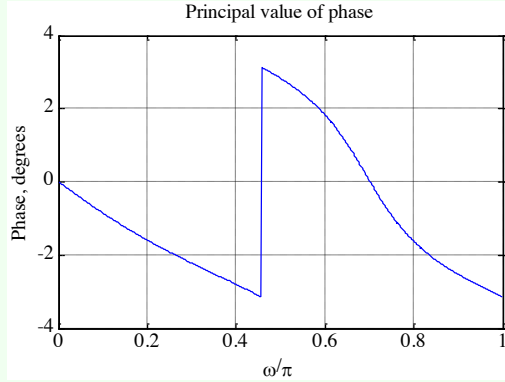
Now, the poles of a causal stable transfer function must lie inside the unit circle in the z -plane. Hence, all zeros of a causal stable allpass transfer function must lie outside the unit circle in a mirror-image symmetry with its poles situated inside the unit circle.

Example 40: Allpass transfer function

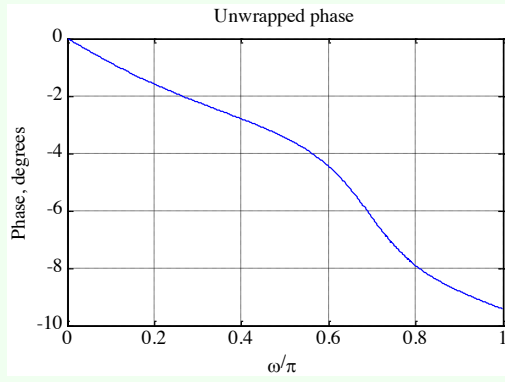
Consider the 3rd order allpass function:

$$A_3(z) = \frac{-0.2 + 0.18z^{-1} + 0.4z^{-2} + z^{-3}}{1 + 0.4z^{-1} + 0.18z^{-2} - 0.2z^{-3}} \quad (6.24)$$

The principal value of phase is showed in the plot below. Note the discontinuity by the amount of 2π in the phase $\theta(\omega)$.



If we unwrap the phase by removing the discontinuity, we arrive at the unwrapped phase function $\theta_c(\omega)$ indicated in the plot below. Note that the unwrapped phase function is a continuous function of ω .



We list now the properties of allpass transfer function:

- a causal stable real-coefficient allpass transfer function is a lossless bounded real (LBR) function or, equivalently, a causal stable allpass filter is a lossless structure;
- the magnitude function of a stable allpass function $A(z)$ satisfies:

$$|A(z)| \begin{cases} < 1 & |z| > 1 \\ = 1 & |z| = 1 \\ > 1 & |z| < 1 \end{cases} \quad (6.25)$$

- let $\tau(\omega)$ denote the group delay function of an allpass filter $A(z)$:

$$\tau(\omega) = -\frac{d}{d\omega}[\theta_c(\omega)] \quad (6.26)$$

The unwrapped phase function $\theta_c(\omega)$ of a stable allpass function is a monotonically decreasing function of ω so that $\tau(\omega)$ is everywhere positive in the range $0 < \omega < \pi$. The group delay of an M^{th} order stable real-coefficient allpass transfer function satisfies:

$$\int_0^\pi \tau(\omega) d\omega = M\pi \quad (6.27)$$

A simple but often used application of an allpass filter is as a delay equalizer. Let $G(z)$ be the transfer function of a digital filter designed to meet a prescribed magnitude

response. The non-linear phase response of $G(z)$ can be corrected by cascading it with an allpass filter $A(z)$ so that the overall cascade has a constant group delay in the band of interest. Since $|A_M(e^{j\omega})| = 1$, we have:

$$|G(e^{j\omega})A(e^{j\omega})| = |G(e^{j\omega})| \quad (6.28)$$

The overall group delay is given by the sum of the group delays of $G(z)$ and $A(z)$.

6.2.4 Phase characteristics

A second classification of a transfer function is with respect to its phase characteristics. In many applications, it is necessary that the digital filter designed does not distort the phase of the input signal components for frequencies in the passband. One way to avoid any phase distortion is to make the frequency response of the filter real and nonnegative, i.e., to design the filter with a zero-phase characteristic. However, it is not possible to design a causal digital filter with a zero phase.

For non-real-time processing of real-valued input signals of finite length, zero-phase filtering can be very simply implemented by relaxing the causality requirement. One zero-phase filtering scheme is sketched in Figure 6.3. It is easy to verify the ladder in the frequency domain.

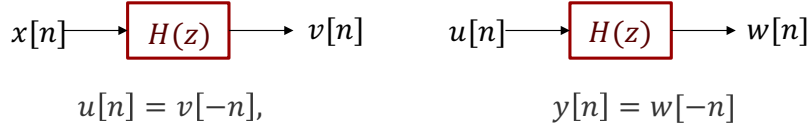


Figure 6.3: A possible zero-phase filtering scheme.

Let $X(e^{j\omega})$, $V(e^{j\omega})$, $U(e^{j\omega})$, $W(e^{j\omega})$ and $Y(e^{j\omega})$ denote the DTFTs of $x[n]$, $v[n]$, $u[n]$, $w[n]$ and $y[n]$, respectively. Making use of the symmetry relations, we arrive at the relations between various DTFTs:

$$V(e^{j\omega}) = H(e^{j\omega})X(e^{j\omega}) \quad (6.29)$$

$$W(e^{j\omega}) = H(e^{j\omega})U(e^{j\omega}) \quad (6.30)$$

$$U(e^{j\omega}) = V^*(e^{j\omega}) \quad (6.31)$$

$$Y(e^{j\omega}) = W^*(e^{j\omega}) \quad (6.32)$$

Combining the above equations we get:

$$\begin{aligned} Y(e^{j\omega}) &= W^*(e^{j\omega}) \\ &= H^*(e^{j\omega})U^*(e^{j\omega}) \\ &= H^*(e^{j\omega})V(e^{j\omega}) \\ &= H^*(e^{j\omega})H(e^{j\omega})X(e^{j\omega}) \\ &= |H(e^{j\omega})|^2 X(e^{j\omega}) \end{aligned} \quad (6.33)$$

The most general type of a filter with a linear phase has a frequency response given by:

$$H(e^{j\omega}) = e^{-j\omega D} \quad (6.34)$$

which has a linear phase from $\omega = 0$ to $\omega = 2\pi$. Note also that:

$$|H(e^{j\omega})| = 1 \quad (6.35)$$

and:

$$\tau(\omega) = -\frac{d}{d\omega}[\theta_c(\omega)] = D \quad (6.36)$$

The output $y[n]$ of this filter to an input $x[n] = Ae^{j\omega n}$ is then given by:

$$y[n] = Ae^{-j\omega D}e^{j\omega n} = Ae^{j\omega(n-D)} \quad (6.37)$$

If $x_a(t)$ and $y_a(t)$ represent the continuous-time signals whose sampled versions, sampled at $t = nT$, are $x[n]$ and $y[n]$ given above, then the delay between $x_a(t)$ and $y_a(t)$ is precisely the group delay of amount D . If D is an integer, then $y[n]$ is identical to $x[n]$, but delayed by D samples. If D is not an integer, $y[n]$, being delayed by a fractional part, is not identical to $x[n]$. In the latter case, the waveform of the underlying continuous-time output is identical to the waveform of the underlying continuous-time input and delayed D units of time.

If it is desired to pass input signal components in a certain frequency range undistorted in both magnitude and phase, then the transfer function should exhibit a unity magnitude response and a linear-phase response in the band of interest. In Figure 6.4 the frequency response of a lowpass filter with a linear-phase characteristic in the passband is showed. Since the signal components in the stopband are blocked, the phase response in the stopband can be of any shape.

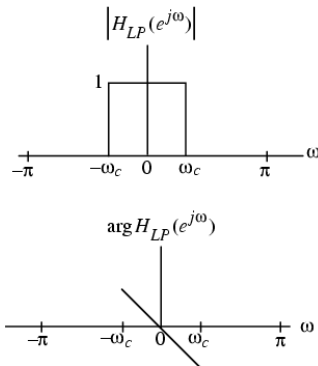


Figure 6.4: Frequency response of a lowpass filter with a linear-phase characteristic in the passband.

Example 41: Linear-phase transfer function

We determine now the impulse response of an ideal lowpass filter with a linear phase response:

$$H_{LP}(e^{j\omega}) = \begin{cases} e^{-j\omega n_0} & 0 < |\omega| < \omega_c \\ 0 & \omega_c \leq |\omega| \leq \pi \end{cases} \quad (6.38)$$

Applying the frequency-shifting property of the DTFT to the impulse response of an ideal zero-phase lowpass filter we arrive at:

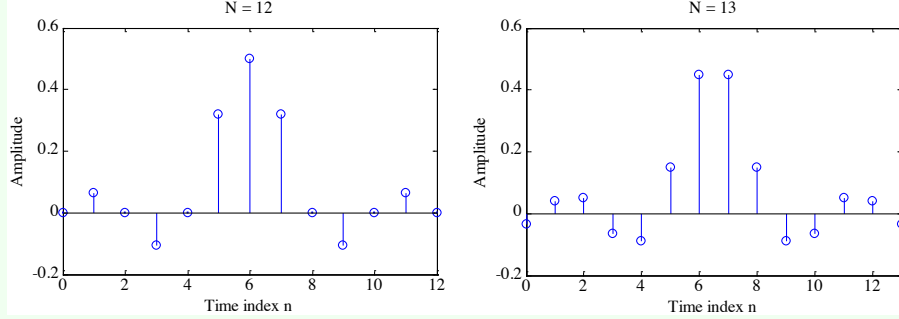
$$h_{LP}[n] = \frac{\sin(\omega(n - n_0))}{\pi(n - n_0)} \quad -\infty < n < \infty \quad (6.39)$$

As before, the above filter is noncausal and of doubly infinite length, and hence, unrealizable. By truncating the impulse response to a finite number of terms, a realizable FIR approximation to the ideal lowpass filter can be developed. The truncated approximation may or may not exhibit linear phase, depending on the value of n_0 chosen.

If we choose $n_0 = \frac{N}{2}$ with N a positive integer, the truncated and shifted approximation:

$$\hat{h}_{LP}[n] = \frac{\sin\left(\omega_c\left(n - \frac{N}{2}\right)\right)}{\pi\left(n - \frac{N}{2}\right)} \quad 0 \leq n \leq N \quad (6.40)$$

will be a length $N + 1$ causal linear-phase FIR filter. In the plot below the filter coefficients are showed. They are obtained using the function sinc for two different values of N .



Because of the symmetry of the impulse response coefficients as indicated in the two plots, the frequency response of the truncated approximation can be expressed as:

$$\hat{H}_{LP}(e^{j\omega}) = \sum_{n=0}^N \hat{h}_{LP}[n] e^{-j\omega n} = e^{-j\omega \frac{N}{2}} \tilde{H}_{LP}(\omega) \quad (6.41)$$

where $\tilde{H}_{LP}(\omega)$, called the zero-phase response or amplitude response, is a real function of ω .

Lecture 19.
Thursday 3rd
December, 2020.

6.2.5 Frequency response from transfer function

If the ROC of the transfer function $H(z)$ includes the unit circle, then the frequency response $H(e^{j\omega})$ of the LTI digital filter can be obtained simply as follows:

$$H(e^{j\omega}) = [H(z)]_{z=e^{j\omega}} \quad (6.42)$$

For a real coefficient transfer function $H(z)$ it can be showed that:

$$|H(e^{j\omega})|^2 = H(e^{j\omega})H^*(e^{j\omega}) = H(e^{j\omega})H(e^{-j\omega}) = [H(z)H(z^{-1})]_{z=e^{j\omega}} \quad (6.43)$$

For a stable rational transfer function in the form:

$$H(z) = \frac{p_0}{d_0} z^{(N-M)} \frac{\prod_{k=1}^M (z - \xi_k)}{\prod_{k=1}^N (z - \lambda_k)} \quad (6.44)$$

the factored form of the frequency response is given by:

$$H(e^{j\omega}) = \frac{p_0}{d_0} e^{j\omega(N-M)} \frac{\prod_{k=1}^M (e^{j\omega} - \xi_k)}{\prod_{k=1}^N (e^{j\omega} - \lambda_k)} \quad (6.45)$$

It is convenient to visualize the contributions of the zero ($z - \xi_k$) and the pole factor ($z - \lambda_k$) from the factored form of the frequency response. The magnitude function is given by:

$$|H(e^{j\omega})| = \left| \frac{p_0}{d_0} \right| \frac{\prod_{k=1}^M |e^{j\omega} - \xi_k|}{\prod_{k=1}^N |e^{j\omega} - \lambda_k|} \quad (6.46)$$

The phase response for a rational transfer function is of the form:

$$\arg H(e^{j\omega}) = \arg \left(\frac{p_0}{d_0} \right) + \omega(N-M) + \sum_{k=1}^M \arg(e^{j\omega} - \xi_k) - \sum_{k=1}^N \arg(e^{j\omega} - \lambda_k) \quad (6.47)$$

The magnitude-squared function of a real-coefficient transfer function can be computed using:

$$|H(e^{j\omega})|^2 = \left| \frac{p_0}{d_0} \right|^2 \frac{\prod_{k=1}^M (e^{j\omega} - \xi_k)(e^{j\omega} - \xi_k^*)}{\prod_{k=1}^N (e^{j\omega} - \lambda_k)(e^{j\omega} - \lambda_k^*)} \quad (6.48)$$

6.2.6 Geometric interpretation of frequency response

The factored form of the frequency response in Eq. 6.45 is convenient to develop a geometric interpretation of the frequency response computation from the pole-zero plot as ω varies from 0 to 2π on the unit circle. The geometric interpretation can be used to obtain a sketch of the response as a function of the frequency. A typical factor in the factored form of the frequency response is given by $(e^{j\omega} - \rho e^{j\varphi})$, where $\rho e^{j\varphi}$ is a zero if it is zero factor or is a pole if it is a pole factor. As showed in Figure 6.5, in the z-plane the factor $(e^{j\omega} - \rho e^{j\varphi})$ represents a vector starting at the point $z = \rho e^{j\varphi}$ and ending on the unit circle at $z = e^{j\omega}$.

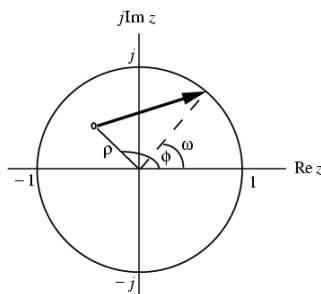


Figure 6.5: Factor $(e^{j\omega} - \rho e^{j\varphi})$ in the z-plane.

As ω is varied from 0 to 2π , the tip of the vector moves counterclockwise from the point $z = 1$, tracing the unit circle, and back to the point $z = 1$.

As indicated by the modulus of $H(e^{j\omega})$, in Eq. 6.46, the magnitude response $|H(e^{j\omega})|$ at a specific value of ω is given by the product of the magnitudes of all zero vectors divided by the product of the magnitudes of all pole vectors. Likewise, from Eq. 6.47, we observe that the phase response at a specific value of ω is obtained by adding the phase of the term $\frac{p_0}{d_0}$ and the linear-phase term $\omega(N - M)$ to the sum of the angles of the zero vectors minus the angles of the pole vectors. Thus, an approximate plot of the magnitude and phase responses of the transfer function of an LTI digital filter can be developed by examining the pole and zero locations.

Now, a zero (pole) vector has the smallest magnitude when $\omega = \varphi$. To highly attenuate signal components in a specified frequency range, we need to place zeros very close to or on the unit circle in this range. Likewise, to highly emphasize signal components in a specified frequency range, we need to place poles very close to or on the unit circle in this range.

6.3 Simple digital filters

Later in the course we shall review various methods of designing frequency-selective filters satisfying prescribed specifications. We now describe several low-order FIR and IIR digital filters with reasonable selective frequency responses that often are satisfactory in a number of applications. FIR digital filters considered here have integer-valued impulse response coefficients. These filters are employed in a number of practical applications, primarily because of their simplicity, which makes them amenable to inexpensive hardware implementations.

6.3.1 Lowpass FIR digital filters

The simplest lowpass FIR digital filter is the 2-point moving-average filter given by:

$$H_0(z) = \frac{1}{2}(1 + z^{-1}) = \frac{z + 1}{2z} \quad (6.49)$$

The above transfer function has a zero at $z = -1$ and a pole at $z = 0$. Note that here the pole vector has a unity magnitude for all values of ω . On the other hand, as ω increases from 0 to π , the magnitude of the zero vector decreases from a value of 2, the diameter of the unit circle, to 0. Hence, the magnitude response $|H_0(e^{j\omega})|$ is a monotonically decreasing function of ω from $\omega = 0$ to $\omega = \pi$. The maximum value of the magnitude function is 1 at $\omega = 0$, and the minimum value is 0 at $\omega = \pi$, i.e.:

$$|H_0(e^{j0})| = 1 \quad (6.50)$$

$$|H_0(e^{j\pi})| = 0 \quad (6.51)$$

The frequency response of the above filter is given by:

$$H_0(e^{j\omega}) = e^{-j\frac{\omega}{2}} \cos\left(\frac{\omega}{2}\right) \quad (6.52)$$

The magnitude response $|H_0(e^{j\omega})| = \cos\left(\frac{\omega}{2}\right)$ can be seen to be a monotonically decreasing function of ω , as showed in Figure 6.6.

The frequency $\omega = \omega_c$ at which:

$$|H_0(e^{j\omega_c})| = \frac{1}{\sqrt{2}} H_0(e^{j0}) \quad (6.53)$$

is of practical interest since here the gain $G(\omega_c)$ in dB is given by:

$$G(\omega_c) = 20 \log_{10} |H(e^{j\omega_c})| = 20 \log_{10} |H(e^{j0})| - 20 \log_{10} \sqrt{2} \approx -3 \text{ dB} \quad (6.54)$$

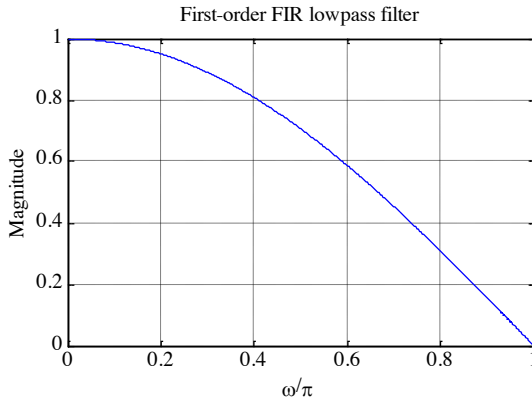


Figure 6.6: Magnitude response of the FIR lowpass filter.

since the dc gain $G(0) = 20 \log_{10} |H(e^{j0})| = 0$.

Thus, the gain $G(\omega)$ at $\omega = \omega_c$ is approximately 3 dB less than the gain at $\omega = 0$. As a result, ω_c is called the 3-dB cutoff frequency. To determine the value of ω_c , we set:

$$|H_0(e^{j\omega_c})|^2 = \cos^2\left(\frac{\omega_c}{2}\right) = \frac{1}{2} \quad (6.55)$$

which yields $\omega_c = \frac{\pi}{2}$.

The 3-dB cutoff frequency ω_c can be considered as the passband edge frequency. As a result, for the filter $H_0(z)$ the passband width is approximately $\frac{\pi}{2}$. The stopband is from $\frac{\pi}{2}$ to π . Note that $H_0(z)$ has a zero at $z = -1$ or $\omega = \pi$, which is in the stopband of the filter.

A cascade of the simple FIR filter:

$$H_0(z) = \frac{1}{2}(1 + z^{-1}) \quad (6.56)$$

results in an improved lowpass frequency response as showed in Figure 6.7 for a cascade of 3 sections.

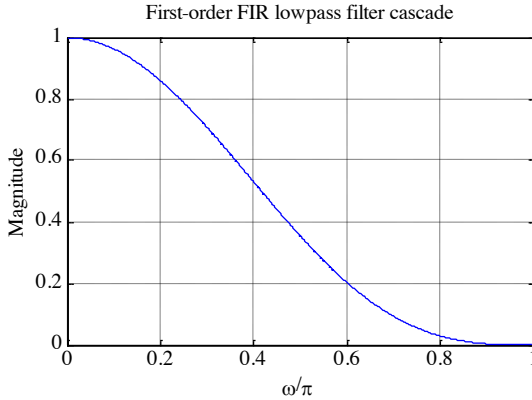


Figure 6.7: Magnitude response of the FIR lowpass filter cascade.

The 3-dB cutoff frequency of a cascade of M sections is given by:

$$\omega_c = 2 \arccos\left(2^{-\frac{1}{2M}}\right) \quad (6.57)$$

For $M = 3$, the above yields $\omega_c = 0.302\pi$. Thus, the cascade of first-order sections yields a sharper magnitude response but at the expense of a decrease in the width of the passband.

A better approximation to the ideal lowpass filter is given by a higher-order moving-average filter. Signals with rapid fluctuations in sample values are generally associated with high-frequency components. These high-frequency components are essentially removed by a moving-average filter resulting in a smoother output waveform.

6.3.2 Highpass FIR digital filters

The simplest highpass FIR filter is obtained from the simplest lowpass FIR filter by replacing z with $-z$. This results in:

$$H_1(z) = \frac{1}{2}(1 - z^{-1}) \quad (6.58)$$

The corresponding frequency response is given by:

$$H_1(e^{j\omega}) = j e^{-j\frac{\omega}{2}} \sin\left(\frac{\omega}{2}\right) \quad (6.59)$$

whose magnitude response is showed in Figure 6.8.

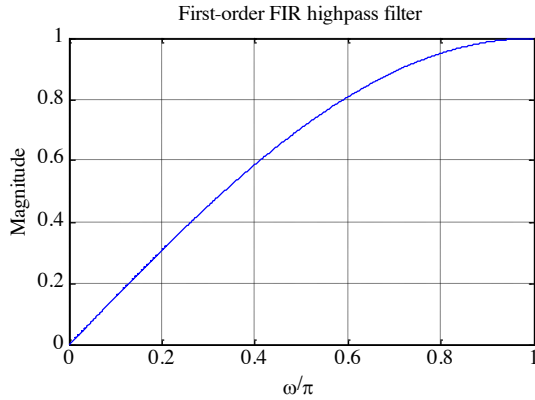


Figure 6.8: Magnitude response of the FIR highpass filter.

The monotonically increasing behavior of the magnitude function can again be demonstrated by examining the pole-zero pattern of the transfer function $H_1(z)$. The highpass transfer function $H_1(z)$ has a zero at $z = 1$ or $\omega = 0$, which is in the stopband of the filter.

Improved highpass magnitude response can be obtained by cascading several sections of the first-order highpass filter. Alternately, a higher-order highpass filter of the form:

$$H_1(z) = \frac{1}{M} \sum_{n=0}^{M-1} (-1)^n z^{-n} \quad (6.60)$$

is obtained by replacing z with $-z$ in the transfer function of a moving average filter. An application of the FIR highpass filters is in moving-target-indicator (MTI) radars. In these radars, interfering signals, called clutters, are generated from fixed objects in the path of the radar beam. The clutter, generated mainly from ground echoes and weather returns, has frequency components near zero frequency (dc). The clutter can be removed by filtering the radar return signal through a two-pulse canceler, which is the first-order FIR highpass filter. For a more effective removal it may be necessary to use a three-pulse canceler obtained by cascading two two-pulse cancelers:

$$H_1(z) = \frac{1}{2}(1 - z^{-1}) \quad (6.61)$$

6.3.3 Lowpass IIR digital filters

We have already shown that the first-order causal IIR transfer function:

$$H(z) = \frac{k}{1 - \alpha z^{-1}} \quad 0 < \alpha < 1 \quad (6.62)$$

has a lowpass magnitude response for $\alpha > 0$. An improved lowpass magnitude response is obtained by adding a factor $(1 + z^{-1})$ to the numerator of the transfer function:

$$H(z) = \frac{k(1 + z^{-1})}{1 - \alpha z^{-1}} \quad 0 < \alpha < 1 \quad (6.63)$$

This forces the magnitude response to have a zero at $\omega = \pi$ in the stopband of the filter. On the other hand, the first-order causal IIR transfer function:

$$H(z) = \frac{k}{1 - \alpha z^{-1}} \quad -1 < \alpha < 0 \quad (6.64)$$

has a highpass magnitude response for $\alpha < 0$. However, the modified transfer function obtained with the addition of a factor $(1 + z^{-1})$ to the numerator:

$$H(z) = \frac{k(1 + z^{-1})}{1 - \alpha z^{-1}} \quad -1 < \alpha < 0 \quad (6.65)$$

exhibits a lowpass magnitude response. The modified first-order lowpass transfer function for both positive and negative values of α is then given by:

$$H_{LP}(z) = \frac{k(1 + z^{-1})}{1 - \alpha z^{-1}} \quad 0 < |\alpha| < 1 \quad (6.66)$$

As ω increases from 0 to π , the magnitude of the zero vector decreases from a value of 2 to 0. The maximum values of the magnitude function is $\frac{2k}{(1-\alpha)}$ at $\omega = 0$ and the minimum value is 0 at $\omega = \pi$, i.e.:

$$|H_{LP}(e^{j0})| = \frac{2k}{(1 - \alpha)} \quad (6.67)$$

$$|H_{LP}(e^{j\pi})| = 0 \quad (6.68)$$

Therefore, $|H_{LP}(e^{j\omega})|$ is a monotonically decreasing function of ω from $\omega = 0$ to $\omega = \pi$.

For most applications, it is usual to have a dc gain of 0 dB, that is to have the maximum magnitude $|H(e^{j0})| = 1$. To this end, we choose $k = \frac{1-\alpha}{2}$, resulting in the first-order IIR lowpass transfer function:

$$H_{LP}(z) = \frac{1 - \alpha}{2} \frac{(1 + z^{-1})}{1 - \alpha z^{-1}} \quad 0 < |\alpha| < 1 \quad (6.69)$$

The above transfer function has a zero at i.e., at $\omega = \pi$, which is in the stopband. It has also a real pole at $z = \alpha$.

As ω increases from 0 to π , the magnitude of the zero vector decreases from a value of 2 to 0, whereas, for a positive value of α , the magnitude of the pole vector increases from a value of $1 - \alpha$ to $1 + \alpha$. The maximum value of the magnitude function is 1 at $\omega = 0$, and the minimum value is 0 at $\omega = \pi$, i.e. $|H_{LP}(e^{j0})| = 1$, $|H_{LP}(e^{j\pi})| = 0$. Therefore, $H_{LP}(e^{j\omega})$ is a monotonically decreasing function of ω from $\omega = 0$ to $\omega = \pi$ as indicated in Figure 6.9.

The squared magnitude function is given by:

$$|H_{LP}(e^{j\omega})|^2 = \frac{(1 - \alpha)^2(1 + \cos \omega)}{2(1 + \alpha^2 - 2\alpha \cos \omega)} \quad (6.70)$$

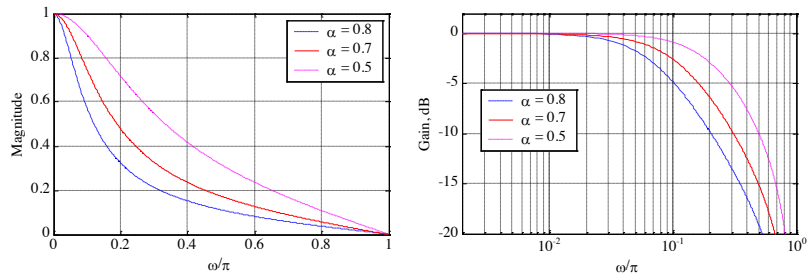


Figure 6.9: Magnitude (left) and gain (right) responses of the IIR lowpass filter.

The derivative of $|H_{LP}(e^{j\omega})|^2$ with respect to ω is given by:

$$\frac{d|H_{LP}(e^{j\omega})|^2}{d\omega} = \frac{-(1-\alpha)^2(1+\alpha^2+2\alpha)\sin\omega}{2(1+\alpha^2-2\alpha\cos\omega)^2} \quad (6.71)$$

The derivative in Eq. 6.71 is less or equal than zero in the range $0 \leq \omega \leq \pi$, verifying again the monotonically decreasing behaviour of the magnitude function. To determine the 3-dB cutoff frequency we set:

$$|H_{LP}(e^{j\omega})|^2 = \frac{1}{2} \quad (6.72)$$

in the expression for the square magnitude function, resulting in:

$$\frac{(1-\alpha)^2(1+\cos\omega_c)}{2(1+\alpha^2-2\alpha\cos\omega_c)} = \frac{1}{2} \quad (6.73)$$

which, when solved, yields:

$$\cos\omega_c = \frac{2\alpha}{1+\alpha^2} \quad (6.74)$$

The above quadratic equation can be solved for a yielding two solutions. The solution resulting in a stable transfer function $H_{LP}(z)$ is given by:

$$\alpha = \frac{1-\sin\omega_c}{\cos\omega_c} \quad (6.75)$$

It follows from:

$$|H_{LP}(e^{j\omega})|^2 = \frac{(1-\alpha)^2(1+\cos\omega_c)}{2(1+\alpha^2-2\alpha\cos\omega_c)} \quad (6.76)$$

that $H_{LP}(z)$ is a BR function for $|\alpha| < 1$.

6.3.4 Highpass IIR digital filters

A first-order causal highpass IIR digital filter has a transfer function given by:

$$H_{HP}(z) = \frac{1+\alpha}{2} \frac{1-z^{-1}}{1-\alpha z^{-1}} \quad (6.77)$$

where $|\alpha| < 1$ in order to have stability. The transfer function in Eq. 6.77 has a zero at $z = 1$, i.e. at $\omega = 0$, which is in the stopband.

Its 3-dB cutoff frequency ω_c is given by:

$$\alpha = \frac{1-\sin\omega_c}{\cos\omega_c} \quad (6.78)$$

which is the same as that of $H_{LP}(z)$. Magnitude and gain responses of $H_{HP}(z)$ are showed in Figure 6.10. $H_{HP}(z)$ is a BR function for $|\alpha| < 1$.

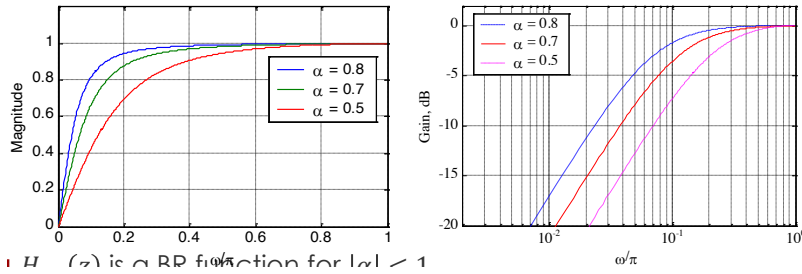


Figure 6.10: Magnitude (left) and gain (right) responses of the IIR highpass filter.

Example 42: Design of a filter

We design a first-order highpass digital filter with a 3-dB cutoff frequency of 0.8π .

Now, we consider that:

$$\begin{aligned}\sin(\omega_c) &= \sin(0.8\pi) = 0.587785 \\ \cos(\omega_c) &= \cos(0.8\pi) = -0.80902\end{aligned}$$

Therefore:

$$\alpha = \frac{1 - \sin \omega_c}{\cos \omega_c} = -0.5095245 \quad (6.79)$$

Therefore:

$$H_{HP}(z) = \frac{1 + \alpha}{2} \frac{1 - z^{-1}}{1 - \alpha z^{-1}} = 0.245238 \left(\frac{1 - z^{-1}}{1 + 0.5095245 z^{-1}} \right) \quad (6.80)$$

6.3.5 Bandpass IIR digital filters

A 2nd-order bandpass digital transfer function is given by:

$$H_{HP}(z) = \frac{1 - \alpha}{2} \left(\frac{1 - z^{-2}}{1 - \beta(1 + \alpha)z^{-1} + \alpha z^{-2}} \right) \quad (6.81)$$

Its squared magnitude function is:

$$|H_{BP}(e^{j\omega})|^2 = \frac{(1 - \alpha)^2(1 - \cos(2\omega))}{2[1 + \beta^2(1 + \alpha)^2 + \alpha^2 - 2\beta(1 + \alpha)^2 \cos \omega + 2\alpha \cos(2\alpha)]} \quad (6.82)$$

$|H_{BP}(e^{j\omega})|^2$ goes to zero at $\omega = 0$ and $\omega = \pi$. It assumes a maximum value of 1 at $\omega = \omega_0$, called the center frequency of the bandpass filter, where:

$$\omega_0 = \cos^{-1}(\beta) \quad (6.83)$$

The frequencies ω_{c1} and ω_{c2} where $|H_{BP}(e^{j\omega})|^2$ becomes $\frac{1}{2}$ are called the 3-dB cutoff frequencies. The difference between the two cutoff frequencies, assuming $\omega_{c2} > \omega_{c1}$ is called the 3-dB bandwidth and is given by:

$$B_w = \omega_{c2} - \omega_{c1} = \cos^{-1} \left(\frac{2\alpha}{1 + \alpha^2} \right) \quad (6.84)$$

The transfer function $H_{BP}(e^{j\omega})$ is a BR function if $|\alpha| < 1$ and $|\beta| < 1$. Some plots of $|H_{BP}(e^{j\omega})|$ are showed in Figure 6.11.

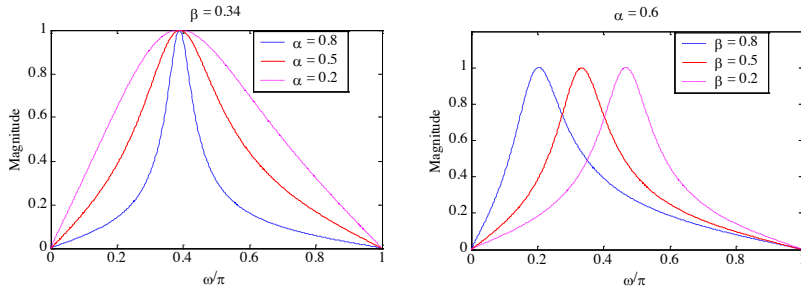


Figure 6.11: Magnitude responses of the IIR bandpass filter.

Example 43: Design of a filter

We design a 2nd-order bandpass digital filter with center frequency at 0.4π and a 3-dB bandwidth of 0.1π . We have:

$$\beta = \cos(\omega_0) = \cos(0.4\pi) = 0.309017 \quad (6.85)$$

and:

$$\frac{2\alpha}{1 + \alpha^2} = \cos(B_w) = \cos(0.1\pi) = 0.9510565 \quad (6.86)$$

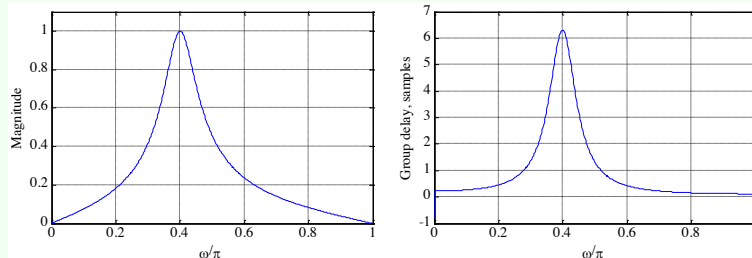
The solution of Eq. 6.86 yields $\alpha = 1.376382$ and $\alpha = 0.72654253$. The corresponding transfer functions are:

$$H'_{BP}(z) = -0.18819 \frac{1 - z^{-2}}{1 - 0.7343424z^{-1} + 1.37638z^{-2}} \quad (6.87)$$

$$H''_{BP}(z) = 0.13673 \frac{1 - z^{-2}}{1 - 0.533531z^{-1} + 0.72654253z^{-2}} \quad (6.88)$$

The poles of $H'_{BP}(z)$ are at $z = 0.3671712 \pm j1.11425636$ and they have a magnitude greater than 1. Thus, the poles of $H'_{BP}(z)$ are outside the unit circle making the transfer function unstable. On the other hand, the poles of $H''_{BP}(z)$ are at $z = 0.2667655 \pm j0.8095546$ and they have a magnitude of 0.8523746. Hence, $H''_{BP}(z)$ is BIBO stable.

In the plot below, the plots of the magnitude function and the group delay of $H''_{BP}(z)$ are showed.



6.3.6 Bandstop IIR digital filters

A 2nd-order bandstop digital filter has a transfer function given by:

$$H_{BS}(z) = \frac{1 + \alpha}{2} \left(\frac{1 - 2\beta z^{-1} + z^{-2}}{1 - \beta(1 + \alpha)z^{-1} + \alpha z^{-2}} \right) \quad (6.89)$$

The transfer function $H_{BS}(z)$ is a BR function if $|\alpha| < 1$ and $|\beta| < 1$. Its magnitude response is showed in Figure 6.12.

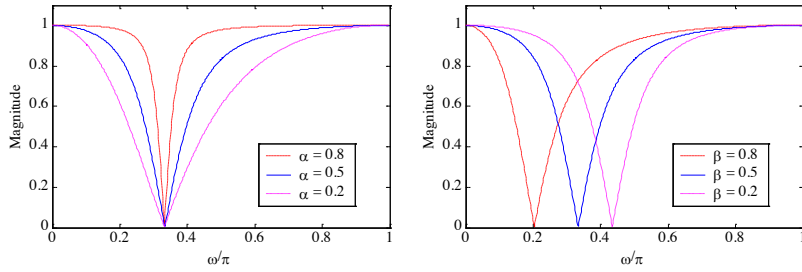


Figure 6.12: Magnitude responses of the IIR bandstop filter.

Here, the magnitude function takes the maximum value of 1 at $\omega = 0$ and $\omega = \pi$. It goes to 0 at $\omega = \omega_0$, where ω_0 , called the notch frequency, is given by:

$$\omega_0 = \cos^{-1}(\beta) \quad (6.90)$$

The digital transfer function $H_{BS}(z)$ is more commonly called a notch filter.

The frequencies ω_{c1} and ω_{c2} where $|H_{BP}(e^{j\omega})|^2$ becomes $\frac{1}{2}$ are called the 3-dB cutoff frequencies. The difference between them, assuming $\omega_{c2} > \omega_{c1}$, is called the 3-dB notch bandwidth and it is given by:

$$B_w = \omega_{c2} - \omega_{c1} = \cos^{-1} \left(\frac{2\alpha}{1 + \alpha^2} \right) \quad (6.91)$$

6.3.7 Higher-Order IIR digital filters

By cascading the simple digital filters discussed so far, we can implement digital filters with sharper magnitude responses. For example, let us consider a cascade of k first-order lowpass sections characterized by the transfer function:

$$H_{LP}(z) = \frac{1 - \alpha}{2} \frac{1 + z^{-1}}{1 - \alpha z^{-1}} \quad (6.92)$$

The overall structure has a transfer function given by:

$$G_{LP}(z) = \left(\frac{1 - \alpha}{2} \cdot \frac{1 + z^{-1}}{1 - \alpha z^{-1}} \right)^k \quad (6.93)$$

The corresponding squared-magnitude function is given by:

$$|G_{LP}(e^{j\omega})|^2 = \left[\frac{(1 - \alpha)^2(1 + \cos \omega)}{2(1 + \alpha^2 - 2\alpha \cos \omega)} \right]^k \quad (6.94)$$

To determine the relation between its 3-dB cutoff frequency ω_c and the parameter α , we set:

$$\left[\frac{(1 - \alpha)^2(1 + \cos \omega_c)}{2(1 + \alpha^2 - 2\alpha \cos \omega_c)} \right]^k = \frac{1}{2} \quad (6.95)$$

which when solved for α , yields for a stable $G_{LP}(z)$:

$$\alpha = \frac{1 + (1 - C) \cos \omega_c - \sin \omega_c \sqrt{2C - C^2}}{1 - C + \cos \omega_c} \quad (6.96)$$

where:

$$C = 2^{\frac{k-1}{k}} \quad (6.97)$$

It should be noted that, for $k = 1$, the expression given in Eq. 6.96 reduces to:

$$\alpha = \frac{1 - \sin \omega_c}{\cos \omega_c} \quad (6.98)$$

Example 44: Design of a filter

We design a lowpass filter with a 3-dB cutoff frequency at $\omega_c = 0.4\pi$ using a single first-order section and a cascade of 4 first-order sections, and we compare their gain responses.

For the single first-order lowpass filter we have:

$$\alpha = \frac{1 + \sin \omega_c}{\cos \omega_c} = \frac{1 + \sin(0.4\pi)}{\cos(0.4\pi)} \quad (6.99)$$

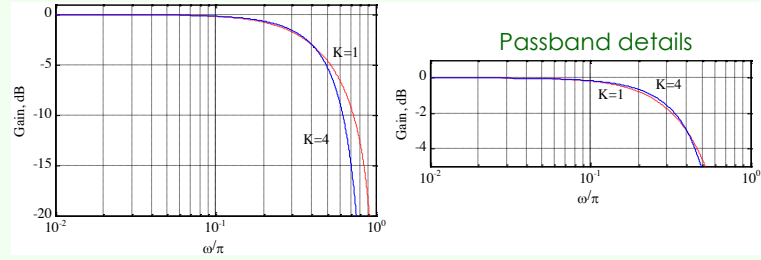
For the cascade of 4 first-order sections, we substitute $k = 4$ and get:

$$C = 2^{\frac{k-1}{k}} = 2^{\frac{4-1}{4}} = 1.6818 \quad (6.100)$$

Next, we compute:

$$\begin{aligned} \alpha &= \frac{1 + (1 - C) \cos \omega_c - \sin \omega_c \sqrt{2C - C^2}}{1 - C + \cos \omega_c} \\ &= \frac{1 + (1 - 1.6818) \cos(0.4\pi) - \sin(0.4\pi) \sqrt{2(1.6818) - (1.6818)^2}}{1 - 1.6818 + \cos(0.4\pi)} \\ &= -0.251 \end{aligned} \quad (6.101)$$

The gain responses of the two filters are showed in the plots below. As can be seen, cascading has resulted in a sharper roll-off in the gain response



Bibliography

- [1] *Signal Processing for Communications*, P. Prandoni and M. Vetterli, https://www.sp4comm.org/docs/sp4comm_corrected.pdf
- [2] *Digital Signal Processing*, A. V. Oppenheim and R. W. Schafer, Prentice Hall
- [3] *Digital Signal Processing: Digital Signal Processing: A Computer-Based Approach*, S. K. Mitra